1998

Interference suppression for DS/CDMA systems in non-Gaussian impulsive channels

Seoyoung Lee
Iowa State University

INFORMATION TO USERS

This manuscript has been reproduced from the microfilm master. UMI films the text directly from the original or copy submitted. Thus, some thesis and dissertation copies are in typewriter face, while others may be from any type of computer printer.

The quality of this reproduction is dependent upon the quality of the copy submitted. Broken or indistinct print, colored or poor quality illustrations and photographs, print bleedthrough, substandard margins, and improper alignment can adversely affect reproduction.

In the unlikely event that the author did not send UMI a complete manuscript and there are missing pages, these will be noted. Also, if unauthorized copyright material had to be removed, a note will indicate the deletion.

Oversize materials (e.g., maps, drawings, charts) are reproduced by sectioning the original, beginning at the upper left-hand corner and continuing from left to right in equal sections with small overlaps. Each original is also photographed in one exposure and is included in reduced form at the back of the book.

Photographs included in the original manuscript have been reproduced xerographically in this copy. Higher quality 6" x 9" black and white photographic prints are available for any photographs or illustrations appearing in this copy for an additional charge. Contact UMI directly to order.

UMI

A Bell & Howell Information Company
300 North Zeeb Road, Ann Arbor MI 48106-1346 USA
313/761-4700 800/521-0600

Interference suppression for DS/CDMA systems in non-Gaussian impulsive channels

by

Seoyoung Lee

A dissertation submitted to the graduate faculty

in partial fulfillment of the requirements for the degree of

DOCTOR OF PHILOSOPHY

Major: Electrical Engineering (Communications and Signal Processing)

Major Professor: Julie Dickerson

Iowa State University

Ames, Iowa

1998

Graduate College
Iowa State University

This is to certify that the Doctoral dissertation of

Seoyoung Lee

has met the dissertation requirements of Iowa State University

Signature was redacted for privacy.

Committee Member

Signature was redacted for privacy.

Committee Member

Signature was redacted for privacy.

Committee Member

Signature was redacted for privacy.

Committee Member

Signature was redacted for privacy.

Major Professor

Signature was redacted for privacy.

For the Major Program

Signature was redacted for privacy.

For the Graduate College

TABLE OF CONTENTS

LIST OF FIGURES

LIST OF TABLES

ACKNOWLEDGEMENTS

I would like to thank Dr. Julie Dickerson, my major professor, for her guidance, patience, encouragement, and support throughout this research and the writing of this dissertation. She gave me insight into the world of a stable process. I would also like to thank Dr. Steve F. Russell, my project co-leader and committee member, for his comments, suggestions, and support during last two semesters. I would also like to thank my committee members, Dr. Satish S. Udpa, Dr. Sung-Yell Song, and Dr. Fritz Keinert, for their efforts and contributions to this work.

I want to thank the Electronics and Telecommunications Research Institute (ETRI), Republic of Korea, for its continuous financial support during my first five years of graduate studies. Especially, I would like to thank Dr. Hyuckjae Lee, Dr. Young Soo Kim, and many other people in the ETRI for their encouragement and help. I would also like to thank Dr. Kaveh Pahlavan, Dr. Hsien-Sen Hung, and Dr. John F. Doherty for their time and advice during initial stages of my graduate career. I would also like to Dr. Dae Young Kim for introducing me to modem technologies when I started my research in the area of digital communications.

I would like to thank my late teacher, Chi Rang (Ziro) Min, for his love and dedication to my young life. He had been my best friend throughout my youth. He inspired me to have a vision of my future and initiate my overseas studies. I feel very sorry for his early death at the age of 41. I would like to share my pleasure with him in heaven.

I would like to express my thanks to my father for his support and encouragement. Without his patience, this work would not have been carried out. I miss my late mother

who passed away a year after my entering the United States of America. I should have stood by her when she went into a coma. I feel very sorry for not attending her funeral service. I would like to share my pleasure with her in heaven. She deserves special appreciation for her endless love and forgiveness. I would also like to thank my mother-in-law, brother-in-law, and sister-in-law for their support and encouragement. Their prayers and love have enriched my family's life.

Finally, special thanks go to my wife, Heasook, my daughter, Yoonhee, and my son, Joohyung. Their patience, insights, and words of encouragement have inspired me and renewed my hopes for completing my graduate studies. Heasook is my best friend in my life. I am very proud of my family. They always make my life enjoyable and valuable. I dedicate this dissertation to my beloved family.

ABSTRACT

Multiple-access interference (MAI) suppression techniques in DS/CDMA systems usually assume additive Gaussian noise. Minimum mean squared error (MMSE) detectors are near-far resistant in additive Gaussian noise channels. But the additive channel noise in many communication channels is often non-Gaussian and impulsive. Signal detection in non-Gaussian impulsive noise is traditionally focused on single-user channels. Symmetric alpha-stable ($S\alpha S$) probability density functions can accurately model large classes of impulsive noise. The MMSE performance criterion cannot be used for $S\alpha S$ processes with $0 < \alpha < 2$ since they have infinite variance. This dissertation considers the problems of MAI suppression for DS/CDMA systems in the presence of additive non-Gaussian impulsive channel noise modeled as a $S\alpha S$ process with $1 < \alpha < 2$. These MAI suppression techniques help combat the near-far problem. First, the minimum dispersion (MD) criterion is introduced to suppress MAI. Linear MD detection can be viewed as expansion of the concept of the MMSE detection for Gaussian multiple-access channels to $S\alpha S$ non-Gaussian impulsive multiple-access channels. The linear MD detector is implemented adaptively using least mean p-norm (LMP) algorithm. The performance of the linear MD detector is analyzed in the context of a $S\alpha S$ process. Simulation results indicate that the adaptive MD detector shows good near-far resistance. Next, this dissertation presents a MAI suppression method using the least L_p-norm criterion. The iteratively reweighted least squares (IRLS) algorithm recursively approximates the least L_p-norm solution from weighted normal equations. Simulation results show that the proposed detector provides remarkable performance improvements over the adaptive MD

detector in a wide range of near-far situations. The proposed detector has much better near-far resistance than the adaptive MD detector. Finally, fuzzy hybrid detector combines the adaptive MD detector and the hard-limiting matched filter (HLMF) detector. The HLMF detector performs well when the additive impulsive noise significantly dominates over MAI. Simulation results indicate significant performance improvements over the adaptive MD detector alone in impulsive noise-limited environments. When MAI dominates, the fuzzy hybrid detector nearly has the same performance as the adaptive MD detector.

ACRONYMS

BER	bit error rate
BPSK	binary phase shift keyed
CIR	carrier-to-interference ratio
DS/CDMA	direct-sequence code-division multiple-access
FIR	finite impulse response
HLMF	hard-limiting matched filter
ISI	intersymbol interference
LC	linear correlation
LMP	least mean p-norm
LMS	least mean square
MAI	multiple-access interference
MD	minimum dispersion
MF	matched filter
MMSE	minimum mean squared error
MSE	mean squared error
NE	normalized error
PRID	power ratio of the interfering users to the desired user
SaS	symmetric α-stable
SIR	signal-to-interference ratio
SNR	signal-to-noise ratio

CHAPTER 1 INTRODUCTION

1.1 Problem Statement

Direct-sequence code-division multiple-access (DS /CDMA) is one of various popular multiple-access techniques in digital wireless communications. CDMA is also referred to as spread-spectrum multiple-access (SSMA) or spread-spectrum communications [1]. In DS/CDMA systems, users can simultaneously access the same channel using their distinct spreading codes, even though all users' signals overlap in time and frequency. The receivers of conventional DS/CDMA systems consists of a bank of matched filters, each of which is matched to each of the users' spreading codes. It is well known that the conventional linear matched filter (MF) or correlation detector is optimal in the sense of minimum probability of error in an additive white Gaussian noise (AWGN) channel. For DS/CDMA systems, this is the case for a single-user channel without interfering users in the presence of AWGN. The conventional MF detector was essentially regarded as optimum due to the belief of many workers in spread spectrum that multiple-access interference (MAI) is accurately modeled as a white Gaussian random process by the Central Limit Theorem [2], [3]. The fact that the MAI can not be any longer Gaussian in multiple-access channels motivated the development of mutiuser detection. Poor demonstrated in 1980 that the Gaussian approximation is completely useless in many practical situations (*e.g.* in near-far environments). He improved the performance of the conventional MF detector in multiple-access channels based on techniques from both minimax robustness and non-Gaussian signal detection [4], [2], [3].

Since the spreading codes are not completely orthogonal, the MAI exists at the output of each of the MF's in conventional DS/CDMA systems. The amount of MAI increases as the number of interfering users increases, and/or the received signal powers of the interfering users increase. Especially, when there exist interfering users with high powers, the strong MAI dominates over a weak received signal, which results in a *near-far* problem. The conventional MF detector is highly sensitive to the near-far problem. The near-far problem is thus a limiting factor to the capacity and performance of the conventional DS/CDMA systems in spite of the fact that spread spectrum, by its very nature, is an interference-tolerant modulation [5]. The performance of the conventional MF detector is acceptable if the received signal powers are not too dissimilar and the cross-correlations of the spreading codes are low enough [2], [3].

In order to mitigate the effect of MAI on the conventional MF detector, various research efforts have focused on several areas such as code waveform design, power control, forward error correction (FEC) codes, and sectored/adaptive antennas. If the spreading codes are completely orthogonal, there exists no MAI in synchronous DS/CDMA systems. However, since some degree of asynchronism is inherent in most practical channels due to their path delays, it is not possible to design complete orthogonal codes over all possible delays (see [1] and references therein). Power control is currently used to solve the near-far problem in DS/CDMA systems based on the IS-95 standard [6], [7], [8], [9]. The power control method equalizes the received signal powers and therefore mitigates the near-far effect.

Above all, the most important approach to solve the near-far problem is *MAI suppression*. This is also known as wideband interference suppression since the MAI is wideband like wideband DS/CDMA signals. Note that narrowband interference suppression is another area in DS/CDMA systems. This narrowband interference occurs in overlaying systems during transitions between the old and new systems. For example, the CDMA overlay or coexistence with the existent analog cellular system, called

advanced mobile phone system (AMPS) results in narrowband interference. The narrowband interference is beyond the scope of this work. A reader is referred to [10], [11], [12], [5] and references therein for details.

This dissertation will focus on wideband interference or MAI suppression. For conceptual clarity, it can be classified into *multiuser* detection and *single-user* detection depending on its detection structure as in [5]. Multiuser detection is fully centralized, while single-user detection is fully decentralized. In general, the single-user detection requires knowledge of only one user's (or desired user's) signal parameters such as spreading code, delay, and power, but not that of the interfering users' parameters. The multiuser detection requires knowledge of all users' signals parameters. The delay and power of each user are usually estimated at the receiver. All users' spreading codes can be available in base stations, but they are not easily available in mobile stations without receiving the spreading codes from base stations. The distribution of that information may be vulnerable to a wireless channel security problem. The complexity of the single-user detection is much lower than that of the multiuser detection. Single-user detection is more favorable in terms of its relative simplicity of implementation and wireless channel security. Thus, the single-user detection may be more appealing to mobile stations rather than to base stations. In this work, we will focus on single-user detection. This work is the communication problem that takes into account the effects of both MAI and additive impulsive channel noise for increasing the system performance and capacity.

1.2 Literature Review

This section briefly reviews several MAI suppression techniques. The results are primarily summarized from two survey papers [1], [5]. The reader is referred to [2], [3], [13], [14], [1], and [5] for detailed information on each scheme. Figure 1.1 shows an organizational chart for MAI suppression in DS/CDMA systems.

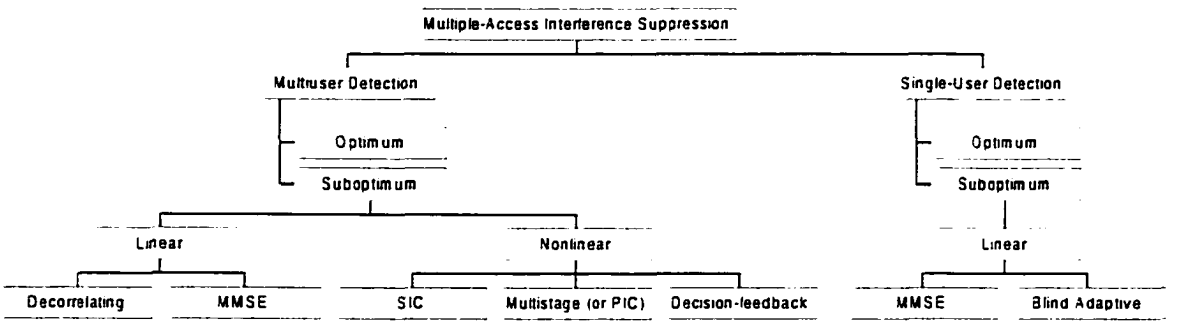

Figure 1.1 Organizational chart for MAI suppression in DS/CDMA systems.

1.2.1 Multiuser Detection

Verdu [15] proposed and analyzed an optimum multiuser detector with minimum probability of error and near-far resistance. The detector consists of a bank of MF's followed by a maximum likelihood sequence detector. The optimum multiuser detector requires knowledge of the spreading codes, delays, and powers of all active users. The computational complexity increases exponentially with the number of users. Since the detector is too complex to be used in practical DS/CDMA systems, most research efforts have focused on the development of suboptimum multiuser detectors which have good near-far resistance, lower computational complexity, and low probability of error. Most suboptimum multiuser detectors can be classified into one of two categories: *linear* and *nonlinear* [1].

A class of linear suboptimum multiuser detectors includes *decorrelating* and *minimum mean squared error* (*MMSE*) detectors. This class of detectors applies a linear mapping to the soft output of the conventional MF's to reduce the MAI seen by each user [1]. Lupas and Verdu [16], [17] introduced the decorrelating detector with the same near-far resistance as the optimum multiuser detector. It completely eliminates the MAI at the expense of noise enhancement. It provides significant performance improvements over the conventional MF detector under most conditions except when the MAI is relatively

low and the background noise is relatively high [3], [17], [1]. The decorrelating detector requires knowledge of the spreading codes and delays of all active users, but does not require knowledge or estimates of the received signal powers of all active users. This detector is analogous to the zero-forcing equalizer which is used to completely eliminate inter-symbol interference (ISI) [1]. The computational complexity increases linearly with the number of users.

Another linear multiuser detector is the MMSE detector [18] which takes into account the background noise. It requires knowledge or estimates of the received signal powers of all active users. Thus, the MMSE detector generally has better performance in terms of probability of error than the decorrelating detector. This detector is exactly analogous to the MMSE linear equalizer which is used to combat ISI. The MMSE detector strikes a balance between complete MAI elimination and noise enhancement [1]. As the background noise goes to zero, the performance of the MMSE detector converges to that of the decorrelating detector, while the performance of the MMSE detector approaches that of the conventional MF detector as the noise gets very large, or the MAI gets very small [18], [13], [1]. Since the performance of the MMSE detector depends on the powers of the interfering users [18], there is some loss of near-far resistance comparing to the decorrelating detector [1].

A class of nonlinear suboptimum multiuser detectors is divided into three classes such as *successive interference cancellation* (*SIC*) [19], [20], [21], *multistage* detection [22] (or *parallel interference cancellation* (*PIC*) [23]), and decision-feedback detection [24], [25]. The basic principle is to subtract out some or all of the MAI by estimates of the MAI at the receiver. These detectors are similar to decision-feedback equalizers used to combat ISI. The detectors have near-far resistance. These detectors requires knowledge of the spreading codes of all active users and estimates of all active users' parameters such as amplitudes and delays. They provide significant performance improvements over the conventional MF detector. The computational complexity increases linearly with the

number of users. A reader is referred to [1] and references therein for a number of variations on these types of detectors.

1.2.2 Single-User Detection

Poor and Verdu [26] investigated optimum decentralized detection for asynchronous Gaussian multiple-access channels by taking into account the structure of the MAI. The detection is the optimum one-shot detection where the detection of each symbol is based on the received signal only in that symbol interval. Detection is modeled by the binary hypothesis testing problem and the optimum (in the sense of maximum likelihood/minimum probability of error) decision is based on comparing the likelihood ratio to a threshold.

Aazhang, Paris, and Orsak [27] proposed two detection schemes such as single-user and multiuser for asynchronous and synchronous Gaussian multiple-access channels using multilayer perceptrons. These detectors approximate the optimum multiuser [15] and single-user [26] detectors. Mitra and Poor [28] also provided an implementation of the optimal single-user detector for synchronous Gaussian multiple-access channels using the radial basis function (RBF) network. Neural network techniques such as supervised clustering and k-means clustering adaptively determine unknown system parameters in unknown or changing communication environments. The adaptive RBF network provides near optimal performance and is robust in realistic communication environments. Since the RBF network with the full user set requires 2^K neurons for K users, it may not be desirable if there are a significant number of active users. But it provides strong performance with reduced user set.

Since a class of the optimum single-user detectors may require knowledge of the interfering users, their complexity may be relatively high. Thus, adaptive single-user detectors using the MMSE criterion have been introduced for MAI suppression in DS/CDMA systems [29], [30], [31], [32], [33], [34], [35], [36], [37], [38], [39], [40], [41]. The adaptive

detectors offer significant performance improvements over the conventional MF detector and near-far resistance in AWGN channels. The adaptive detectors do not require knowledge of the interfering users' parameters such as spreading codes, delays, and powers, but they require training sequences for their adaptation to changing or unknown communication environments. Adaptive single layer perceptrons using the MMSE criterion were considered to suppress MAI [39]. Their convergence analysis were performed in a multiuser communications environment and the performance of various algorithms such as least mean square (LMS), MF, and decorrelating was compared via computer simulation. An adaptive correlator using the MMSE criterion was proposed to suppress narrowband interference and mitigate multipath [42]. The performance of the adaptive correlator is nearly comparable to that of a RAKE receiver with perfect channel information in the presence of multipath only. The RAKE receiver degrades significantly, while the adaptive correlator still performs well in the presence of both narrowband interference and multipath. The adaptive MMSE detectors can be attractive not only in base stations but also in mobile stations. Even though the adaptive MMSE detectors primarily aims at combating the MAI, the previous works of [43] and [42] implicitly suggests that those detectors can simultaneously treat multipath and narrowband interference as well as MAI [38].

Blind adaptive interference suppression for near-far resistant CDMA was proposed in [44]. It requires only knowledge of the desired user's spreading code and associated timing. The received amplitudes do not need to be known or estimated. The criterion is to minimize the mean output energy, which is equivalent to minimizing the MSE without training sequences.

1.3 Motivation

There are several factors that motivate us to consider the problems of MAI suppression for DS/CDMA systems in non-Gaussian impulsive channels:

- **Non-Gaussian impulsive channel noise models** - The existing detectors for MAI suppression have mainly been considered under the assumption of additive Gaussian noise. Many communications links are often corrupted by non-Gaussian impulsive noise which is generated by either natural or man-made noise [45], [46], [47], [48], [49], [50]. Man-made electromagnetic noise in urban mobile-radio channels has a noise density in which the tails decay at a rate slower than that of the Gaussian noise density [45], [51]. Therefore, more accurate noise models need to be considered to avoid a significant performance degradation. Many models of non-Gaussian impulsive noise can be divided into two classes of models: physical models such as Middleton class A, B, and C [45], [52], [53], [54] and empirical models such as an ϵ-mixture [48]. These models have widely been used for signal detection in impulsive environments [55], [56], [57], [49], [58], [51]. It was shown that a general class of man-made and natural impulsive noise indeed has a symmetric stable distribution under appropriate assumptions on the spatial and temporal distributions of noise source and the propagation conditions [59], [60]. Recently, symmetric α-stable ($S\alpha S$) noise models have been used in [61], [62], [50]. A mixture model of Gaussian and $S\alpha S$ noise was especially taken into account in [61] and [62]. Binary detection in a mixture of Gaussian and α-stable noise was investigated in [61]. In [62], the mixture noise was used to model the interference of frequency-hopping (FH) spread-spectrum (SS) radio networks in a Poisson field of interfering users [62]. A reader is referred to Section 2.5 for more description of impulsive noise models. In this work, we model the additive non-Gaussian impulsive noise as a $S\alpha S$ random process [60], [63].

- **Linear estimation within the framework of a $S\alpha S$ process** [60], [64], [65] - Since the second moment of a $S\alpha S$ noise process is not finite for $0 < \alpha < 2$, the MMSE criterion is not valid anymore. The *minimum dispersion* (MD) criterion is addressed in linear theory of stable processes. Under the MD criterion, the best estimate of a $S\alpha S$ random variable in the linear space of observations is the one that minimizes the dispersion of the estimation error. Note that the dispersion of a stable random variable plays a role analogous to the variance. A reader is referred to Section 2.4 for details of $S\alpha S$ random process.

- **Interference suppression in non-Gaussian impulsive noise channels** - Lots of research efforts have made in the area of signal detection over a single-user impulsive noise channel (see [49], [58], [66] and references therein for details). In [49], performance of discrete-time linear and nonlinear correlation detectors was studied in the presence of both MAI and additive impulsive noise. When the MAI dominates over the additive impulsive noise, the conventional linear correlation (or MF) detector still suffers from the near-far problem like in the Gaussian channels. But the problem of MAI suppression for DS/CDMA systems in the presence of additive non-Gaussian impulsive noise has not been given much attention. As far as we know, there have been few works [67], [68], [51], [69] on MAI suppression in additive non-Gaussian impulsive channels. Mandayam [67], [68] proposed adaptive linear detection to minimize the average probability of bit-error using an infinitesimal perturbation analysis (IPA) based stochastic gradient algorithm. In [51], detection of spread-spectrum signals in a multiuser environment with additive impulsive noise was considered to determine the presence of a new user and integrate knowledge of this new user into the multiuser detector. In [69], a near single-user performance of the HLMF detector was achieved by incorporating a *sgn* function and using the steepest descent method for multiuser detection. Cheng, Shen,

and Nikias [70] developed a family of optimal $\mathcal{L}^{(p,q)}$-metric interference estimators for arbitrary i.i.d. interference sequence and any discrete-type complex measurement noise (or signal) sequence. The proposed interference estimators were tested via computer simulation under the assumption that the additive interference is modeled as an autoregressive (AR) sequence driven by the $S\alpha S$ process and binary random sequence. In [10], [11], and [12], nonlinear filtering techniques were introduced to predict an narrowband interference in the presence of additive non-Gaussian noise. Rusch and Poor [12] modeled the CDMA signal as non-Gaussian noise in the interference suppression process. Garth and Poor [11] considered the effect of non-Gaussian noise corrupted by impulsive background noise as well as the CDMA signal. Even if the interference suppression techniques given in [11], [12], and [70] are considered in non-Gaussian impulsive environments, they modeled the relevant interference as a sinusoidal or an AR signal and therefore it is not clear that these techniques will still be effective in real situations, where the relevant interference is a digital communications or CDMA signal. The relevant interference is quite likely to be poorly modeled as a sinusoidal or an AR signal. Multiuser detection theory was first applied to solve this modeling problem of the narrowband interference suppression [71]. When the narrowband interference is indeed a digital communications signal, the existing techniques are less effective than those based on the multiuser detection theory.

1.4 Objectives and Expected Contributions

The purpose of this work is to consider the problems of MAI suppression for asynchronous binary phase shift keyed (BPSK) DS/CDMA systems in the presence of additive non-Gaussian impulsive noise modeled as a $S\alpha S$ process. The interference suppression techniques help mitigate the near-far problem. The expected contributions of the

proposed research includes:

- Expanding the concept of the MMSE MAI suppression for Gaussian multiple-access channels to $S\alpha S$ non-Gaussian impulsive multiple-access channels.
- Presenting MAI suppression techniques, for DS/CDMA systems in additive $S\alpha S$ non-Gaussian impulsive channels, such as adaptive MD detection, least L_p-norm detection, and fuzzy hybrid detection.
- Analyzing the performance of the linear MD detector in the context of a $S\alpha S$ process.
- Assessing the performance of the proposed detectors by extensive Monte Carlo simulation.

1.5 Dissertation Organization

Chapter 2 presents some preliminary results used throughout this dissertation. It includes a mathematical description of a system model for a conventional DS/CDMA system, an illustration of the effect of MAI on conventional discrete-time MF detector, a brief summary of the classical theory of stable processes, and a review of both channel noise models and optimum detection based on Bayes rule. Chapter 3 through Chapter 5 consider the problems of MAI suppression for DS/CDMA systems in the presence of additive non-Gaussian impulsive noise modeled as a $S\alpha S$ process. Chapter 3 presents a linear minimum dispersion (MD) detector. It includes a performance analysis of the linear MD detector in the context of a $S\alpha S$ process. Chapter 4 introduces a least L_p-norm detector. Chapter 5 describes a fuzzy hybrid detector. These detectors for MAI suppression are to combat the near-far problem. Simulation results are included at the end of each of the chapters. Finally, Chapter 6 concludes the dissertation and recommends future work.

CHAPTER 2 BACKGROUND

In this chapter, we introduce useful preliminary results used widely throughout this dissertation. In Section 2.1, we describe a system model for a conventional DS/CDMA system to be considered throughout this dissertation. The system model uses the assumptions made in [49], [58] and the approaches given in [34], [49], and [58]. Section 2.2 provides simulation environments and some simulation results on the system model. Section 2.3 illustrates the effect of MAI on the conventional MF (or correlation) detector using discrete-time system model. Section 2.4 presents a brief summary of the classical theory of stable processes. This includes the stable distribution and characterizations and statistical properties. For further information, a reader is referred to [60], [64], and [63]. Next we briefly present an introduction to linear theory of stable processes. These materials will be primarily employed in Chapter 3. Most of the preliminary results are extracted from [64], [60], [63], [72] and [65]. Section 2.5 discusses noise models. Section 2.6 describes optimum detection based on Bayes rule.

2.1 System Description

Consider an asynchronous binary phase shift keyed (BPSK) DS/CDMA system with K users. The system model is shown in Figure 2.1. K users share the channel which consists of K paths. Each path has a unity path gain and some fixed path delay.

The transmitted signal for the kth user is given by

$$s_k(t) = \sqrt{2P_k}b_k(t)c_k(t)\cos(\omega_c t + \theta_k),\ k = 1, 2, \cdots, K \tag{2.1}$$

where P_k and θ_k are the transmitter power and carrier phase, respectively. ω_c is the carrier frequency. $b_k(t)$ is the baseband signal generated by the binary data symbol $b^{(k)}(i) \in \{-1, +1\}, -\infty < i < \infty$, and $c_k(t)$ is the spreading signal generated by the spreading sequence $\left\{c_0^{(k)}, c_1^{(k)}, \cdots, c_{N-1}^{(k)}\right\}$ with a processing gain N. It is assumed that $b_k(t)$ and $c_k(t)$ are polar signals of duration T and T_c, respectively. Then they are of the forms

$$b_k(t) = \sum_{i=-\infty}^{\infty} b^{(k)}(i) p_T(t - iT) \tag{2.2}$$

and

$$c_k(t) = \sum_{n=-\infty}^{\infty} c_n^{(k)} p_{T_c}(t - nT_c) \tag{2.3}$$

where $c_n^{(k)} = c_{n+N}^{(k)}$ and $c_n^{(k)} \in \{-1, +1\}$, $p_T(t)$ and $p_{T_c}(t)$ are the unity rectangular pulses of duration T and T_c, respectively. Assuming $T = NT_c$, there exists one code sequence $\left\{c_0^{(k)}, c_1^{(k)}, \cdots, c_{N-1}^{(k)}\right\}$ per data symbol $b^{(k)}(i)$. This assumption is not usually required for a DS/CDMA system to function properly, but is essential for the system studied in this dissertation as in [38]. The resulting received signal for a given receiver is given by

$$\begin{aligned} r(t) &= \sum_{k=1}^{K} s_k(t - \tau_k) + v(t) \\ &= \sum_{k=1}^{K} \sqrt{2P_k} b_k(t - \tau_k) c_k(t - \tau_k) \cos(\omega_c t + \varphi_k) + v(t), \; k = 1, 2, \cdots, K \end{aligned} \tag{2.4}$$

where $v(t)$ is the additive non-Gaussian impulsive noise modeled as a $S\alpha S$ process with zero location parameter μ, τ_k is the time delay due to the channel propagation delay and the lack of time synchronism between the transmitter and receiver, and $\varphi_k \triangleq \theta_k - \omega_c \tau_k$.

After the front-end chip-matched filtering, the received signal is sampled at the chip rate $1/T_c$. The signal samples over a symbol interval T can be considered as a signal vector. Without any loss of generality, we can assume that the user of interest is user number 1, who is referred as the desired user, and that the receiver is synchronized to

this transmitter. Hence only relative time delays and carrier phase angles need to be considered. The nth sample over ith symbol interval at the output of the chip-matched filter is given by

$$r_n(i) \triangleq r(nTc) = \int_{nT_c+\tau_1}^{(n+1)T_c+\tau_1} r(t)\cos(\omega_c t + \varphi_1)dt \tag{2.5}$$

for $0 \leq n \leq N-1$. We can assume $\theta_1 = 0$ and $\tau_1 = 0$ due to the above assumption. Furthermore, there is no loss of generality in assuming $\varphi_k \in [0, 2\pi)$ and $\tau_k \in [0, T)$, $2 \leq k \leq K$ since we are concerned only with carrier phase shifts modulo 2π and time delays modulo T .

Figure 2.2 shows relative time delays of asynchronous CDMA systems. Without loss of generality, we order the users such that $0 = \tau_1 \leq \tau_2 \leq \cdots \leq \tau_K$. Since we are interested in a symbol-by-symbol detection through this dissertation, we need to consider the received samples within the single symbol period, i.e., ith symbol interval of T. During this symbol interval the kth interfering spreading sequence is modulated by the data symbol $b^{(k)}(i-1)$, for $t \in [0, \tau_k]$, and by the data symbol $b^{(k)}(i)$, for $t \in [\tau_k, T]$. For $2 \leq k \leq K$, the relative delay for the kth user is written as $\tau_k = m_k T_c + \delta_k$ where m_k is an integer between 0 and $N-1$ and $0 \leq \delta_k < T_c$ (see [34] and [58]). When τ_k is zero for every k, the asynchronous system reduces to a synchronous system.

We assume that the integrator has a scaling factor of $\sqrt{2/P_1}/T_c$ associated with the desired user. Then from (2.4) and (2.5), it follows that at time $t = iT$

$$r_n(i) = b^{(1)}(i)c_n^{(1)} + \sum_{k=2}^{K} \frac{1}{T_c}\sqrt{\frac{P_k}{P_1}}\cos(\varphi_k)\left[b^{(k)}(i-1)\hat{c}_{i-1}^{(k)}(n) + b^{(k)}(i)\hat{c}_i^{(k)}(n)\right] + v_n(i) \tag{2.6}$$

for $0 \leq n \leq N-1$ where

$$v_n(i) \triangleq v(nTc) = \frac{\sqrt{2/P_1}}{T_c}\int_{nT_c+\tau_1}^{(n+1)T_c+\tau_1} v(t)\cos(\omega_c t + \varphi_1)dt. \tag{2.7}$$

$$\begin{aligned}\hat{c}_{i-1}^{(k)}(n) &\triangleq \hat{c}_{i-1}^{(k)}(n; m_k, \delta_k) \\ &= c_{n-m_k-1+N}^{(k)} \cdot \delta_k \cdot \Psi_{0\leq n\leq m_k} + c_{n-m_k+N}^{(k)} \cdot (T_c - \delta_k) \cdot \Psi_{0\leq n\leq m_k-1}.\end{aligned} \tag{2.8}$$

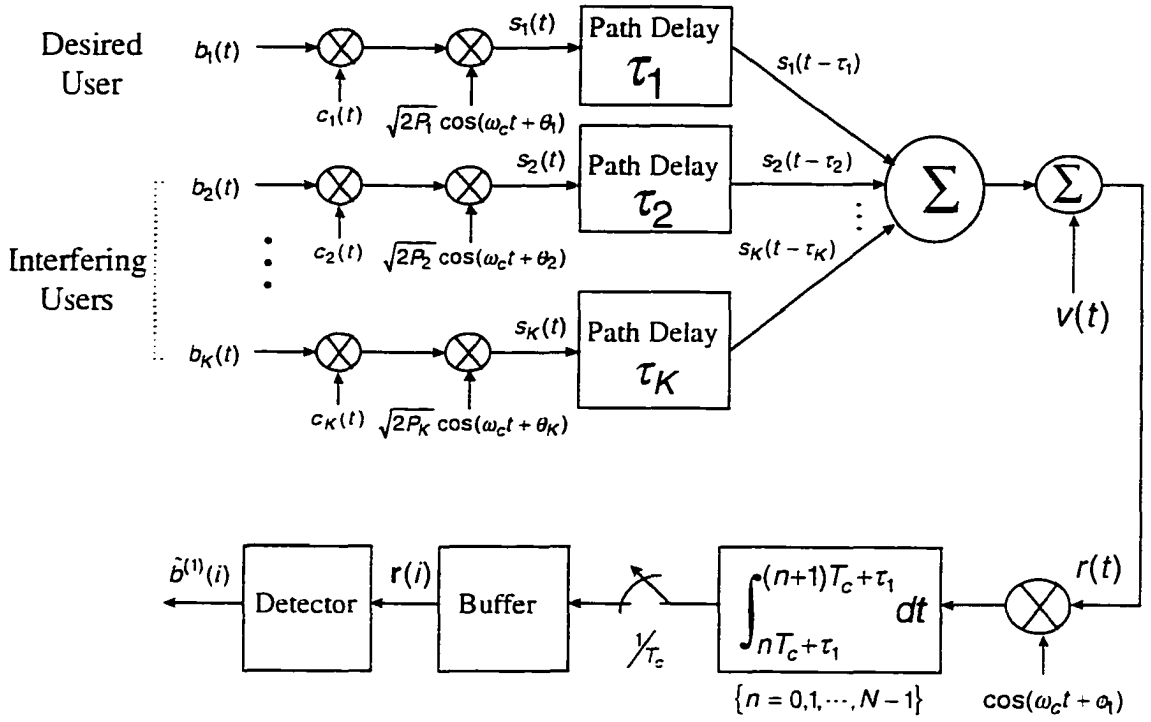

Figure 2.1 Asynchronous BPSK DS/CDMA system.

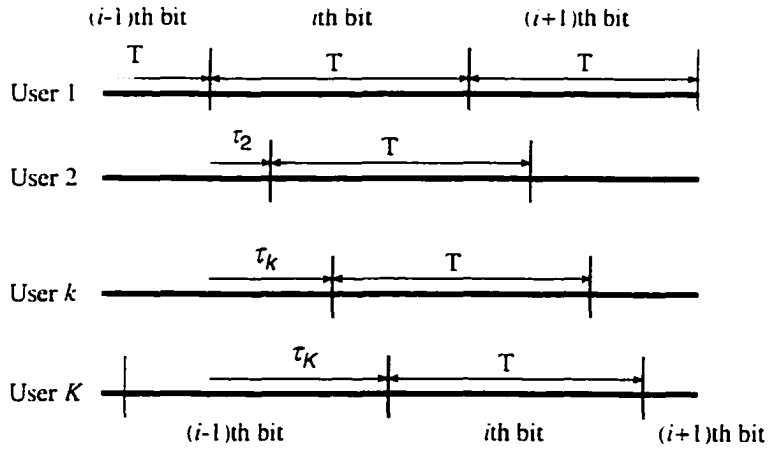

Figure 2.2 Relative time delays of asynchronous DS/CDMA systems.

and

$$\begin{aligned}\hat{c}_i^{(k)}(n) &\triangleq \hat{c}_i^{(k)}(n; m_k, \delta_k) \\ &= c_{n-m_k-1}^{(k)} \cdot \delta_k \cdot \Psi_{N-1\geq n\geq m_k+1} + c_{n-m_k}^{(k)} \cdot (T_c - \delta_k) \cdot \Psi_{N-1\geq n\geq m_k}. \end{aligned} \quad (2.9)$$

Here $\Psi_{S(n)}$ is the characteristic function of the set $S(n)$, i.e.,

$$\Psi_{S(n)} = \begin{cases} \Psi_{S(n)} = 1 \text{ if } n \in S \\ \Psi_{S(n)} = 0 \text{ otherwise.} \end{cases} \quad (2.10)$$

Let

$$\begin{aligned}\hat{\mathbf{c}}_{i-1}^{(k)} &\triangleq \hat{\mathbf{c}}_{i-1}^{(k)}(m_k, \delta_k) \\ &= \left[\hat{c}_{i-1}^{(k)}(0; m_k, \delta_k), \hat{c}_{i-1}^{(k)}(1; m_k, \delta_k), \cdots, \hat{c}_{i-1}^{(k)}(N-1; m_k, \delta_k)\right]^T \in \Re^N. \quad (2.11) \\ \hat{\mathbf{c}}_i^{(k)} &\triangleq \hat{\mathbf{c}}_i^{(k)}(m_k, \delta_k) \\ &= \left[\hat{c}_i^{(k)}(0; m_k, \delta_k), \hat{c}_i^{(k)}(1; m_k, \delta_k), \cdots, \hat{c}^{(k)}(i)(N-1; m_k, \delta_k)\right]^T \in \Re^N. \quad (2.12) \\ \mathbf{c}^{(1)} &\triangleq \left[c_0^{(1)}, c_1^{(1)}, \cdots, c_{N-1}^{(1)}\right]^T \in \Re^N. \quad (2.13) \\ \mathbf{r}(i) &\triangleq [r_0(i), r_1(i), \cdots, r_{N-1}(i)]^T \in \Re^N. \quad (2.14) \end{aligned}$$

and

$$\mathbf{v}(i) \triangleq [v_0(i), v_1(i), \cdots, v_{N-1}(i)]^T \in \Re^N. \quad (2.15)$$

Then, in vector-form, (2.6) can be written as

$$\mathbf{r}(i) = b^{(1)}(i)\mathbf{c}^{(1)} + \sum_{k=2}^{K} \frac{1}{T_c}\sqrt{\frac{P_k}{P_1}}\cos(\varphi_k)\left[b^{(k)}(i-1)\hat{\mathbf{c}}_{i-1}^{(k)} + b^{(k)}(i)\hat{\mathbf{c}}_i^{(k)}\right] + \mathbf{v}(i) \quad (2.16)$$

where $\mathbf{r}(i)$ is the received signal vector at time $t = iT$, $\mathbf{c}^{(1)}$ is the spreading sequence vector of user 1 at time $t = iT$, $\mathbf{v}(i)$ is the additive noise vector at time $t = iT$. It is usually assumed that the binary data bits $b^{(k)}(i)$'s are independent, equiprobable and have zero mean. Note that $\hat{\mathbf{c}}_{i-1}^{(k)}(m_k, \delta_k)$ and $\hat{\mathbf{c}}_i^{(k)}(m_k, \delta_k)$ are linearly independent and are modulated by independent, different bits $b^{(k)}(i-1)$ and $b^{(k)}(i)$, so that the kth

asynchronous user actually contributes two interference vectors during a single symbol interval. We can therefore view the asynchronous system as the equivalent synchronous system with additional K fictitious users, or interferers, as shown in Figure 2.2. The total number of interference vector can range from $K-1$ to $2(K-1)$ according to the relative delays of the actual $K-1$ interfering users (see [34]). Suppose that

$$\mathbf{j}(i) = \sum_{k=2}^{K} \frac{1}{T_c}\sqrt{\frac{P_k}{P_1}}\cos(\phi_k)\left[b^{(k)}(i-1)\hat{\mathbf{c}}_{i-1}^{(k)} + b^{(k)}(i)\hat{\mathbf{c}}_i^{(k)}\right] \tag{2.17}$$

$$= \sum_{l=1}^{L-1}\mathbf{j}_l(i) \tag{2.18}$$

where $L = 2(K-1)+1$ and

$$\mathbf{j}_l(i) \triangleq \begin{cases} \frac{1}{T_c}\sqrt{\frac{P_{l+1}}{P_1}}\cos(\phi_{l+1})b^{(l+1)}(i-1)\hat{\mathbf{c}}_{i-1}^{(l+1)} & \text{for } 1 \le l \le K-1 \\ \frac{1}{T_c}\sqrt{\frac{P_{l-K+2}}{P_1}}\cos(\phi_{l-K+2})b^{(l-K+2)}(i)\hat{\mathbf{c}}_i^{(l-K+2)} & \text{for } K \le l \le 2(K-1) = L-1. \end{cases} \tag{2.19}$$

Note that $\mathbf{j}_l(i)$ is a function of all random parameters such as powers, phase angles, delays, symbols, and associated spreading codes (i.e., other users' spreading codes and their path delays). It is clear that $\mathbf{j}_l(i)$ are generated by $L-1$ interference symbols, $\mathbf{b}_J(i) = \left(b_J^{(1)}, b_J^{(2)}, \cdots, b_J^{(L-1)}\right)$ where

$$b_J^{(l)} = \begin{cases} b^{(l+1)}(i-1) & \text{for } 1 \le l \le K-1 \\ b^{(l-K+2)}(i) & \text{for } K \le l \le 2(K-1) = L-1. \end{cases} \tag{2.20}$$

Then the received signal vector $\mathbf{r}(i)$ at time $t = iT$ is given by

$$\mathbf{r}(i) = b^{(1)}(i)\mathbf{c}^{(1)} + \mathbf{j}(i) + \mathbf{v}(i), \quad -\infty < i < \infty \tag{2.21}$$

where $\mathbf{j}(i) \triangleq [j_0(i), \cdots, j_{N-1}(i)]^T \in \Re^N$. We will use (2.21) as the discrete-time received signal vector at time $t = iT$ throughout this dissertation.

For mathematical tractability, throughout this dissertation, the noise samples given in (2.7) are assumed to be statistically independent as in [58] and [49]. This assumption is

valid when the noise process $v(t)$ is white and Gaussian. When the noise process is white but not Gaussian, the noise samples are uncorrelated but not necessarily independent at the appropriate sampling rate after the low-pass filtering of integrator shown in (2.7) [57], [58], [49].

2.2 Simulation Environments

Next, we present simulation environments and some simulation results such as MAI and additive noise samples generated by our system model. Relevant simulation results corresponding to each of the interference schemes will be presented at the end of the following chapters. We consider an asynchronous BPSK DS/CDMA system with $K = 5$ users, unless stated otherwise. We use an m-sequence of length $N = 31$ chips as the PN-spreading sequence. The additive $S\alpha S$ noise process is assumed to have a location parameter, μ, of zero. We consider the cases of the characteristic exponents $\alpha = 1.1$, 1.5, and 1.9. The reader is referred to [73] for simulation of stable random variables. The detector of the desired user is assumed to have perfect synchronization for timing, carrier phase, and carrier frequency. The relative time delays and carrier phases of the interfering users are assumed to be uniformly distributed. The power ratio of the interfering users to the desired user (PRID) is defined as

$$\text{PRID} = \frac{\sum_{k=2}^{K} P_k}{P_1} \tag{2.22}$$

where P_k is the transmitter power of user k. P_1 is set to 0.3 watt. Among K users, only the transmitter powers of K_s strong interfering users are varied and the transmitter powers of the other $K - K_s - 1$ interfering users are equal to that of the desired user. These simulation environments will be used throughout this dissertation, unless stated otherwise. To obtain reliable bit error rates for all simulation conditions except for very small values of BER (*e.g.* small PRID values of HLMF detectors), we choose each sample

size (or number of transmitted bits) of Monte Carlo simulation so that each normalized accuracy of about 10 % may be assured. The normalized error (NE) [74] is given by

$$\mathrm{NE} = \frac{100\%}{\sqrt{N_{sap} P_e}} \tag{2.23}$$

where P_e is the estimate bit error rate P_e and N_{sap} is the sample size of Monte Carlo simulation.

Figure 2.3 shows the amplitudes of the MAI ($K = 5$ and $K_s = 2$) samples after the front-end chip-matched filtering for different values of PRID. Figure 2.3 (a) represents the amplitude of the MAI with PRID = 6.021 dB, i.e., for equal powers of the interfering users. It is clear that the amplitudes of the MAI becomes larger as the PRID increases. Figure 2.4 and Figure 2.5 show the amplitudes of the additive $S\alpha S$ samples after the front-end chip-matched filtering for different values of characteristic exponent α and dispersion γ. These plots denote that the additive noise become more impulsive as α gets smaller.

2.3 Conventional Matched Filter Detector and MAI Effect

Figure 2.6 shows a generalized correlation (GC) detector [75]. The test statistic is written as

$$Z(i)_{GC} = \sum_{n=0}^{N-1} g(r_n(i)) c_n^{(1)} \tag{2.24}$$

where $g : \Re \rightarrow \Re$ is a memoryless nonlinearity. For example, $g(r_n(i)) = r_n(i)$ corresponds to a linear correlation (LC) or matched filter (MF) detector whose test statistic reduces to

$$Z(i)_{LC} = \sum_{n=0}^{N-1} r_n(i) c_n^{(1)} = \left\langle \mathbf{r}(i), \mathbf{c}^{(1)} \right\rangle = \mathbf{r}(i)^T \mathbf{c}^{(1)} \tag{2.25}$$

where $\left\langle \mathbf{r}(i), \mathbf{c}^{(1)} \right\rangle$ represents an inner product. For single-user AWGN channels, the MF detector is optimum and offers a sufficient statistic, while the MF detector is

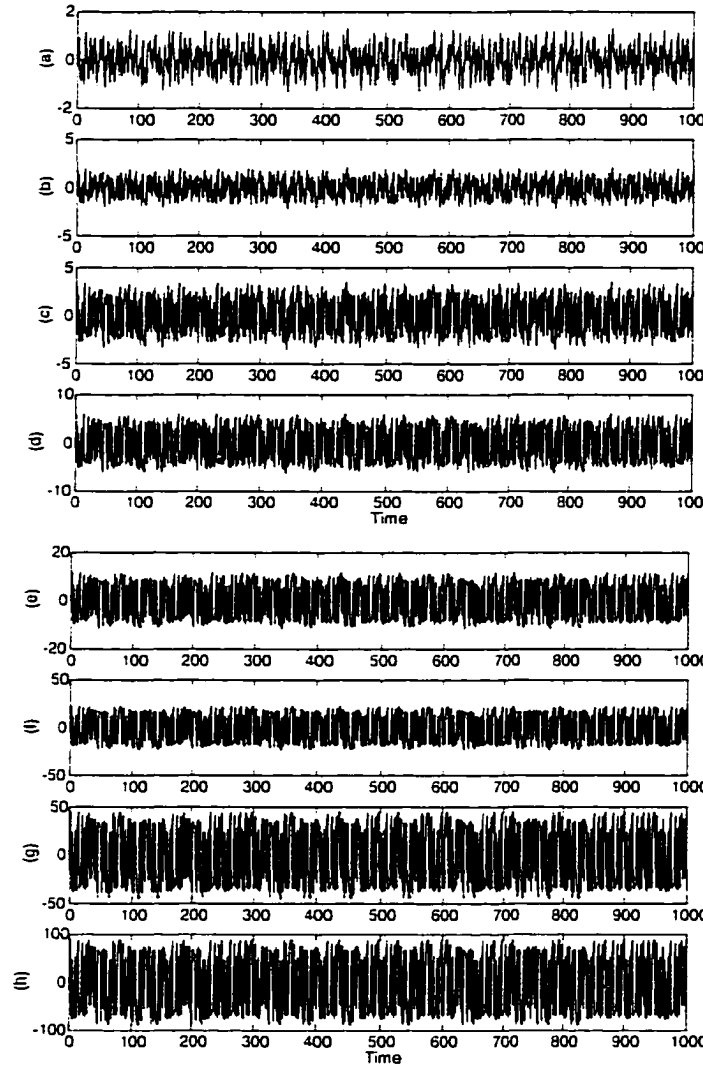

Figure 2.3 Amplitude of the MAI samples after the front-end chip-matched filtering with $K = 5$ and $K_s = 2$: (a) PRID = 6.021 dB. (b) PRID = 12.02 dB. (c) PRID = 18.02 dB. (d) PRID = 24.02 dB. (e) PRID = 30.02 dB. (f) PRID = 36.02 dB. (g) PRID = 42.02 dB. and (h) PRID = 48.02 dB.

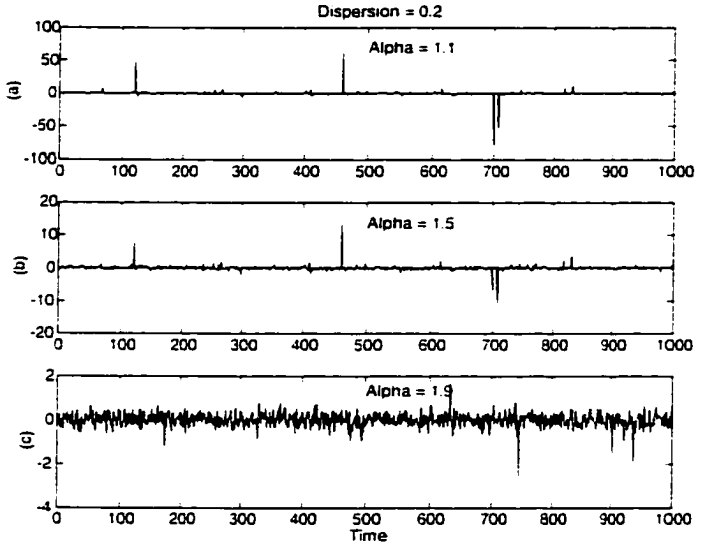

Figure 2.4 Amplitude of the $S\alpha S$ impulsive noise samples after the front-end chip-matched filtering with $\gamma = 0.2$: (a) $\alpha = 1.1$, (b) $\alpha = 1.5$, and (c) $\alpha = 1.9$.

suboptimal for multiple-access channels regardless of the additive noise density [58]. $g(r_n(i)) = sign(r_n(i))$ corresponds to a hard-limiting correlation(or, hard-limiting MF, sign correlation, sign) detector. It is a locally optimum detector for a single-user Laplacian noise channel [75].

Next, we describe the effect of MAI on the test statistic of the MF detector. Substituting (2.21) into (2.25) yields

$$\begin{aligned} Z(i)_{LC} &= \left\langle b^{(1)}(i)\mathbf{c}^{(1)} + \mathbf{j}(i) + \mathbf{v}(i), \mathbf{c}^{(1)} \right\rangle \\ &= \left\langle b^{(1)}(i)\mathbf{c}^{(1)}, \mathbf{c}^{(1)} \right\rangle + \left\langle \mathbf{j}(i), \mathbf{c}^{(1)} \right\rangle + \left\langle \mathbf{v}(i), \mathbf{c}^{(1)} \right\rangle \\ &= b^{(1)}(i) \left\langle \mathbf{c}^{(1)}, \mathbf{c}^{(1)} \right\rangle + \left\langle \mathbf{j}(i), \mathbf{c}^{(1)} \right\rangle + \left\langle \mathbf{v}(i), \mathbf{c}^{(1)} \right\rangle \\ &= N \cdot b^{(1)} + \left\langle \mathbf{j}(i), \mathbf{c}^{(1)} \right\rangle + \left\langle \mathbf{v}(i), \mathbf{c}^{(1)} \right\rangle . \end{aligned} \tag{2.26}$$

Again, substituting (2.17) into (2.26), we obtain

$$\begin{aligned} Z(i)_{LC} &= N \cdot b^{(1)} + \sum_{k=2}^{K} \frac{1}{T_c} \sqrt{\frac{P_k}{P_1}} \cos(\varphi_k) \left[b^{(k)}(i-1) \left\langle \hat{\mathbf{c}}_{i-1}^{(k)}, \mathbf{c}^{(1)} \right\rangle + b^{(k)}(i) \left\langle \hat{\mathbf{c}}_{i}^{(k)}, \mathbf{c}^{(1)} \right\rangle \right] \\ &\quad + \left\langle \mathbf{v}(i), \mathbf{c}^{(1)} \right\rangle . \end{aligned} \tag{2.27}$$

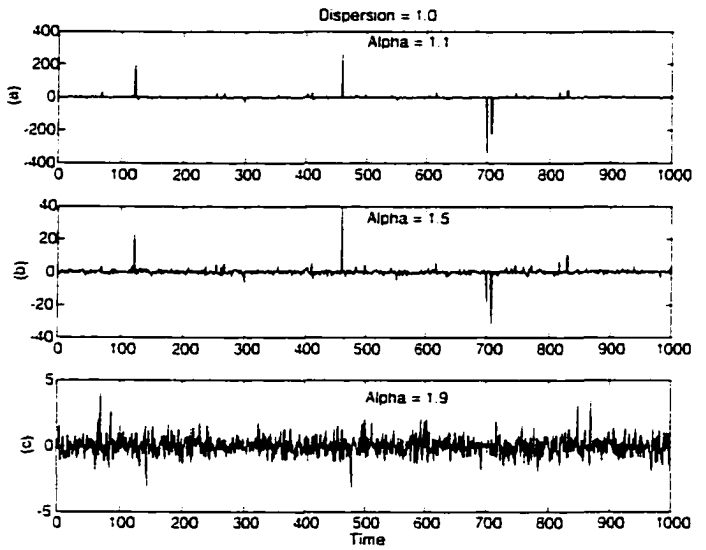

Figure 2.5 Amplitude of the $S\alpha S$ impulsive noise samples after the front-end chip-matched filtering with $\gamma = 1$: (a) $\alpha = 1.1$, (b) $\alpha = 1.5$, and (c) $\alpha = 1.9$.

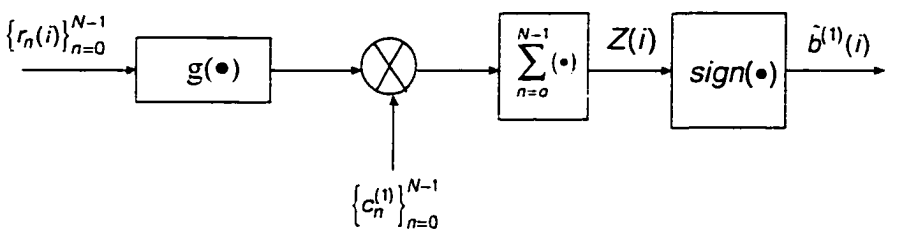

Figure 2.6 Generalized correlator (GC) detector.

The first term of the right-hand side in (2.27) denotes the desired signal. The second term indicates the MAI due to the interfering signals of other users. The last term denotes the inner product of the additive noise and the spreading code vector of the desired user. It is evident that the MAI mainly depends on $\frac{P_k}{P_1}$, K, and the cross-correlation between $\tilde{\mathbf{c}}_{i-1}^{(k)}/\tilde{\mathbf{c}}_i^{(k)}$ and $\mathbf{c}^{(1)}$. The most dominant factor is $\frac{P_k}{P_1}$ which can cause the near-far problem. Hence the MAI is a limiting factor for the conventional MF detector. Assuming a synchronous system and $\phi_k = 0$ for simplicity, (2.27) reduces to

$$Z(i)_{LC} = N \cdot b^{(1)} + \sum_{k=2}^{K} \frac{1}{T_c} \sqrt{\frac{P_k}{P_1}} \left[b^{(k)}(i) \left\langle \mathbf{c}^{(k)}, \mathbf{c}^{(1)} \right\rangle \right] + \left\langle \mathbf{v}(i), \mathbf{c}^{(1)} \right\rangle \qquad (2.28)$$

where the cross-correlation for the spreading codes is given by

$$\rho_{kl} = \left\langle \mathbf{c}^{(k)}.\mathbf{c}^{(l)} \right\rangle = \begin{cases} N. & k = l \\ 0 \leq \left\langle \mathbf{c}^{(k)}.\mathbf{c}^{(l)} \right\rangle < 1. & k \neq l. \end{cases} \tag{2.29}$$

2.4 Theory of $S\alpha S$ Processes

2.4.1 Definitions and Properties

The theory of univariate stable distributions was essentially developed in the 1920s and 1930s by Paul Lévy and Aleksander Yakovlevich Khinchine [63]. Classics of the theory include [76]. [77] [78]. Two equivalent definitions of a stable distribution are given as follows:

Definition 1 *A random variable X is said to have a stable distribution if for any positive numbers a_1 and a_2, there is a positive number a and a real number b such that*

$$a_1 X_1 + a_2 X_2 \stackrel{d}{=} aX + b \tag{2.30}$$

where X_1 and X_2 are independent copies of X and the notation $\stackrel{d}{=}$ indicates that the random variables $a_1 X_1 + a_2 X_2$ and $aX + b$ have the same distribution. That is, these random variables are said to be equal in distribution.

A random variable X is called *strictly* stable if (2.30) holds with $b = 0$. A stable random variable X is called *symmetric* stable if its distribution is symmetric, that is, if X and $-X$ have the same distribution. A symmetric stable random variables is strictly stable [63].

Definition 2 *A random variable X is said to have a stable distribution if there are real parameters $0 < \alpha \leq 2$, $-1 \leq \beta \leq 1$, $\gamma \geq 0$, and $-\infty < \mu < \infty$ such that its*

characteristic function has the following form:

$$\varphi_X(\omega) = E\left[\exp j\omega X\right] = \exp\left\{j\mu\omega - \gamma|\omega|^\alpha\left[1 + j\beta\,\mathrm{sign}(\omega)\,\kappa(\omega,\alpha)\right]\right\} \tag{2.31}$$

where

$$\kappa(\omega,\alpha) = \begin{cases} \tan\frac{\alpha\pi}{2}, & \text{if } \alpha \neq 1 \\ \frac{2}{\pi}\log|\omega|, & \text{if } \alpha = 1 \end{cases} \tag{2.32}$$

$$\mathrm{sign}(\omega) = \begin{cases} 1. & \text{if } \omega > 0 \\ 0. & \text{if } \omega = 0 \\ -1. & \text{if } \omega < 0. \end{cases} \tag{2.33}$$

The parameters $\alpha, \beta, \gamma, \mu$ are called the characteristic exponent (or stability index), symmetry (or skewness), dispersion (or scale), and location (or shift) parameters, respectively. The parameters β, γ, μ are unique except that β is irrelevant when $\alpha = 2$. These parameters are characterized as follows:

- α controls the distribution type. It measure the thickness of tails of the distribution. As α decreases, the tails of the distribution get heavier. A stable distribution with parameter α is often called *α-stable*. When $\alpha = 2$ for any β, the distribution reduces to a Gaussian distribution, while when $\alpha = 1$ and $\beta = 0$, the distribution becomes a Cauchy distribution.

- β denotes the departure from a symmetric distribution about μ. An α-stable distribution with $\beta = 0$ is symmetric about μ and called *symmetric α-stable* ($S\alpha S$). The $S\alpha S$ distributions belongs to an important subclass of stable distributions. The Gaussian and Cauchy distributions are both $S\alpha S$.

- γ represents the range of likely values. It is analogous to the variance of the Gaussian distribution ($\alpha = 2$). When $\alpha = 2$, γ equals a half of the variance of the Gaussian distribution.

- μ denotes the shift from zero. For $S\alpha S$ distribution, it is the mean when $1 < \alpha \leq 2$ and the median when $0 < \alpha \leq 1$. A stable distribution is called *standard* if $\mu = 0$ and $\gamma = 1$.

A stable probability density function (pdf) is given by taking the inverse Fourier transform of the characteristic function

$$f_X(x; \alpha, \beta, \gamma, \mu) = \frac{1}{2\pi} \int_{-\infty}^{\infty} \varphi_X(\omega) e^{-j\omega x} d\omega \tag{2.34}$$

In general, there do not exist closed-form expressions for the stable distributions except for the Gaussian ($\alpha = 2$), Pearson ($\alpha = \frac{1}{2}$, $\beta = -1$), and Cauchy ($\alpha = 1$, $\beta = 0$) pdf's. But power series expansions of stable pdf's are available. The Gaussian pdf is given by

$$f_X(x; 2.0, \gamma, \mu) = \frac{1}{\sqrt{4\pi\gamma}} \exp\left[-\frac{(x-\mu)^2}{4\gamma}\right] \tag{2.35}$$

where $\gamma = \frac{1}{2}\mathrm{Var}(X)$. The Cauchy pdf is given by

$$f_X(x; \mu, \gamma, 1) = \frac{1}{\pi} \frac{\gamma}{(x-\mu)^2 + \gamma^2}. \tag{2.36}$$

where μ is the median.

The main difference between the Gaussian and non-Gaussian $S\alpha S$ distributions is their tails. The $S\alpha S$ pdf's have algebraic (i.e., inverse power) tails, while the Gaussian pdf has exponential tails. Thus, the $S\alpha S$ pdf's have heavier tails than the Gaussian pdf ($\alpha = 2$) as shown in Figure 2.7.

We will be concerned about $S\alpha S$ distributions throughout this dissertation. Next, we present some of the useful properties and theorems of $S\alpha S$ distributions. These are largely extracted from [60], [64] and [63].

Theorem 1 (Generalized Central Limit Theorem) *A random variable X is the limit in distribution of normalized sums of the form*

$$S_n = \frac{X_1 + X_2 + \cdots + X_n}{a_n - b_n} \tag{2.37}$$

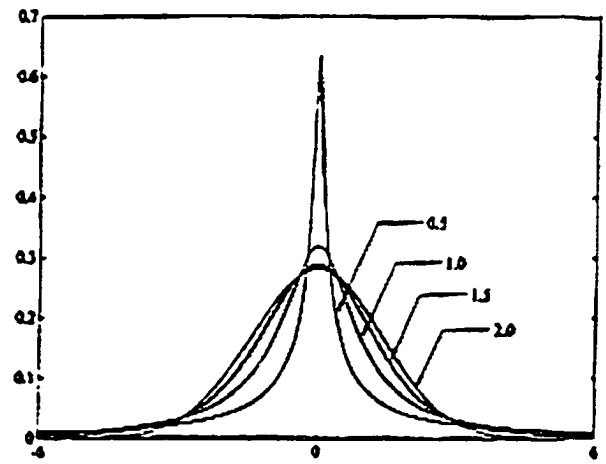

Figure 2.7 Standard $S\alpha S$ probability density functions for different valuse of α [64].

where the random variables $X_1, X_2, \cdots, X_n$ *are i.i.d. and* $n \to \infty$, *if and only if* X *is stable.*

This implies that stable distributions are the only possible limit distributions for sums of i.i.d. random variables. Note that if the $X_i's$ are i.i.d. and have finite variance, then the limit distribution is Gaussian. This is the result of the ordinary Central Limit Theorem.

Theorem 2 *Let* X *be a* α*-stable random variable with* $0 < \alpha < 2$. *Then*

$$E\left[|X|^p\right] < \infty \quad \text{if } 0 \leq p < \alpha. \tag{2.38}$$

$$E\left[|X|^p\right] = \infty \quad \text{if } p \geq \alpha. \tag{2.39}$$

If $\alpha = 2$, *then*

$$E\left[|X|^p\right] < \infty \quad \text{for all } p \geq 0. \tag{2.40}$$

Hence for $0 < \alpha \leq 1$, α-stable distributions have no finite first or higher order moments. This excludes the use of statistical expectations: for $1 < \alpha < 2$, they have

the first order moment and all the *fractional lower order moments* (FLOM's) of order p where $p < \alpha$: for $\alpha = 2$, all order moments exist. In particular, all non-Gaussian stable distributions have infinite variance. The FLOM's can be easily obtained by using the following Proposition 1.

Proposition 1 *Let X be a $S\alpha S$ random variable with zero location parameter μ and dispersion γ. Then*

$$E\left[|X|^p\right] = C(p,\alpha)\gamma^{\frac{p}{\alpha}} \quad \text{for } 0 < p < \alpha \tag{2.41}$$

where

$$C(p,\alpha) = \frac{2^{p+1}\Gamma(\frac{p+1}{2})\Gamma(-p/\alpha)}{\alpha\sqrt{\pi}\Gamma(-p/2)} \tag{2.42}$$

depends only on α and p, not on X. Here Γ is the gamma function defined by

$$\Gamma(x) = \int_0^\infty t^{x-1}e^{-t}dt. \tag{2.43}$$

Since $S\alpha S$ random variables with $\alpha < 2$ have infinite second moment (i.e., variance), the covariance does not apply to $S\alpha S$ random variables. Instead, we use the covariation proposed in [60], [65], [76], [77], [78], and [79].

Definition 3 *Let X_1 and X_2 be jointly $S\alpha S$ random variables with $1 < \alpha \leq 2$. Then the covariation of X_1 on (or with, or and) X_2 is defined by*

$$[X_1, X_2]_\alpha = \int_S s_1 s_2^{<\alpha-1>}\Gamma(ds) \tag{2.44}$$

where S is the unit circle of $\Re^2$ and $\Gamma(\cdot)$ is the spectral measure of the $S\alpha S$ random vector $X = (X_1, X_2)$.

Here $(\cdot)^{<a>}$ is known as signed power which is defined as

$$t^{<a>} \triangleq |t|^a sign(t) \tag{2.45}$$

for any real numbers t and $a \geq 0$. We now list some of the useful properties of the covariation. Suppose throughout that $1 < \alpha \leq 2$.

Definition 4 *Let X and Y be jointly $S\alpha S$ random variables with $1 < \alpha \leq 2$. Then the covariation coefficient of X with Y is defined by*

$$\lambda_{X,Y} = \frac{[X,Y]_\alpha}{[Y,Y]_\alpha}. \tag{2.46}$$

These definitions for the covariation and covariation coefficient are not very convenient in practice since they require the calculation of the spectral measure $\Gamma(\cdot)$. This difficulty can be avoided by using the FLOM's as illustrated in **Lemma 1**.

Lemma 1 *Let X and Y are jointly $S\alpha S$. Suppose that the dispersion of Y is γ_y. Then*

$$[X,Y]_\alpha = \frac{E[XY^{<p-1>}]}{E[|Y|^p]}\gamma_y \quad \text{for all } 1 \leq p < \alpha. \tag{2.47}$$

$$\lambda_{X,Y} = \frac{E[XY^{<p-1>}]}{E[|Y|^p]} \quad \text{for all } 1 \leq p < \alpha. \tag{2.48}$$

Property 1 (Additivity in the first argument) *If X_1, X_2, and Y are jointly $S\alpha S$, then*

$$[X_1 + X_2, Y]_\alpha = [X_1, Y]_\alpha + [X_2, Y]_\alpha. \tag{2.49}$$

Property 2 (Scaling) *Let X and Y be jointly $S\alpha S$. Then*

$$[aX, bY]_\alpha = ab^{<\alpha-1>}[X,Y]_\alpha \tag{2.50}$$

for any real numbers a and b.

Property 3 *If X, Y_1, and Y_2 are jointly $S\alpha S$ and Y_1 and Y_2 are independent, then*

$$[X, Y_1 + Y_2]_\alpha = [X, Y_1]_\alpha + [X, Y_2]_\alpha. \tag{2.51}$$

Corollary 1 *Although the covariation is linear in its first argument, it is in general not linear in its second argument. That is,*

$$[a_1X_1 + a_2X_2, Y]_\alpha = a_1 [X_1, Y]_\alpha + a_2 [X_2, Y]_\alpha$$

and

$$[X, Y_1 + Y_2]_\alpha \neq [X, Y_1]_\alpha + [X, Y_2]_\alpha .$$

Corollary 2 *The covariation is in general not symmetric in its arguments. That is,*

$$[X, Y]_\alpha \neq [Y, X]_\alpha .$$

Property 4 *If X and Y are jointly $S\alpha S$ and independent, then*

$$[X, Y]_\alpha = 0. \tag{2.52}$$

while the converse is not true in general.

Property 5 *If X and Y are jointly $S\alpha S$ with $\alpha = 2$ and zero mean, then*

$$[X, Y]_\alpha = \frac{1}{2} E [XY] = \frac{1}{2} \mathrm{Cov}(XY). \tag{2.53}$$

where $Cov(\cdot)$ is the covariance defined for the Gaussian process.

Proposition 2 *Let U_i's be independent $S\alpha S$ random variables with dispersions γ_i, $i = 1, 2, \cdots, n$. Suppose X and Y are both finite linear combinations of U_i's:*

$$X = \sum_{i=1}^{n} a_i U_i,$$

$$Y = \sum_{i=1}^{n} b_i U_i$$

where a_i's and b_i's are any numbers and all b_i's are not zero. Then X and Y are $S\alpha S$ and

$$
\begin{aligned}
[X.X]_\alpha &= \sum_{i=1}^{n} \gamma_i |a_i|^\alpha . \\
[Y.Y]_\alpha &= \sum_{i=1}^{n} \gamma_i |b_i|^\alpha . \\
[X.Y]_\alpha &= \sum_{i=1}^{n} \gamma_i a_i b_i^{<\alpha-1>}. \qquad (2.54) \\
\lambda_{X,Y} &= \frac{\sum_{i=1}^{n} \gamma_i a_i b_i^{<\alpha-1>}}{\sum_{i=1}^{n} \gamma_i |b_i|^\alpha}. \qquad (2.55)
\end{aligned}
$$

Let L_α be a linear space of jointly $S\alpha S$ random variables. When $1 < \alpha \leq 2$, the covariation induces a norm on L_α.

Definition 5 *The covariation norm of $X \in L_\alpha$ with $1 < \alpha \leq 2$ is*

$$\|X\|_\alpha = ([X.X]_\alpha)^{1/\alpha} \qquad (2.56)$$

Property 6 *If X is $S\alpha S$ with $1 < \alpha \leq 2$, then*

$$\|X\|_\alpha = \gamma_x^{1/\alpha}. \qquad (2.57)$$

where γ_x is the dispersion of X.

2.4.2 Linear Estimation of Stable Processes

Gaussian processes belong to a class of second order processes which have finite second order moments. Stochastic processes with finite pth order moments are called pth order processes. A class of stable processes includes the Gaussian processes or the second order processes as special examples. The linear estimation problem of stochastic processes can be stated as follows: *Let $\{X(t), t \in T_{ob}\}$ be a stochastic process, where T_{ob} is a finite or infinite interval. Given a set of observations of a stochastic process $\{X(t),$*

$t \in T_{ob}\}$. *find the best estimate of an unknown random variable* Y *from the linear space spanned by* $\{X(t).\ t \in T_{ob}\}$ [60]. This estimation problem is called either smoothing, filtering, or prediction according to the relationship between observation ending time and estimation time.

Linear theory of second-order processes (Gaussian processes in particular) has been fully developed because the linear space $L\{X(t).\ t \in T_{ob}\}$ is a Hilbert space. Under the minimum mean squared error (MMSE) criterion, the best linear estimate of the unknown Y can be obtained by an orthogonal projection of Y onto $L\{X(t).\ t \in T_{ob}\}$ [60]. Minimum error dispersion linear filtering for scalar symmetric stable processes was early presented in [80]. The development of the linear theory of stable processes has been limited due to the fact that the linear space of a stable process is a Banach space when $1 \leq \alpha < 2$ and only a metric space when $0 < \alpha < 1$ [65], [60]. Nevertheless much attention has recently been paid to the linear theory of stable processes and their applications.

Linear Estimation using the MD Criterion *Let* $\{Y, X(t), t \in T_{ob}\}$ *be stable processes with* $1 < \alpha < 2$ *and* $L(X(t), t \in T_{ob})$ *be the linear space of the observations of the stable process* $\{X(t), t \in T_{ob}\}$, *where* T_{ob} *is an finite interval. Then, given the observations* $\{X(t), t \in T_{ob}\}$, *the linear estimate* $\hat{Y}$ *of* Y *is defined as the best approximation to* Y *in the linear space* $L(X(t), t \in T_{ob})$, *i.e., the random variable* $\hat{Y}$ *in* $L(X(t), t \in T_{ob})$ *such that*

$$\left\| Y - \hat{Y} \right\|_{\alpha} = \inf_{Z \in L(X(t), t \in T_{ob})} \|Y - Z\|_{\alpha} \tag{2.58}$$

or equivalently

$$E\left[\left|Y - \hat{Y}\right|^{p}\right] = \inf_{Z \in L(X(t), t \in T_{ob})} E\left[|Y - Z|^{p}\right] \tag{2.59}$$

for $0 < p < \alpha$ [65], [60].

(2.58) means that the best estimate $\hat{Y}$ of the stable random variables Y in the linear space $L(X(t).t \in T_{ob})$ is the one that minimizes the dispersion of the estimation error. Note that the dispersion (or covariation) of a stable random variable with $1 < \alpha < 2$ plays an analogous role of the variance (or covariance) in the Gaussian case ($\alpha = 2$). Since $L(X(t).t \in T_{ob})$ is a Banach space, $\hat{Y}$ always exists and is unique for $1 < \alpha < 2$ [81]. It is obtained by a metric projection of Y onto the convex Banach space $L(X(t).t \in T_{ob})$. For $1 < \alpha < 2$, $\hat{Y}$ is also uniquely determined [65] by

$$\left[Z.Y - \hat{Y}\right]_{\alpha} = 0 \quad \text{for all } Z \in L(X(t).t \in T_{ob}) \tag{2.60}$$

or

$$\left[X(t).Y - \hat{Y}\right]_{\alpha} = 0 \quad \text{for all } t \in T_{ob}. \tag{2.61}$$

This is analogous to the *orthogonality principle* for the linear estimation problem of second-order processes. When $\alpha = 2$, (2.61) is linear and thus a closed-form solution exists for $\hat{Y}$. For $\alpha < 2$, it is highly nonlinear and hard to solve for the estimate $\hat{Y}$ (see [60]).

2.5 Additive Non-Gaussian Impulsive Channel Noise Models

The additive white Gaussian noise model has been widely used in communication theory due to its mathematical tractability for analysis and optimum solutions and design simplicity. The Gaussian noise assumption is justified by Central Limit Theorem in many situations. However, Rappaport and Kurz [82] said:

> It has been common in technical literature treating signal detection in non-Gaussian noise to assume that if the receiver integrates a sufficiently large number of independent noise bursts, the resulting distribution of the test statistic would be Gaussian. However, if one assumes that the noise amplitude is a random variable

having large variance. the fundamental limit theorem can not be invoked unless there is some noise suppression before integration.

These comments represent that the Gaussian noise assumption may not be adequate and justified any more in some situations. These situations are often caused by additive non-Gaussian noise sources. The non-Gaussian noise is characterized as being of *impulsive* nature because it occurs with noticeable probabilities of large amplitudes for short duration. The empirical data indicate that the pdf's of the associated noise processes have a similarity to the Gaussian pdf. being bell-shaped. smooth. and symmetric. as well as significantly heavier tails [50]. [83].

The non-Gaussian impulsive noise comes from either natural or man-made noise sources. The natural noise sources include atmospheric noise in radio links due to lightning discharges. ambient acoustic noise in underwater sonar and submarine communications due to ice cracking in the arctic regions [84]. and noisy aquatic animals such as snapping shrimps [85]. The man-made noise sources include automobile ignitions. neon lights. switching transients. accidental hits in telephone lines. heavy electrically-powered machinery. and other electronic devices [45]. [46]. [47]. [48]. [49]. [83]. [50].

Many models of non-Gaussian noise have been developed (see [50]. [49]. [48]. [54]. [45]. and references therein for details). These models can be divided into two classes of models: empirical models and physical models. Empirical models are developed to fit collected data. often with little attention to the underlying physical mechanisms. while physical models are developed to model these mechanisms directly [48].

Middleton class A. B. and C models [45]. [52]. [53]. [54] are widely used physical models. Class A noise is narrow-band in which spectra of noise sources are comparable to or narrower than the passband of the receiver. Class B noise is broad-band in which spectra of noise sources are broader than the passband of the receiver. Class C noise is the sum of Class A and Class B types.

An ε-mixture (or ε-contaminated) model [48] is one of commonly used empirical models. The first-order pdf of this noise model has the form

$$f_\varepsilon(x) = (1-\epsilon)\cdot f_{bg}(x) + \epsilon \cdot f_{im}(x) \tag{2.62}$$

where $\epsilon\,[0.1]$ and $f_{bg}(\cdot)$ and $f_{im}(\cdot)$ are the pdf's corresponding to background noise and impulsive (or contaminating) noise, respectively. The pdf $f_{bg}(\cdot)$ is usually taken to be Gaussian. The pdf $f_{im}(\cdot)$ is chosen as one of various heavy-tailed pdf's such as the Laplacian or double-exponential and the Gaussian with large variance. In case of Gaussian pdf $f_{im}(\cdot)$, the ratio of the variance of impulsive component to the variance of the background one, defined as $\gamma^2 = \sigma_{im}^2/\sigma_{bg}^2$, is usually taken to be between 1 and 100 [48], [49], [58]. This model is analytically tractable. This model frequently represents a noise environment that is nominally Gaussian with an additive impulsive noise component.

The $S\alpha S$ probability density functions can accurately model large classes of impulsive noise [59], [60]. For example, the Cauchy pdf, as a family of $S\alpha S$ pdf's, was already used as a model for severe impulsive noise [82]. A reader is referred to Section 2.4 for detailed description of $S\alpha S$ pdf's. In this dissertation, we will model additive non-Gaussian noise as a $S\alpha S$ process.

2.6 Optimum Detection using Likelihood-Ratio Test

Let $\mathbf{r}(i)$ in (2.21) be an observation random vector. Suppose that $p_0\,(\mathbf{r}(i))$ and $p_1\,(\mathbf{r}(i))$ are the probability density functions for the observation vector $\mathbf{r}(i)$ under hypothesis H_0 and H_1, respectively. We can write binary hypothesis testing problem [86] as

$$\begin{aligned} H_0 &: \quad \mathbf{r}(i) = \mathbf{s}_0(i) + \breve{\mathbf{v}}(i) \backsim p_0\,(\mathbf{r}(i)) \\ H_1 &: \quad \mathbf{r}(i) = \mathbf{s}_1(i) + \breve{\mathbf{v}}(i) \backsim p_1\,(\mathbf{r}(i)) \end{aligned} \tag{2.63}$$

where

$$\mathbf{s}(i) \triangleq b^{(1)}(i)\mathbf{c}^{(1)} = \begin{cases} \mathbf{s}_0(i) = +\mathbf{c}^{(1)} & \text{for } b^{(1)}(i) = +1 \\ \mathbf{s}_1(i) = -\mathbf{c}^{(1)} & \text{for } b^{(1)}(i) = -1. \end{cases} \tag{2.64}$$

are completely known (i.e., deterministic) vectors from two possible signal vectors and

$$\breve{\mathbf{v}}(i) \triangleq \mathbf{j}(i) + \mathbf{v}(i) \tag{2.65}$$

are a combined noise vector of additive non-Gaussian impulsive noise and MAI. Here the associated vectors are denoted as follows:

$$\breve{\mathbf{v}}(i) \triangleq [\breve{v}_0(i), \breve{v}_1(i), \cdots, \breve{v}_{N-1}(i)]^T. \tag{2.66}$$

$$\mathbf{s}_0(i) \triangleq [s_{0,0}(i), s_{0,1}(i), \cdots, s_{0,N-1}(i)]^T. \tag{2.67}$$

$$\mathbf{s}_1(i) \triangleq [s_{1,0}(i), s_{1,1}(i), \cdots, s_{1,N-1}(i)]^T. \tag{2.68}$$

The likelihood ratio can be written as

$$\begin{aligned} L(\mathbf{r}(i)) &= \frac{p_1(\mathbf{r}(i))}{p_0(\mathbf{r}(i))} \\ &= \frac{p_{\breve{\mathbf{v}}}(\mathbf{r}(i) - \mathbf{s}_1(i))}{p_{\breve{\mathbf{v}}}(\mathbf{r}(i) - \mathbf{s}_0(i))} \\ &= \frac{p_{\breve{\mathbf{v}}}(r_0(i) - s_{1,0}(i), r_1(i) - s_{1,1}(i), \cdots, r_{N-1}(i) - s_{1,N-1}(i))}{p_{\breve{\mathbf{v}}}(r_0(i) - s_{0,0}(i), r_1(i) - s_{0,1}(i), \cdots, r_{N-1}(i) - s_{0,N-1}(i))}. \end{aligned} \tag{2.69}$$

(2.69) is used to implement the optimum detector based on *Bayes rule* which is known as *likelihood-ratio test*:

$$\delta_B(\mathbf{r}(i)) = \begin{cases} 1 & \text{if } L(\mathbf{r}(i)) \geq \tau \\ 0 & \text{if } L(\mathbf{r}(i)) < \tau. \end{cases} \tag{2.70}$$

where τ is a threshold and the value of $\delta_B(\mathbf{r}(i))$ denote the index of the chosen hypothesis. Bayes decision rule with uniform cost assignment becomes a *minimum probability-of-error decision rule*. This rule is sometimes known as the *maximum a posteriori probability* (MAP) decision rule for the binary hypothesis test because the minimum

probability-of-error decision rule chooses the hypothesis that has the maximum a posteriori probability [86]. It is very hard to find (2.69) in our scenario and in practice because the distributions of the combined noise vector $\check{\mathbf{v}}(i)$ are unknown. If we make an assumption that the elements of $\check{\mathbf{v}}(i)$ are statistically independent, (2.69) reduces to a simpler form

$$\begin{aligned} L(\mathbf{r}(i)) &= \frac{p_{\check{\mathbf{v}}}\left(r_0(i)-s_{1,0}(i), r_1(i)-s_{1,1}(i), \cdots, r_{N-1}(i)-s_{1,N-1}(i)\right)}{p_{\check{\mathbf{v}}}\left(r_0(i)-s_{0,0}(i), r_1(i)-s_{0,1}(i), \cdots, r_{N-1}(i)-s_{0,N-1}(i)\right)} \\ &= \frac{\prod_{n=0}^{N-1} p_{\check{v}_n}\left(r_n(i)-s_{1,n}(i)\right)}{\prod_{n=0}^{N-1} p_{\check{v}_n}\left(r_n(i)-s_{0,n}(i)\right)} \\ &= \prod_{n=0}^{N-1} \frac{p_{\check{v}_n}\left(r_n(i)-s_{1,n}(i)\right)}{p_{\check{v}_n}\left(r_n(i)-s_{0,n}(i)\right)}. \end{aligned} \tag{2.71}$$

where $p_{\check{v}_n}(\cdot)$ is a marginal probability density function of $\check{v}_n(i)$. Since $log(\cdot)$ is monotonically increased, (2.70) is equivalent to

$$\check{\delta}_B(\mathbf{r}(i)) = \begin{cases} 1 & \text{if } \log L(\mathbf{r}(i)) \geq \log \tau \\ 0 & \text{if } \log L(\mathbf{r}(i)) < \log \tau. \end{cases} \tag{2.72}$$

This is often called *log-likelihood-ratio test*. Note that the above assumption of independence is not true in practice.

On the other hand, in the same way as in [26], [27], and [28], this likelihood test can be written as

$$\begin{aligned} L(\mathbf{r}(i)) &= \frac{E\left[p_1\left(\mathbf{r}(i)\right)\right]}{E\left[p_0\left(\mathbf{r}(i)\right)\right]} \\ &= \frac{E\left[p_{\mathbf{v}}\left(\mathbf{r}(i)-\mathbf{s}_1(i)-\mathbf{j}(i)\right)\right]}{E\left[p_{\mathbf{v}}\left(\mathbf{r}(i)-\mathbf{s}_0(i)-\mathbf{j}(i)\right)\right]} \end{aligned} \tag{2.73}$$

where the expectation is taken with respect to all random parameters of the interference vector $\mathbf{j}(i)$ such as powers, phase angles, delays, symbols, and associated spreading codes. (2.73) is also formidable to evaluate due to the computational complexity [27], [26]. Multilayer peceptrons [27] were presented to approximate the likelihood-ratio test based on (2.73) for asynchronous and synchronous Gaussian multiple-access channels.

For synchronous Gaussian multiple-access channels, the likelihood-ratio test using (2.73) was implemented by radial basis function (RBF) [28].

CHAPTER 3 LINEAR MINIMUM DISPERSION INTERFERENCE SUPPRESSION

3.1 Introduction

This work was originally presented in [87] and motivated by the work presented in [49], [60], [34], [38], [50], [67], [68], and [70]. This chapter covers the problem of linear MD detection for MAI suppression in non-Gaussian impulsive noise channels. Additive impulsive noise is modeled as a $S\alpha S$ process. The linear MD detector is adaptively implemented by the least mean p-norm (LMP) algorithm proposed in [60] and [88]. The performance of the linear MD detector is analyzed in the context of a $S\alpha S$ process. We compare the bit error rates of the proposed detector with those of the conventional MF [49], hard-limiting MF [49], and MMSE [30], [34], [38] detectors by extensive Monte Carlo computer simulation.

This chapter is organized as follows. In Section 3.2, we describe the problem formulation of the linear MD detector in the context of a $S\alpha S$ process. In Section 3.3, we analyze the performance of the linear MD detector in the context of a $S\alpha S$ process. The adaptive implementation is presented in Section 3.4. In Section 3.5, we present and discuss simulation results.

3.2 Problem Formulation in the Context of a $S\alpha S$ Process

The MD detector minimizes the dispersion of the estimation error. This is similar to the MMSE criterion for Gaussian channels, since the dispersion is analogous to the variance. The detection scheme presented here is based on symbol-by-symbol detection. It estimates the transmitted symbol $b^{(1)}(i)$ from the received signal vector $\mathbf{r}(i)$ at time $t = iT$. The received signal vector $\mathbf{r}(i)$ is passed to the linear MD detector which consists of an finite-impulse-response (FIR) filter $\mathbf{w}^T(i)$ as shown in Figure 3.1. The output of the detector is sampled at the bit rate $1/T$. The test statistic for the ith desired data bit is written as $Z(i) = \mathbf{w}^T(i)\mathbf{r}(i)$, $-\infty < i < \infty$, where $\mathbf{w}(i) \triangleq [w_0(i), w_1(i), \cdots, w_{N-1}(i)]^T$ is the vector of tap weights of the FIR filter. The decision rule is given by $\hat{b}^{(1)}(i) = sign(Z(i))$. Note that if $\mathbf{w}(i) = \mathbf{c}^{(1)}$ for all i, the detector reduces to the conventional MF detector.

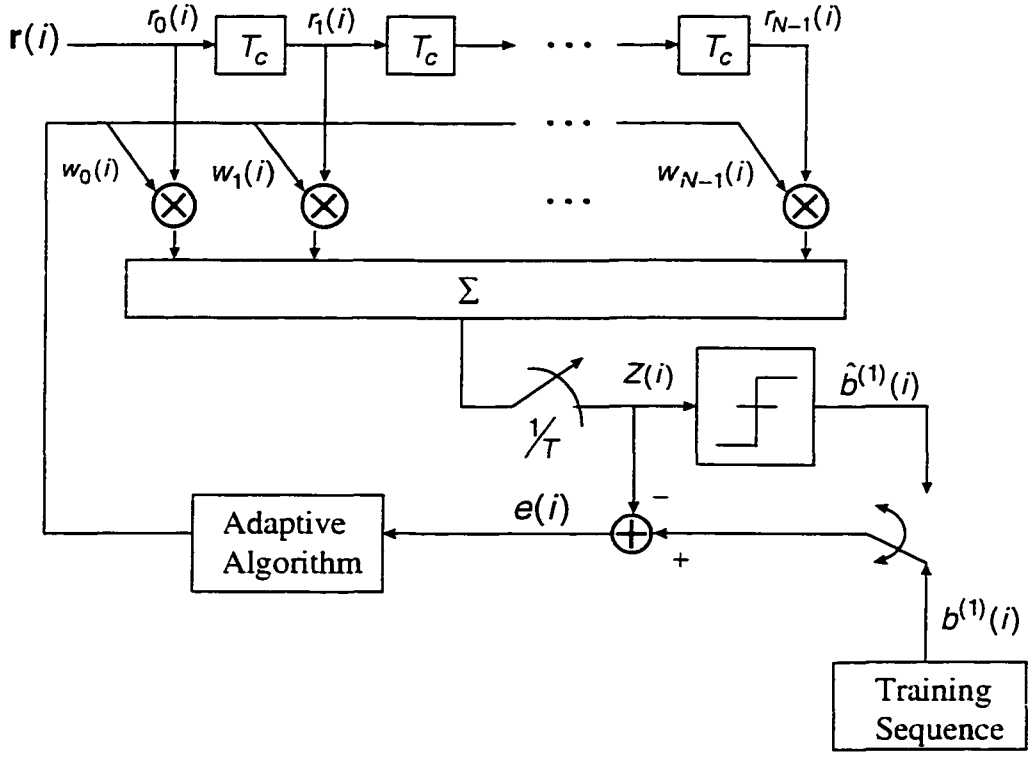

Figure 3.1 Adaptive MD detector for an asynchronous BPSK DS/CDMA system.

Define the estimation error $e(i)$ at time $t = iT$ as $e(i) \triangleq b^{(1)}(i) - Z(i)$, where $b^{(1)}(i)$ is the binary data bit of user 1 at time $t = iT$. The problem can be viewed as finding the FIR filter $\mathbf{w}(i)^T$ such that the dispersion of the estimation error $e(i)$ is minimized. Let $\tilde{Z}(i)$ and $\tilde{e}(i)$ be the test statistic and the estimation error corresponding to the MD, respectively. Then $\tilde{e}(i) = b^{(1)}(i) - \tilde{Z}(i) = b^{(1)}(i) - \bar{\mathbf{w}}(i)^T\mathbf{r}(i)$, where $\bar{\mathbf{w}}(i)$ is the MD solution for $\mathbf{w}(i)$. Using the results of the linear estimation problem for a $S\alpha S$ process given in [60] and [65], $\tilde{Z}(i) = \bar{\mathbf{w}}(i)^T\mathbf{r}(i)$ must satisfy:

$$\left[r_n(i), b^{(1)}(i) - \tilde{Z}(i)\right]_\alpha = 0, \text{ for all } n \in [0, N-1], \ 1 < \alpha \leq 2 \tag{3.1}$$

which is analogous to the *orthogonality principle* used in the linear estimation problem of second-order processes. Here $[\cdot,\cdot]_\alpha$ is the covariation defined in Section 2.4.1. When $\alpha = 2$, this converges to the *orthogonality principle* used in the linear estimation problem of second-order processes:

$$E[r_n(i)(b^{(1)}(i) - \tilde{Z}(i))] = E[r_n(i)e(i)] = 0. \tag{3.2}$$

3.3 Performance Analysis in the Context of a $S\alpha S$ Process

In this section, we study the performance of the linear MD detector in the context of a $S\alpha S$ random process. For mathematical tractability, we assume that $b^{(1)}(i)\mathbf{c}^{(1)}$ and $\mathbf{j}(i)$ are stationary $S\alpha S$ random vectors with the same characteristic exponent α as the noise vector $\mathbf{v}(i)$ and that $r_n(i)$ and $e(i)$ are jointly $S\alpha S$ for all $n \in [0, N-1]$. It is usually assumed that $b^{(1)}(i)\mathbf{c}^{(1)}$, $\mathbf{j}(i)$, and $\mathbf{v}(i)$ in (2.21) are mutually independent for all $i \in (-\infty, \infty)$. In order to use the pseudo-linearity property with the second argument of the covariation, it is also assumed that the interference elements $\{j_n(i)\}_{n=0}^{N-1}$ and the noise elements $\{v_n(i)\}_{n=0}^{N-1}$ are independent for all $n \in [0, N-1]$, respectively. The covariation matrices of the interference vector and the noise vector can thus be written

as

$$\Gamma_j = diag(\gamma_{j_0}, \gamma_{j_1}, \cdots, \gamma_{j_{N-1}})$$

and

$$\Gamma_v = diag(\gamma_{v_0}, \gamma_{v_1}, \cdots, \gamma_{v_{N-1}}).$$

respectively, where

$$[\Gamma_j]_{n,p} = [j_n, j_p]_\alpha = \gamma_{j_n} \delta_{n,p}$$

and

$$[\Gamma_v]_{n,p} = [v_n, v_p]_\alpha = \gamma_{v_n} \delta_{n,p}.$$

Here $\delta_{n,p}$ is the Kronecker delta function and γ is the dispersion of the corresponding $S\alpha S$ random variable. By the above assumption we can also let $\left[b^{(1)}(i), b^{(1)}(i)\right]_\alpha = \gamma_b$. For notational simplicity, we will let $b(i) = b^{(1)}(i)$ and $\mathbf{c} = \mathbf{c}^{(1)}$.

Under the assumptions made above, the MD solution formula is given in APPENDIX A by

$$\bar{\mathbf{w}}_\alpha = \gamma_b \left(1 - \bar{\mathbf{w}}^T \mathbf{c}\right)^{<\alpha-1>} \Gamma^{-1} \mathbf{c} \tag{3.3}$$

where

$$\bar{\mathbf{w}}_\alpha \triangleq \left[\tilde{w}_0^{<\alpha-1>}, \tilde{w}_1^{<\alpha-1>}, \cdots, \tilde{w}_{N-1}^{<\alpha-1>}\right]^T$$

and

$$\Gamma \triangleq \Gamma_j + \Gamma_v.$$

For $1 < \alpha < 2$, (3.3) is hard to solve for $\bar{\mathbf{w}}$ because it is highly nonlinear. When $\alpha = 2$, (3.3) is linear and a closed-form solution exists for $\bar{\mathbf{w}}_\alpha = \bar{\mathbf{w}}$. The solution for $\bar{\mathbf{w}}$ is shown in APPENDIX A as

$$\bar{\mathbf{w}} = \frac{\sigma_b^2}{1 + \sigma_b^2 \mathbf{c}^T \mathbf{R}^{-1} \mathbf{c}} \mathbf{R}^{-1} \mathbf{c} \tag{3.4}$$

which is equivalent to the MMSE solution derived in [34].

For $1 < \alpha \leq 2$. it is also shown in APPENDIX A that in matrix-form the dispersion of the estimation error is given by

$$J_\alpha^\alpha(\mathbf{w}(i)) = \gamma_b(1 - \mathbf{w}(i)^T\mathbf{c})(1 - \mathbf{w}(i)^T\mathbf{c})^{<\alpha-1>} + \mathbf{w}(i)^T\Gamma\mathbf{w}_\alpha(i) \tag{3.5}$$

where

$$\mathbf{w}_\alpha(i) \triangleq [w_0(i)^{<\alpha-1>}, w_1(i)^{<\alpha-1>}, \cdots, w_{N-1}(i)^{<\alpha-1>}]^T.$$

The minimum solution for $J_\alpha^\alpha(\mathbf{w}(i))$ is derived in APPENDIX A as

$$\begin{aligned} J_{\alpha,\min}^\alpha &= J_\alpha^\alpha|_{\mathbf{w}(i)=\bar{\mathbf{w}},\mathbf{w}_\alpha(i)=\bar{\mathbf{w}}_\alpha} \\ &= \gamma_b(1 - \bar{\mathbf{w}}^T\mathbf{c})^{<\alpha-1>}. \end{aligned} \tag{3.6}$$

When $\alpha = 2$. the minimum mean-squared error $J_{\min}$ is shown in APPENDIX A as

$$J_{\min} = \sigma_b^2(1 - \bar{\mathbf{w}}^T\mathbf{c}) \tag{3.7}$$

which is also equivalent to the MMSE solution derived in [38] and [34].

As another performance measure. we define the signal-to-interference ratio (SIR) at the output of the linear MD filter $\mathbf{w}(i)^T$ as

$$\text{SIR} \triangleq \frac{[\mathbf{w}(i)^T b(i)\mathbf{c}, \mathbf{w}(i)^T b(i)\mathbf{c}]_\alpha}{[\mathbf{w}(i)^T(\mathbf{j}(i) + \mathbf{v}(i)), \mathbf{w}(i)^T(\mathbf{j}(i) + \mathbf{v}(i))]_\alpha} \text{ for } 1 < \alpha \leq 2. \tag{3.8}$$

Then by using the properties of the covariation and independence assumptions made above. the output SIR can be shown in APPENDIX A as

$$\text{SIR} = \frac{\gamma_b\,|\mathbf{w}^T(i)\mathbf{c}|^\alpha}{\mathbf{w}^T(i)\Gamma\mathbf{w}_\alpha(i)} \tag{3.9}$$

for $1 < \alpha \leq 2$. The output SIR corresponding the MD solution of $\mathbf{w}(i) = \bar{\mathbf{w}}$ and $\mathbf{w}_\alpha(i) = \bar{\mathbf{w}}_\alpha$ is given in APPENDIX A by

$$\begin{aligned} \text{SIR}_{MD} &= \text{SIR}|_{\mathbf{w}(i)=\bar{\mathbf{w}};\mathbf{w}_\alpha(i)=\bar{\mathbf{w}}_\alpha} \\ &= \frac{\gamma_b}{J_{\alpha,\min}^\alpha}(\bar{\mathbf{w}}^T\mathbf{c})^{<\alpha-1>} = \text{SIR}_{\max}. \end{aligned} \tag{3.10}$$

When $\alpha = 2$. (3.10) can be written in APPENDIX A as

$$\mathrm{SIR}_{\max} = \left(\frac{\sigma_b^2}{J_{\min}} - 1\right) \tag{3.11}$$

which is also equivalent to the MMSE solution derived in [38] and [34]. The performance analysis shows that the MD solution for $\mathbf{w}$ minimizes the dispersion of estimation error and thus maximizes the output SIR under the independence assumptions.

For a particular sequence of $L-1$ interference symbols, $\mathbf{b}_J(i) = \left(b_J^{(1)}, b_J^{(2)}, \cdots, b_J^{(L-1)}\right)$, the interfering symbol vector is fixed as $\mathbf{j}(i) = \mathbf{j}_J(i)$. To analyze the probability of error, we condition on the desired symbol $b(i) = 1$ and the interfering symbol vector $\mathbf{b}_J(i) = \left(b_J^{(1)}, b_J^{(2)}, \cdots, b_J^{(L-1)}\right)$. Assuming that $\Pr\{b(i) = +1\} = \Pr\{b(i) = -1\} = 1/2$, the conditional probability of error can be written as

$$\begin{aligned} P_e(\mathbf{b}_J(i)) &= \frac{1}{2}\Pr\{Z(i) < 0 \mid b(i) = +1, \mathbf{b}_J(i)\} + \frac{1}{2}\Pr\{Z(i) \geq 0 \mid b(i) = -1, \mathbf{b}_J(i)\} \\ &= \Pr\{Z(i) < 0 \mid b(i) = +1, \mathbf{b}_J(i)\} \\ &= \int_{-\infty}^{0} f_\alpha(\xi; \gamma_{\hat{Z}(i)}, \tilde{\mu}_0) d\xi \end{aligned} \tag{3.12}$$

where $f_\alpha(\xi; \gamma_{\hat{Z}(i)}, \tilde{\mu}_0)$ is the $S\alpha S$ pdf with location parameter $\tilde{\mu}_0$ and dispersion $\gamma_{\hat{Z}(i)}$ given in APPENDIX A. Assume that all the interference symbols are equally likely. Then the average probability of error is given by

$$\begin{aligned} \bar{P}_e &= \sum_{\mathbf{b}_J(i)} P_e(\mathbf{b}_J(i)) \Pr\{\mathbf{b}_J(i)\} \\ &= \frac{1}{2^{L-1}} \sum_{\mathbf{b}_J(i)} P_e(\mathbf{b}_J(i)) \\ &\leq \frac{1}{2^{L-1}} \sum_{\mathbf{b}_J(i)} P_e(\mathbf{b}_J^*(i)) = P_e(\mathbf{b}_J^*(i)) \end{aligned}$$

where an upper bound $P_e(\mathbf{b}_J^*(i))$ on the average probability of error is caused by the worst case sequence of interference symbols $\mathbf{b}_J^*(i)$.

When $\alpha = 2$, in APPENDIX A, (3.12) reduces to

$$P_e(\mathbf{b}_J(i)) = Q\left(\frac{\mathbf{w}(i)^T(\mathbf{c} + \mathbf{j}_J(i))}{\sqrt{\mathbf{w}(i)^T \mathbf{R}_v \mathbf{w}_\alpha(i)}}\right) \tag{3.13}$$

where $Q(x) = \frac{1}{\sqrt{2\pi}} \int_x^\infty e^{-t^2/2} dt$. Note that (3.13) is equivalent to the conditional probability of error given in [34].

(A.17), (A.18), and (3.12) imply that the conditional probability of error of the linear MD detector is lowered if the dispersion of estimation error is minimized and thus the output SIR is maximized.

3.4 Adaptive Implementation

Since a closed-form MD solution in general does not exist for $1 < \alpha < 2$, we consider an adaptive solution. Assume that the input vector $\mathbf{r}(i)$ applied to the FIR filter is stationary $S\alpha S$ process. We also assume that $b^{(1)}(i)$ and each element of $\mathbf{r}(i)$ are jointly $S\alpha S$. Consider the problem of finding the MD solution for $\mathbf{w}(i)$ such that the cost function

$$J_\alpha(\mathbf{w}(i)) = \|e(i)\|_\alpha = \left\|b^{(1)}(i) - \mathbf{w}(i)^T \mathbf{r}(i)\right\|_\alpha$$

is minimized. The cost function $J_\alpha(\mathbf{w}(i))$ is quite intractable as given in (3.5). An equivalent cost function can be written as

$$J_p(\mathbf{w}(i)) = E\left\{|e(i)|^p\right\} = E\left\{\left|b^{(1)}(i) - \mathbf{w}(i)^T \mathbf{r}(i)\right|^p\right\}$$

for $0 < p < \alpha$ and $0 < \alpha \leq 2$. We use the least mean p-norm(LMP) algorithm proposed in [60] and [89] to solve for the tap weight vector $\mathbf{w}(i)$ that minimizes the cost function $J_p(\mathbf{w}(i))$. Its adaptation formula is given by

$$\mathbf{w}(i+1) = \mathbf{w}(i) + \mu_{lmp} \cdot p \cdot |e(i)|^{p-1} \, sign(e(i)) \cdot \mathbf{r}(i) \tag{3.14}$$

where $\mu_{lmp} > 0$ is the step size and $1 \leq p < \alpha$. Note that the LMP algorithm reduces to the conventional LMS algorithm for $p = \alpha = 2$. Defining an effective step size μ_{eff} as $\mu_{eff}(e(i)) = \mu_{lmp} \cdot p \cdot |e(i)|^{p-1}$, (3.14) can be rewritten as

$$\mathbf{w}(i+1) = \mathbf{w}(i) + \mu_{eff}(e(i)) \cdot sign(e(i)) \cdot \mathbf{r}(i). \tag{3.15}$$

Thus the LMP algorithm can be viewed as the signed-LMS algorithm with a time-varying step size. Note that for $p = 1$, $\mu_{eff}(e(i)) = \mu_{lmp}$ is constant. For $1 < p < \alpha$, $\mu_{eff}(e(i))$ depends on p and $e(i)$. In general, $\mu_{eff}(e(i))$ is large before convergence since the absolute error $|e(i)|$ is large , while $\mu_{eff}(e(i))$ is small after convergence. Thus the convergence rate of the LMP algorithm is fast at the transient state and gets slower as the LMP algorithm converges. This phenomenon is noticeable as p increases. It is shown in [88] that when input process and desired process are non-Gaussian, the LMP converges to solutions other than the Wiener solution for various p.

3.5 Simulation Results

We performed an extensive Monte Carlo simulation to show the improved performance of the proposed adaptive MD detector in non-Gaussian impulsive noise. The bit error rates are compared for several detectors such as the conventional MF, hard-limiting MF (HLMF), and MMSE detectors. We present several simulation results for different values of the characteristic exponent α and the dispersion γ of the additive $S\alpha S$ noise. In all simulation results, we consider asynchronous BPSK DS/CDMA systems with $K = 2$, 5, 12, and 24 users. We use $K_s = 1$, $K_s = 2$, $K_s = 5$, and $K_s = 10$ for $K = 2$, $K = 5$, $K = 12$, and $K = 24$, respectively.

Figures 3.2 - 3.10 show the bit error rate (BER) performance as a function of the PRID for the nine condition sets: $\{\alpha = 1.1, \gamma = 0.05,$ and $K = 5$ users$\}$, $\{\alpha = 1.1, \gamma = 0.2,$ and $K = 5$ users$\}$, $\{\alpha = 1.5, \gamma = 1,$ and $K = 2$ users$\}$, $\{\alpha = 1.5, \gamma = 0.2,$ and $K = 5$ users$\}$, $\{\alpha = 1.5, \gamma = 1,$ and $K = 5$ users$\}$, $\{\alpha = 1.5, \gamma = 1,$ and $K = 12$ users$\}$, $\{\alpha = 1.5, \gamma = 1,$ and $K = 24$ users$\}$, $\{\alpha = 1.9, \gamma = 0.2,$ and $K = 5$ users$\}$, and $\{\alpha = 1.9, \gamma = 1,$ and $K = 5$ users$\}$, respectively. When $\alpha = 1.1$, γ is set to 0.05 and 0.2 instead of 1, since none of the detectors perform decently with highly impulsive noise with $\gamma = 1$. The first PRID value of each plot corresponds to equal powers (or

perfect power control). The BER performance of the proposed adaptive MD detector remains nearly constant for most PRID levels. This reflects the near-far resistance of the proposed detector for most degrees of near-far environment. The performance of the adaptive MD detector is much better than that of the other detectors at high PRID, while it is comparable to that of the conventional MF detector at low PRID. The HLMF detector has much better performance at lower PRID levels, but its performance rapidly degrades as the PRID increases, since it is locally optimum for single-user non-Gaussian (Laplacian) noise channels. The MMSE detector performs significantly worse than the adaptive MD and conventional MF detectors. The MMSE detector is shown not to be effective in additive non-Gaussian impulsive noise channels modeled as $S\alpha S$ processes as expected. When the system is heavily loaded (or $K = 12$ and $K_s = 5$), the adaptive MD detector provides substantial performance gains over the conventional MF detector. In addition, the HLMF detector is less effective for low PRID levels. This implies that the adaptive MD detector can be globally superior over all PRID levels as the system gets more heavily loaded. When the system is more heavily loaded (or $K = 24$ and $K_s = 10$), the adaptive MD detector outperforms the other detectors and the HLMF is not effective anymore for any low PRID level.

Figure 3.11 through Figure 3.15 show the BER performance as a function of the mixed signal-to-noise ratio (SNR) for the five condition sets: $\{\alpha = 1.1$, PRID = 40 dB, and $K = 5$ users$\}$, $\{\alpha = 1.5$, PRID = 23.01 dB, and $K = 2$ users$\}$, $\{\alpha = 1.5$, PRID = 35 dB, and $K = 5$ users$\}$, $\{\alpha = 1.5$, PRID = 40 dB, and $K = 5$ users$\}$, and $\{\alpha = 1.9$, PRID = 40 dB, and $K = 5$ users$\}$, respectively. Here, the mixed SNR is defined as

$$\text{mixed SNR} \triangleq 10\log\left(\frac{E\left[|s_1(t)|^2\right]}{\gamma}\right) = 10\log\left(\frac{P_1}{\gamma}\right) \tag{3.16}$$

where γ is the dispersion of the additive $S\alpha S$ noise process and $s_1(t)$ is the transmitted signal for user 1 given in [58]. Table 3.1 shows the mixed SNR for each dispersion γ of the additive $S\alpha S$ noise.

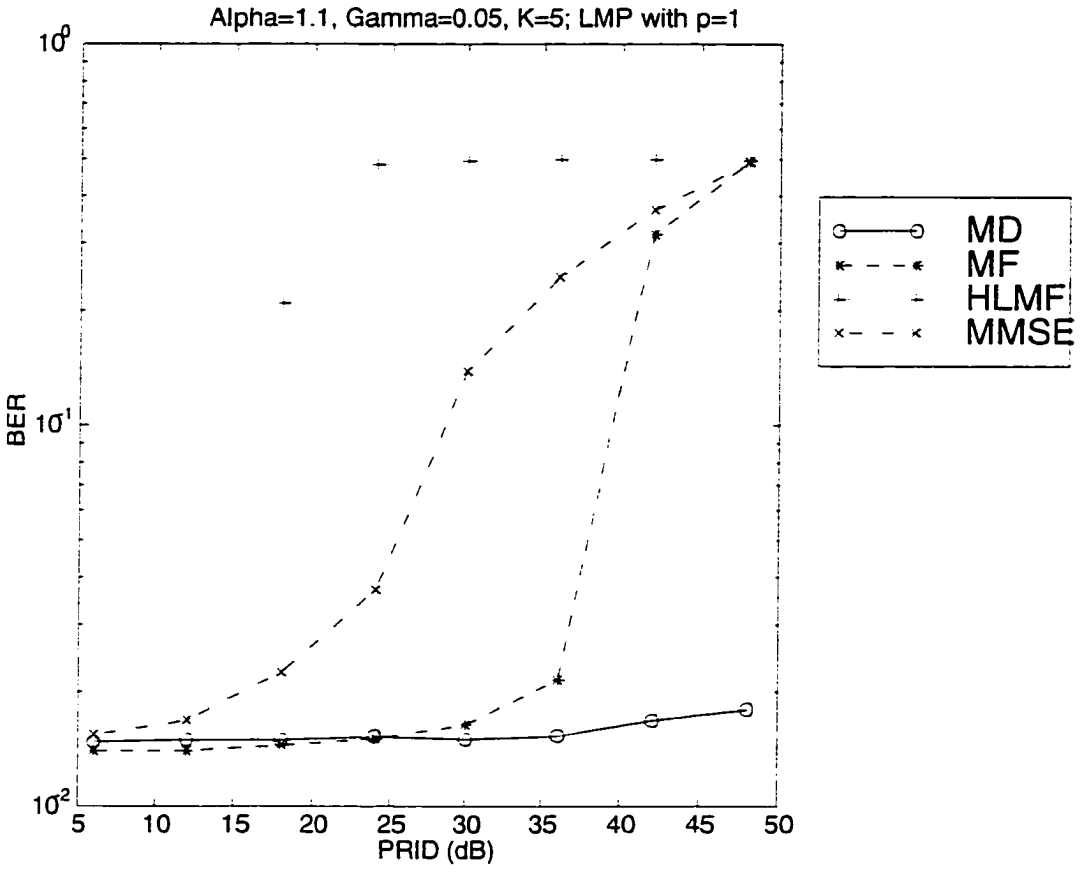

Figure 3.2 BER as a function of the PRID for an asynchronous DS/CDMA system: $\alpha = 1.1$, $\gamma = 0.05$, $K = 5$, and $K_s = 2$.

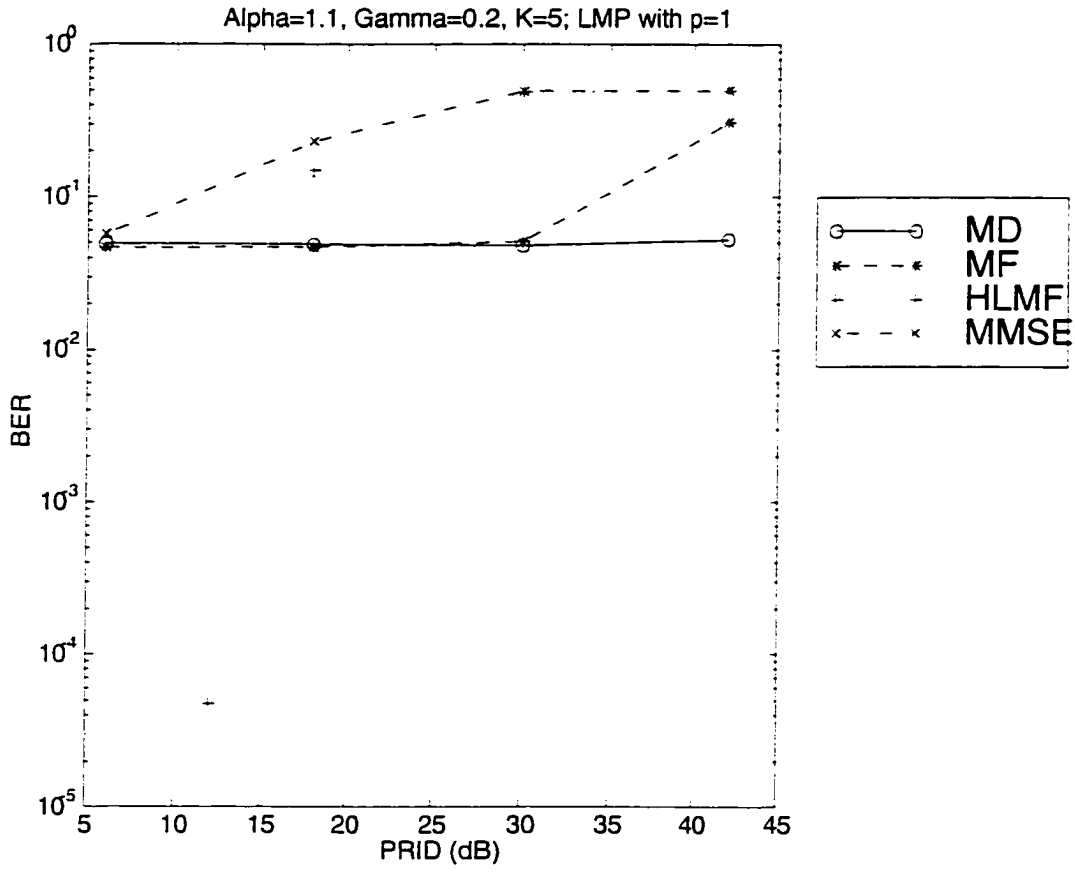

Figure 3.3 BER as a function of the PRID for an asynchronous DS/CDMA system; $\alpha = 1.1$, $\gamma = 0.2$, $K = 5$, and $K_s = 2$.

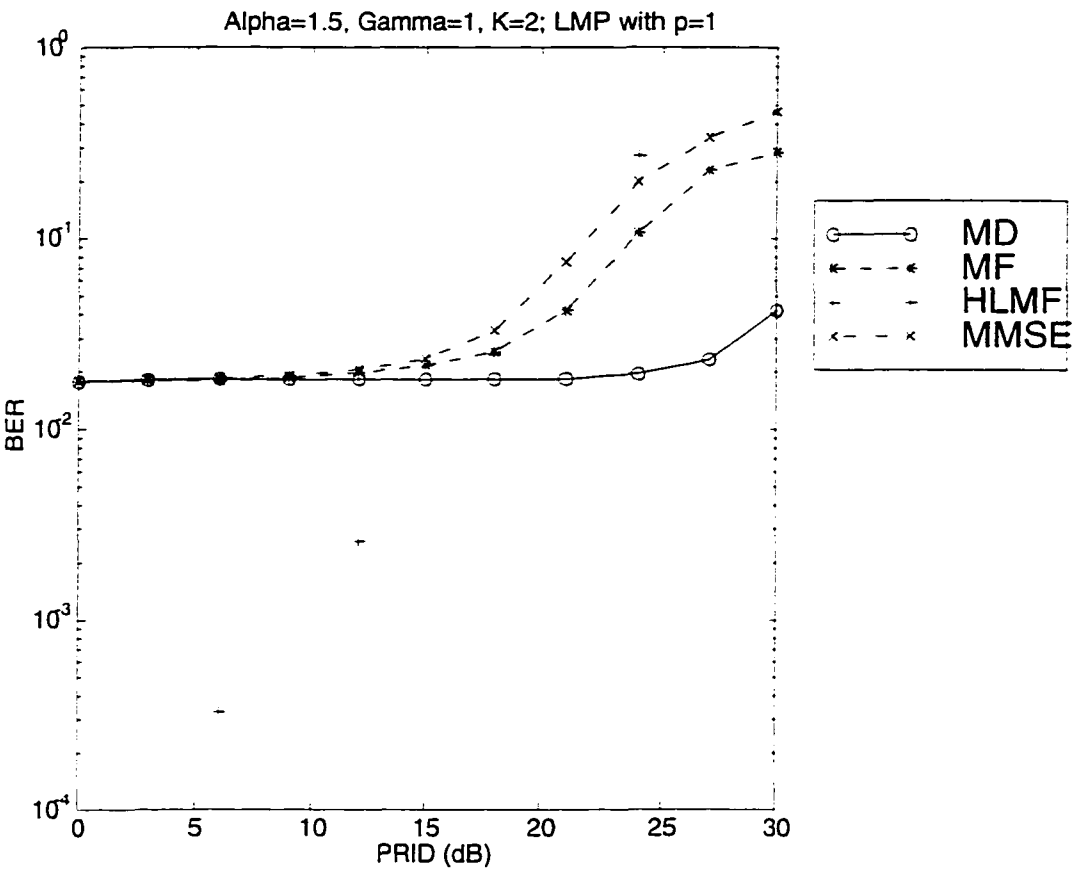

Figure 3.4 BER as a function of the PRID for an asynchronous DS/CDMA system; $\alpha = 1.5$, $\gamma = 1$, $K = 2$, and $K_s = 1$.

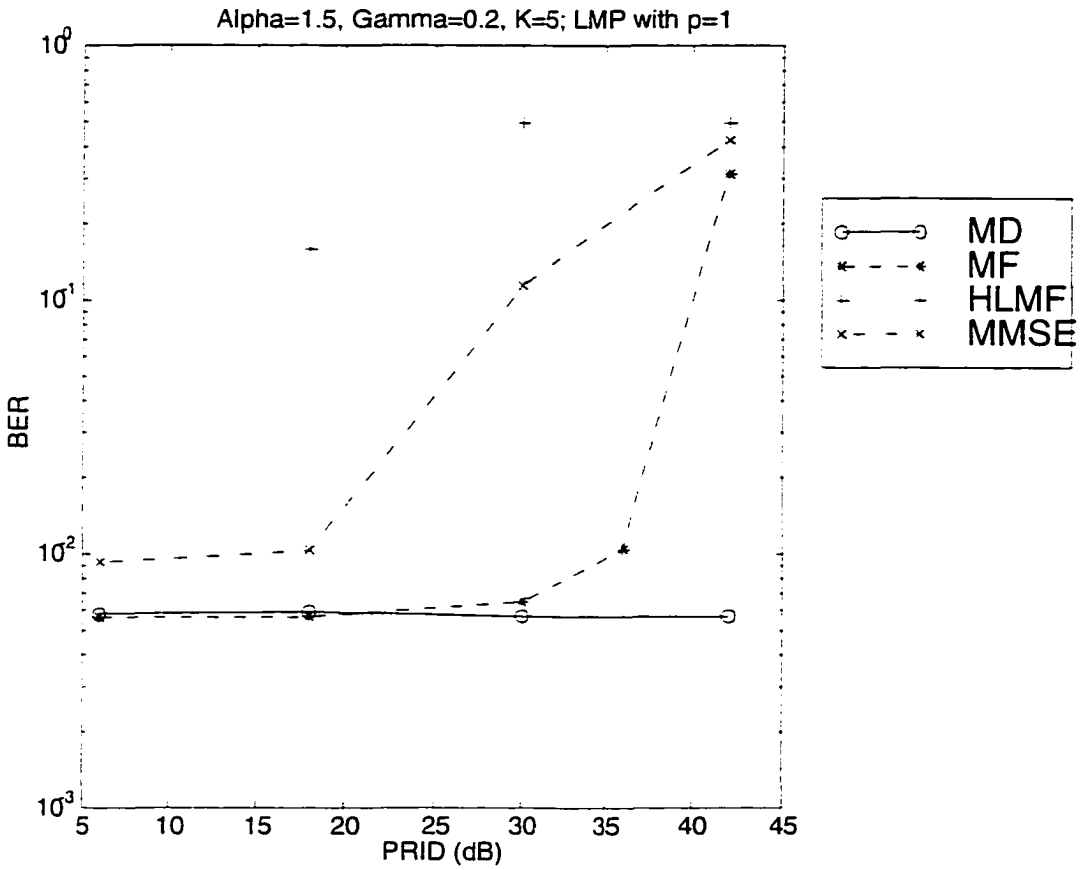

Figure 3.5 BER as a function of the PRID for an asynchronous DS/CDMA system: $\alpha = 1.5$, $\gamma = 0.2$, $K = 5$, and $K_s = 2$.

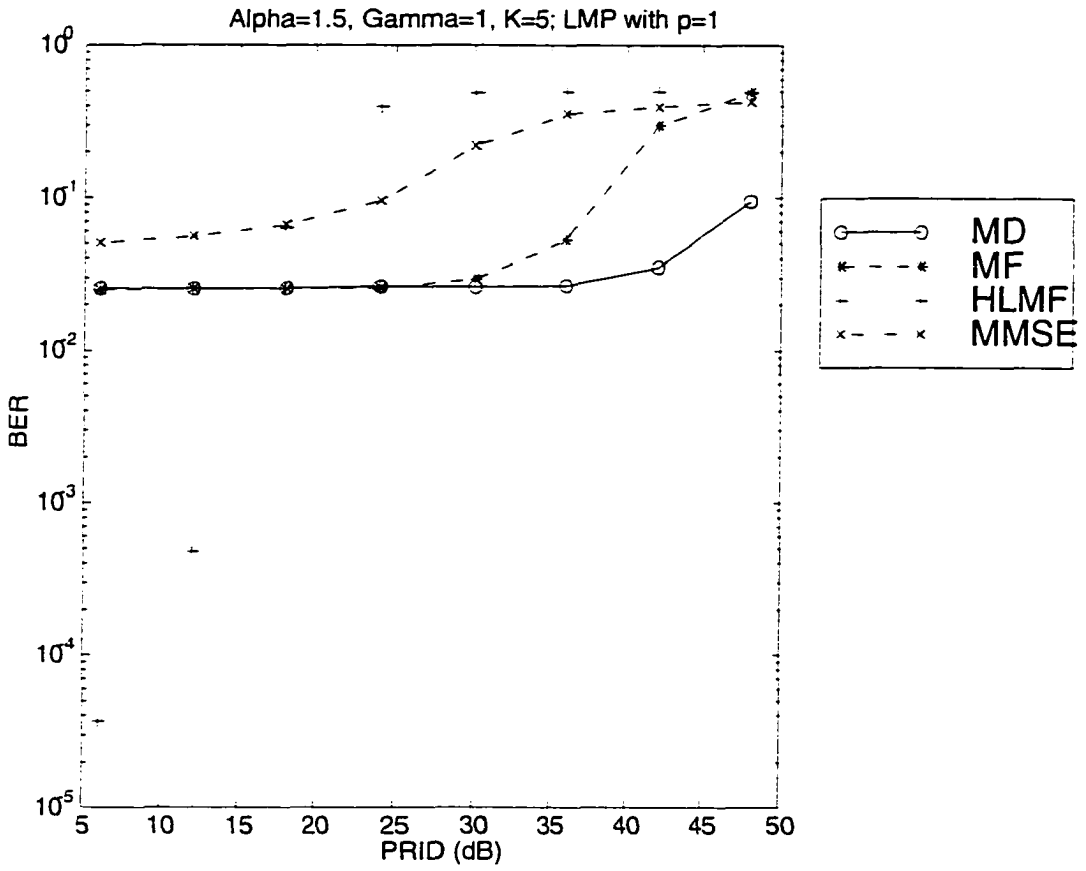

Figure 3.6 BER as a function of the PRID for an asynchronous DS/CDMA system: $\alpha = 1.5$, $\gamma = 1$, $K = 5$, and $K_s = 2$.

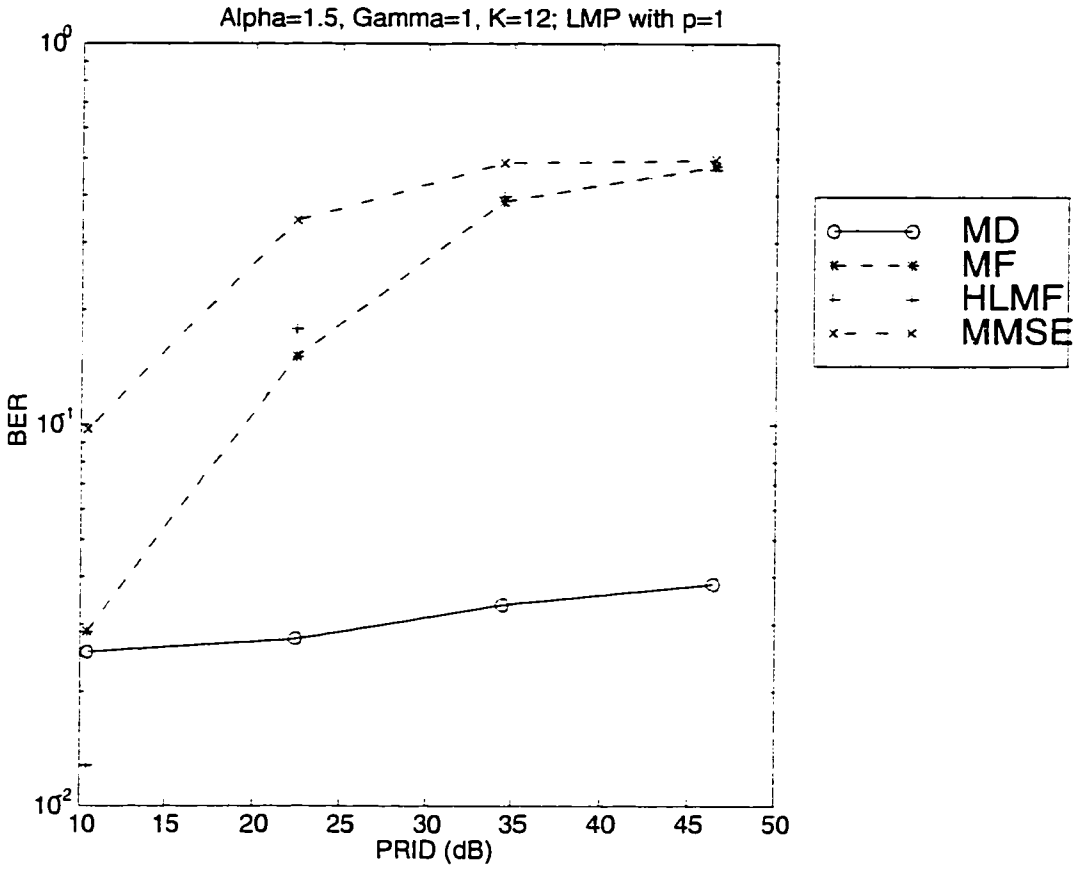

Figure 3.7 BER as a function of the PRID for an asynchronous DS/CDMA system: $\alpha = 1.5$, $\gamma = 1$, $K = 12$, and $K_s = 5$.

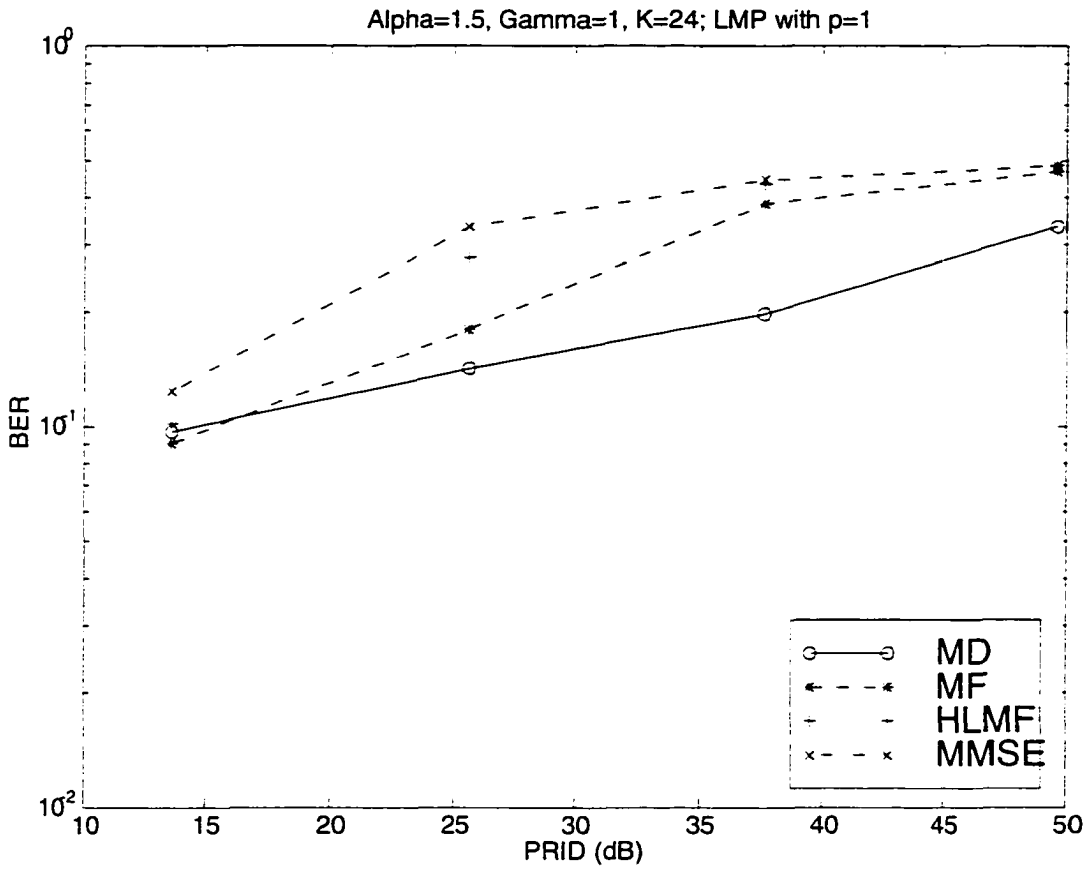

Figure 3.8 BER as a function of the PRID for an asynchronous DS/CDMA system: $\alpha = 1.5$, $\gamma = 1$, $K = 24$, and $K_s = 10$.

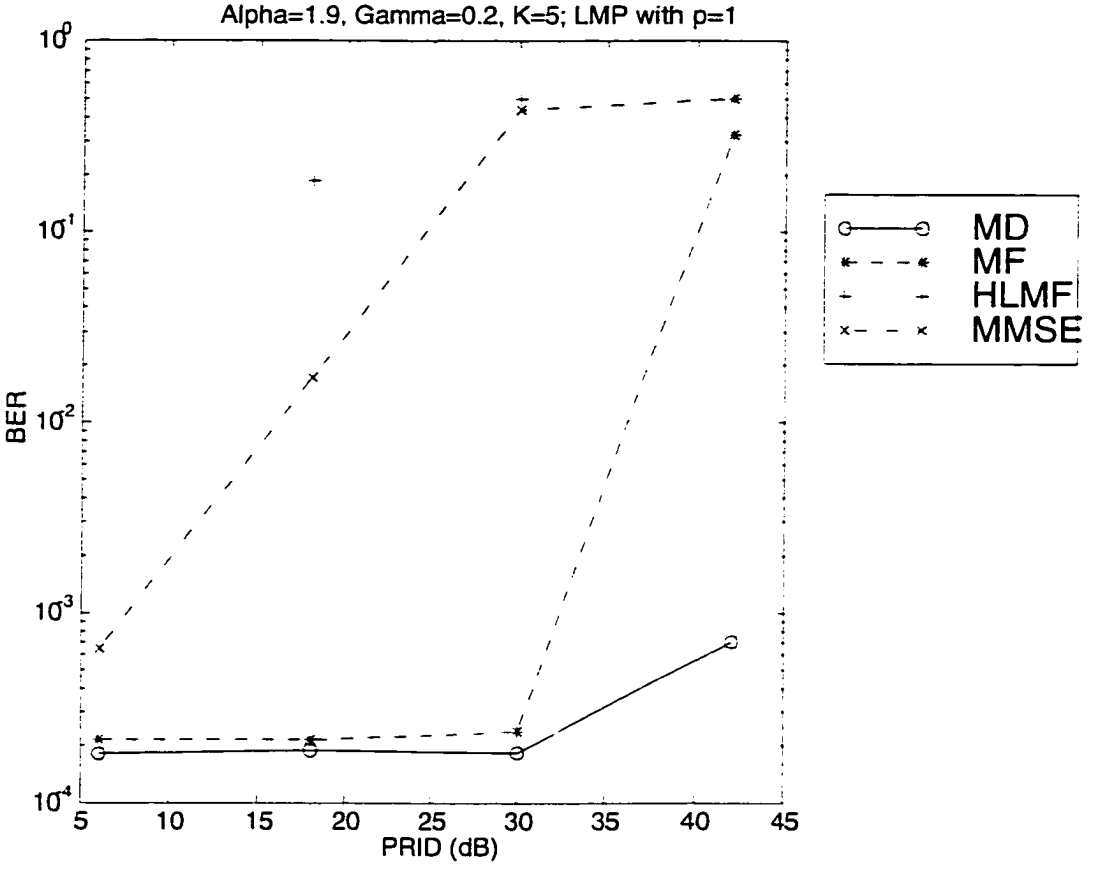

Figure 3.9 BER as a function of the PRID for an asynchronous DS/CDMA system: $\alpha = 1.9$, $\gamma = 0.2$, $K = 5$, and $K_s = 2$.

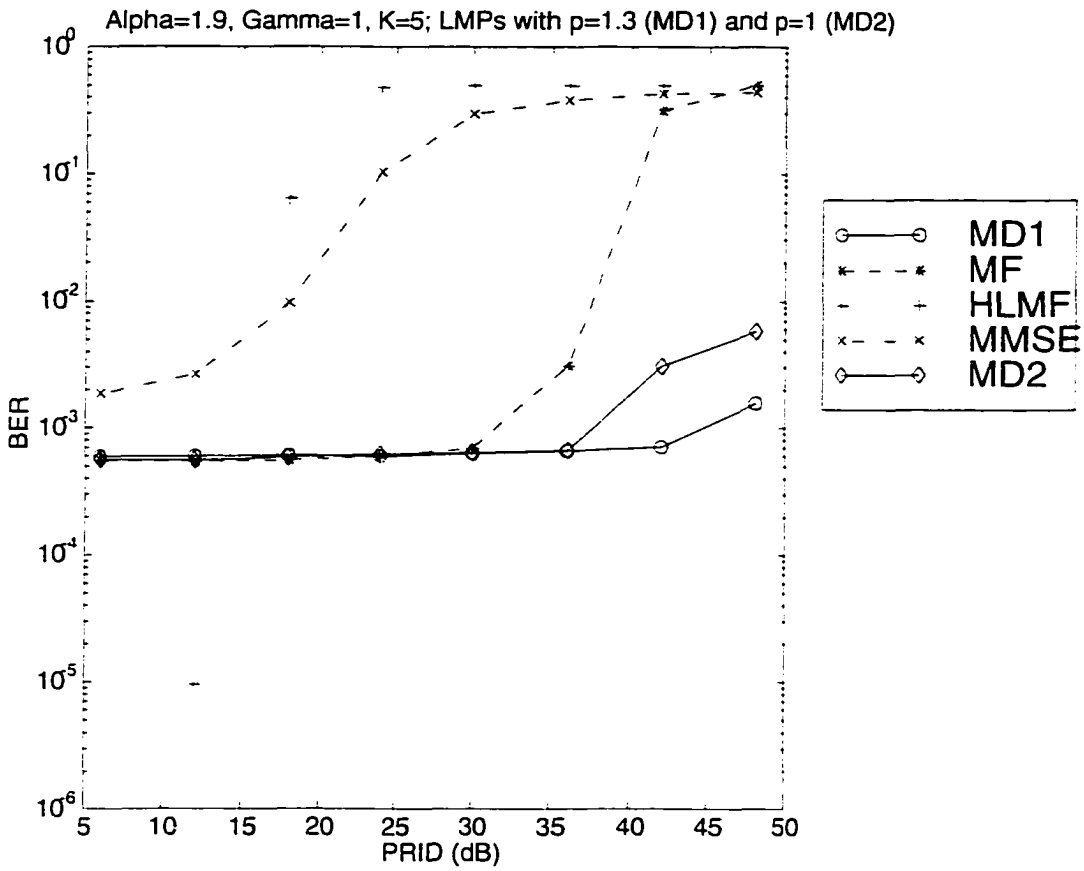

Figure 3.10 BER as a function of the PRID for an asynchronous DS/CDMA system: $\alpha = 1.9$, $\gamma = 1$, $K = 5$, and $K_s = 2$.

Table 3.1 Mixed SNR vs. γ

SNR (dB)	γ	SNR (dB)	γ
−16.37	13	−10.00	3.00
−15.64	11	−5.23	1.00
−14.77	9	−2.22	0.50
−13.68	7	4.77	0.10
−12.22	5	7.78	0.05

The PRID is set to 35 dB or 40 dB to simulate severe near-far environments. The adaptive MD detector gives a much lower BER than the conventional MF detector except in the extreme case of small SNR (i.e., large dispersion of the additive noise process). It is apparent that the adaptive MD detector outperforms the conventional MF detector in MAI-limited environments in which MAI dominates over the additive $S\alpha S$ noise. It is also observed that the HLMF and MMSE detectors always perform poorly. This is due to the fact that the HLMF is not designed for MAI suppression, but for single-user non-Gaussian impulsive noise channels, while the MMSE criterion is not effective since $S\alpha S$ processes have infinite variance.

Figure 3.16 shows the BER performance as a function of the number of active users K for $\alpha = 1.5$ and $\gamma = 1$. Figure 3.16 (a) denotes the case for equal powers. Each of the associated PRID values is 0, 6.02, 10.41, and 13.62 dB for $K = 2, 5, 12$, and 24, respectively. Figure 3.16 (b) denotes the case for unequal powers. Each of the associated PRID values is 21.00 (24.00 only for HLMF with $K = 2$), 36.02, 46.41, 49.62 dB for $K = 2, 5, 12$, and 24, respectively. For equal powers (or perfect power control) the HLMF detector always outperforms the remaining detectors. But as K increases, the performance of the HLMF detector rapidly deteriorates in the range of between $K = 2$ and $K = 12$ and slowly approaches that of the adaptive MD and MF detectors in the range of between $K = 12$ and $K = 24$.

Figure 3.17 and Figure 3.18 show the BER performance as a function of the characteristic exponent α of the additive $S\alpha S$ impulsive noise for $K = 5$ and $K_s = 2$. Figure

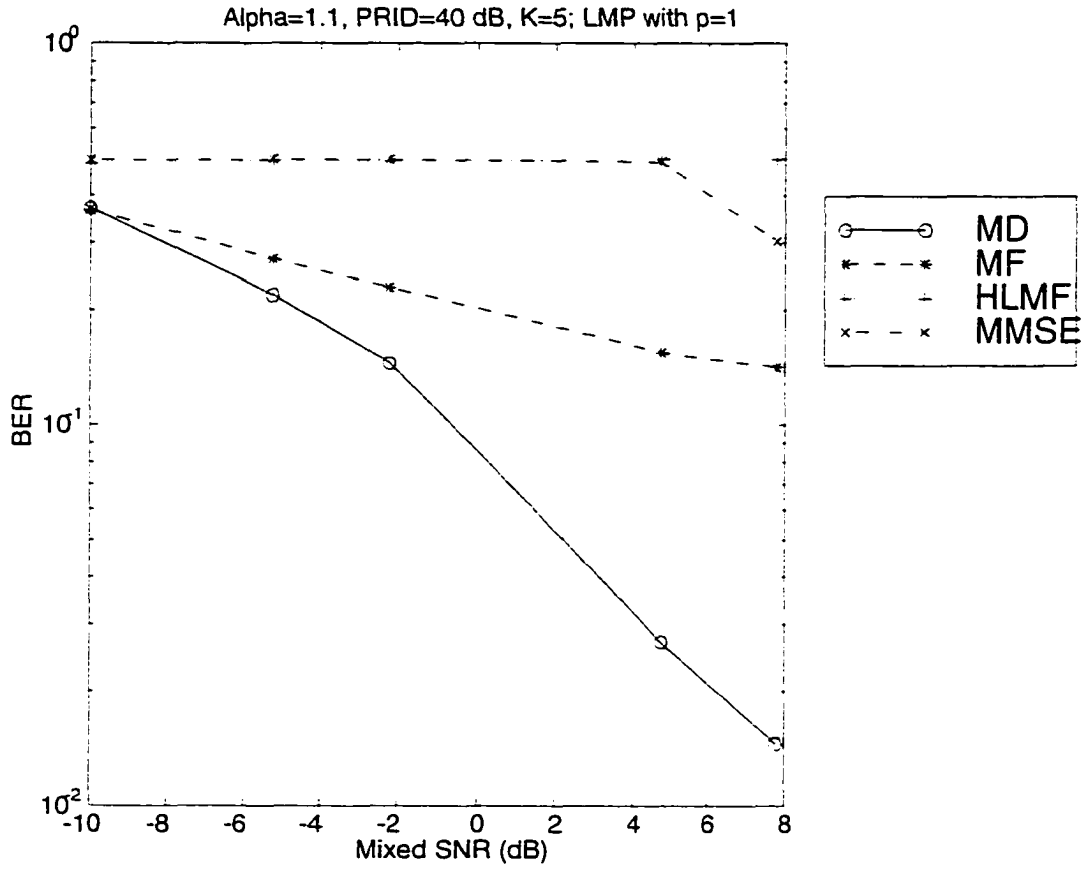

Figure 3.11 BER as a function of the mixed SNR for an asynchronous DS/CDMA system: $\alpha = 1.1$, PRID = 40 dB, $K = 5$, and $K_s = 2$.

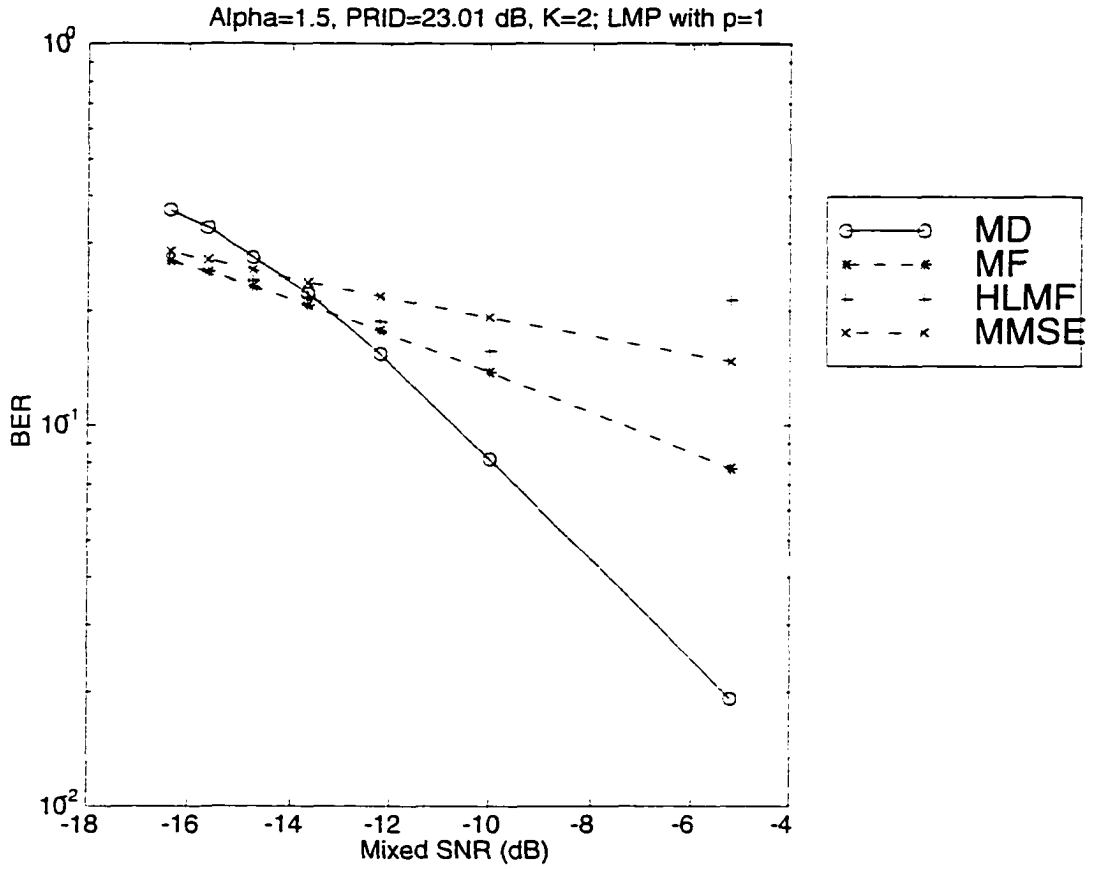

Figure 3.12 BER as a function of the mixed SNR for an asynchronous DS/CDMA system: $\alpha = 1.5$, PRID = 23.01 dB, $K = 2$, and $K_s = 1$.

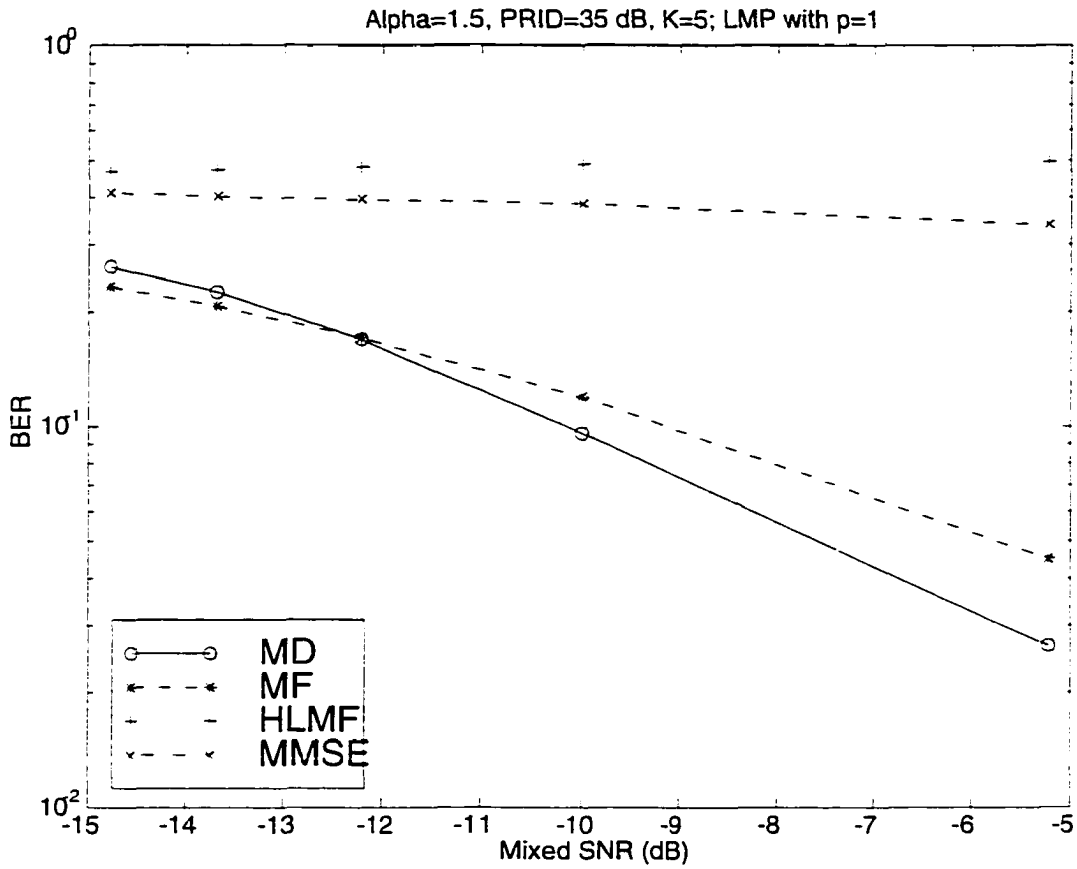

Figure 3.13 BER as a function of the mixed SNR for an asynchronous DS/CDMA system: $\alpha = 1.5$, PRID = 35 dB, $K = 5$, and $K_s = 2$.

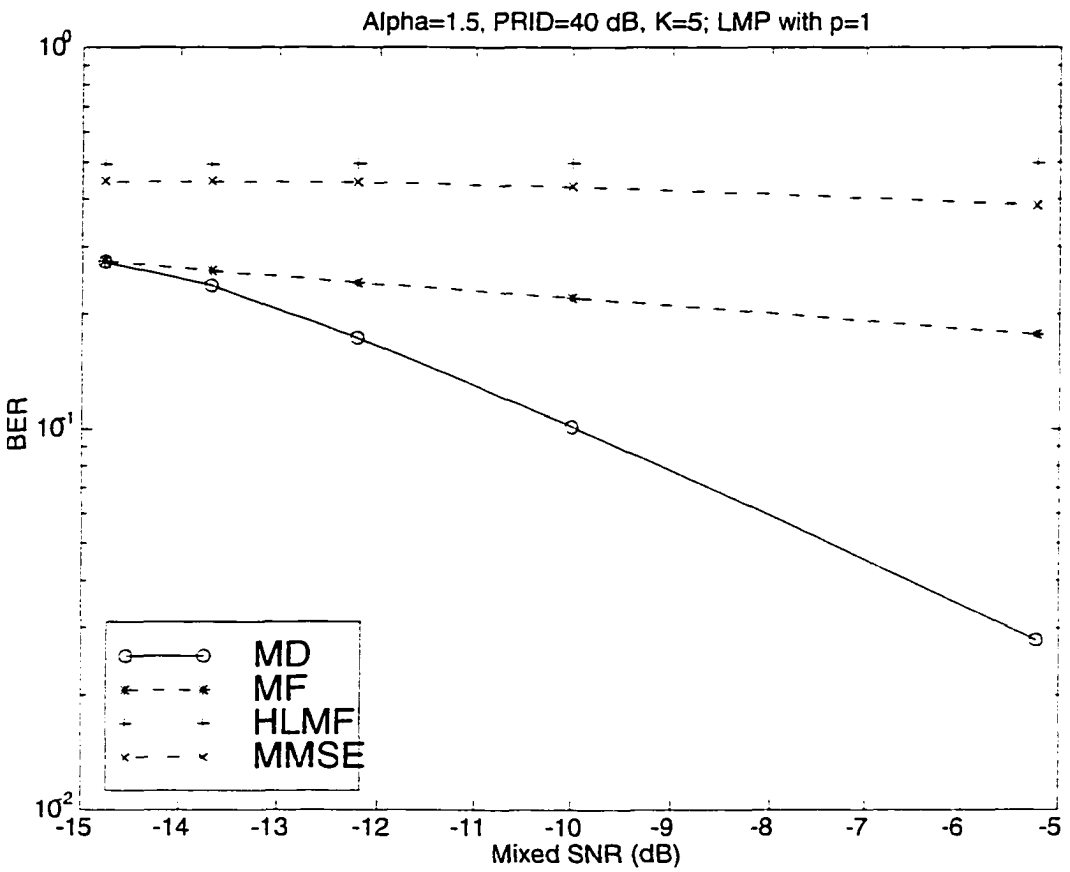

Figure 3.14 BER as a function of the mixed SNR for an asynchronous DS/CDMA system: $\alpha = 1.5$, PRID = 40 dB, $K = 5$, and $K_s = 2$.

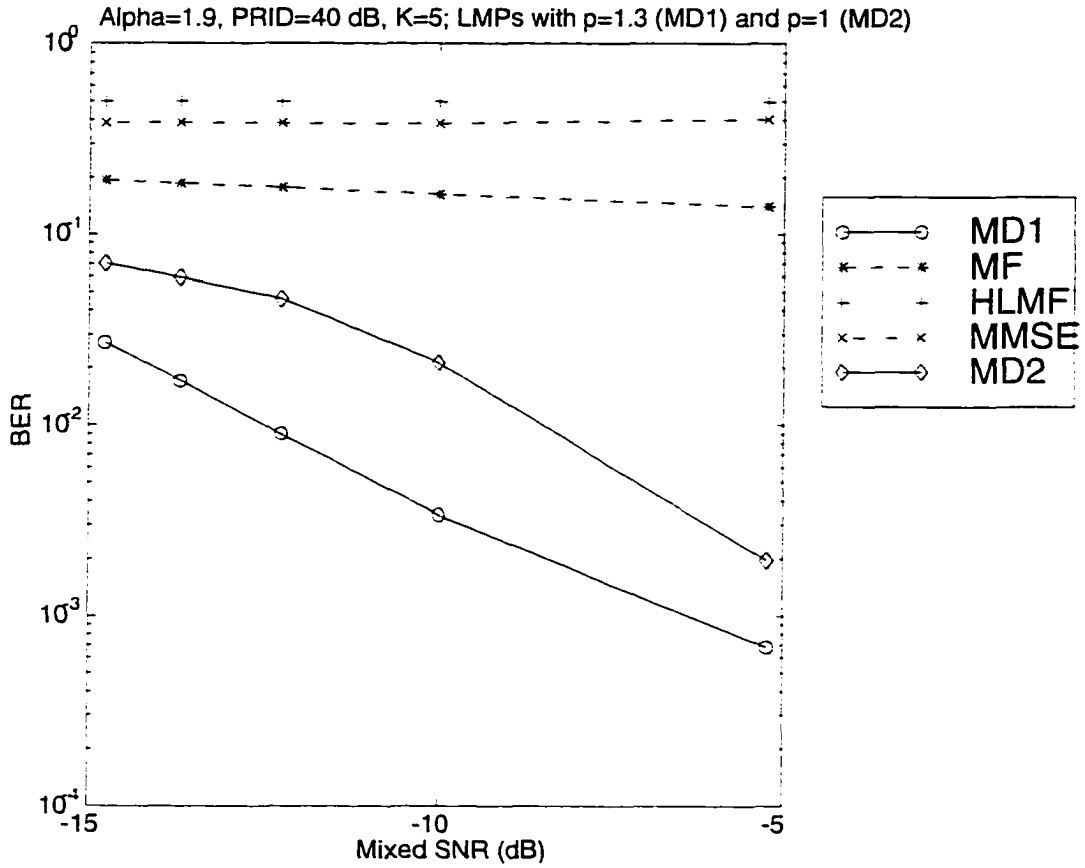

Figure 3.15 BER as a function of the mixed SNR for an asynchronous DS/CDMA system: $\alpha = 1.9$, PRID = 40 dB, $K = 5$, and $K_s = 2$.

3.17 represents the case for $\gamma = 0.2$. For equal powers with PRID = 6.02 dB (or perfect power control), the BER performance of the HLMF detector does not appear due to its very small values. The HLMF detector outperforms the other detectors for all values of α. For unequal powers with PRID = 42.02 dB, the adaptive MD detector significantly outperforms the other detectors for all values of α. As α increases, the BER performance of the adaptive MD detector increases, while that of the remaining detectors nearly remains unchanged. This implies that the adaptive MD detector is very effective for this channel condition, but the remaining detectors are not. Figure 3.18 represents the case for $\gamma = 1$. For equal powers, the HLMF detector outperforms the other detectors for all values of α. The performance of each of the detectors clearly improves as α increases as expected. For unequal powers with PRID = 36.02 dB, the adaptive MD detector outperforms the remaining detectors when α is approximately larger than 1.2, while the MF detector does when α is approximately less than 1.2. The HLMF and MMSE detectors are not effective anymore in this channel situation since the BER performance does not matter with α. For unequal powers with PRID = 48.02 dB, the adaptive MD detector significantly outperforms the remaining detectors except when α is less than or equal to 1.1. When α is less than or equal to 1.1, $\gamma = 1$ is severely impulsive enough to make all of the detectors deteriorate.

Figure 3.19 and Figure 3.20 show the transient behavior of the adaptive MD detector using the LMP algorithm with $p = 1$ for PRID = 46.4 dB (or no power control) and PRID = 10.4 dB (or perfect power control). The results show that the output SIR after the adaptive MD filtering converges to the maximum value as the estimation error $e(i)$ converges to the minimum one as shown analytically in Section 3.3. It is observed that the LMP algorithm takes on the order of several (ten) thousand bits to converge to a steady state. Various simulation results show that the convergence rate depends on the number of active users, PRID level, and α.

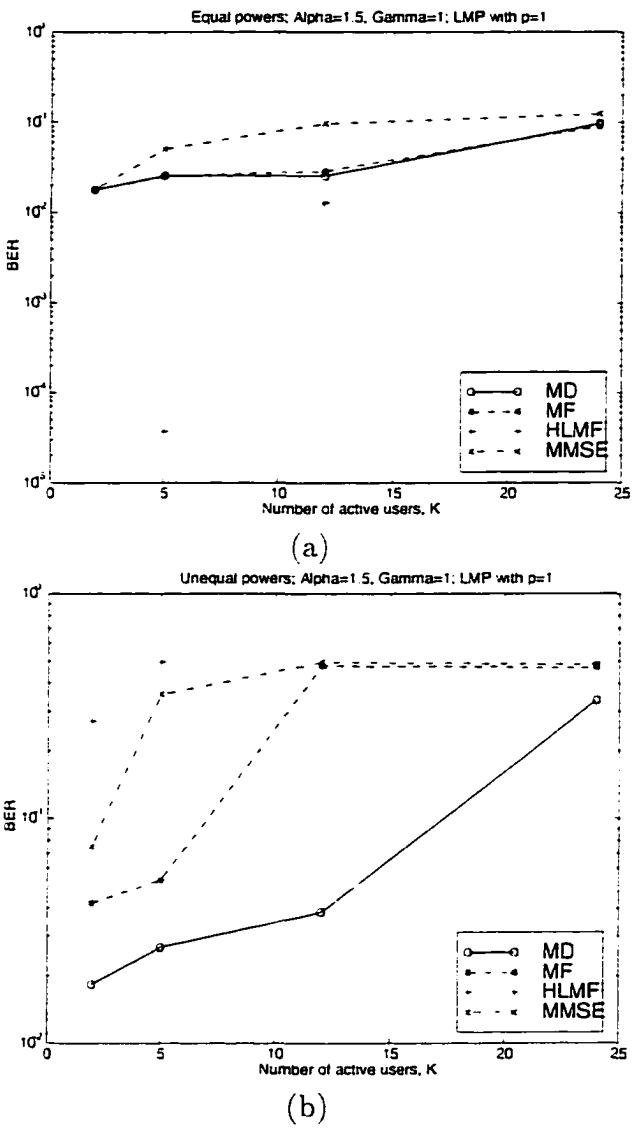

Figure 3.16 BER as a function of the number of active users K for an asynchronous DS/CDMA system: $\alpha = 1.5$, $\gamma = 1$, and LMP with $p = 1$: (a) equal powers and (b) unequal powers.

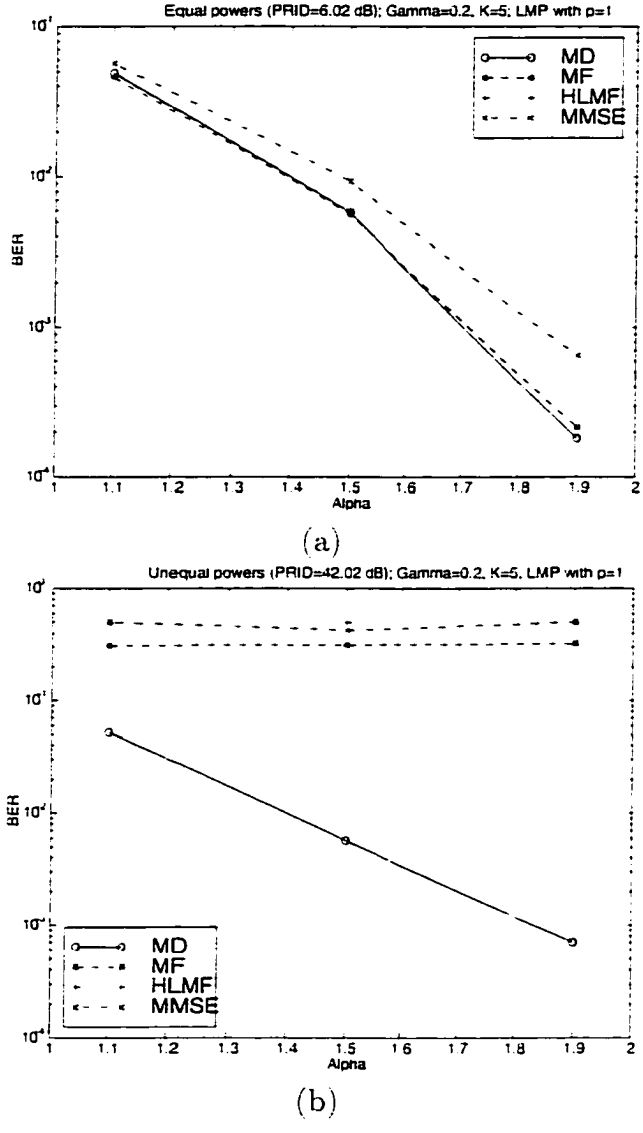

Figure 3.17 BER as a function of the charcteristic exponent α of the additive channel noise for an asynchronous DS/CDMA system: $\gamma = 0.2$, $K = 5$, $K_s = 2$, and LMP with $p = 1$: (a) equal powers (PRID = 6.02 dB) and (b) unequal powers (PRID = 42.02 dB).

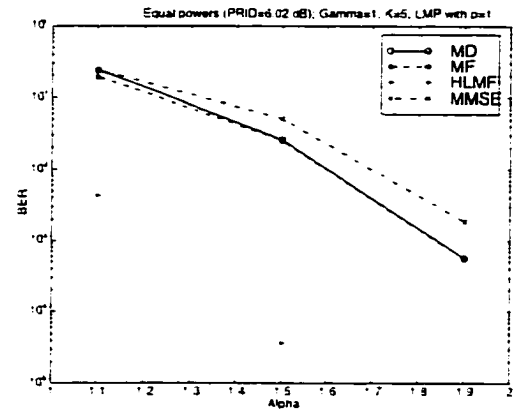

(a)

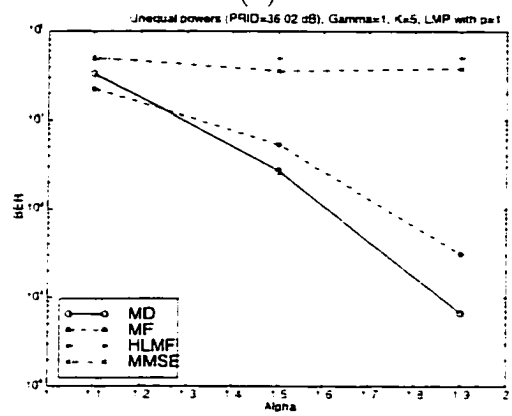

(b)

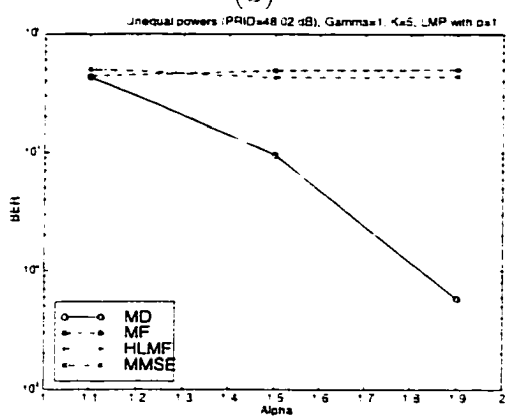

(c)

Figure 3.18 BER as a function of the charcteristic exponent α of the additive channel noise for an asynchronous DS/CDMA system: $\gamma = 1$, $K = 5$, $K_s = 2$, and LMP with $p = 1$: (a) equal powers (PRID = 6.02 dB), (b) unequal powers (PRID = 36.02 dB), and (c) unequal powers (PRID = 48.02 dB).

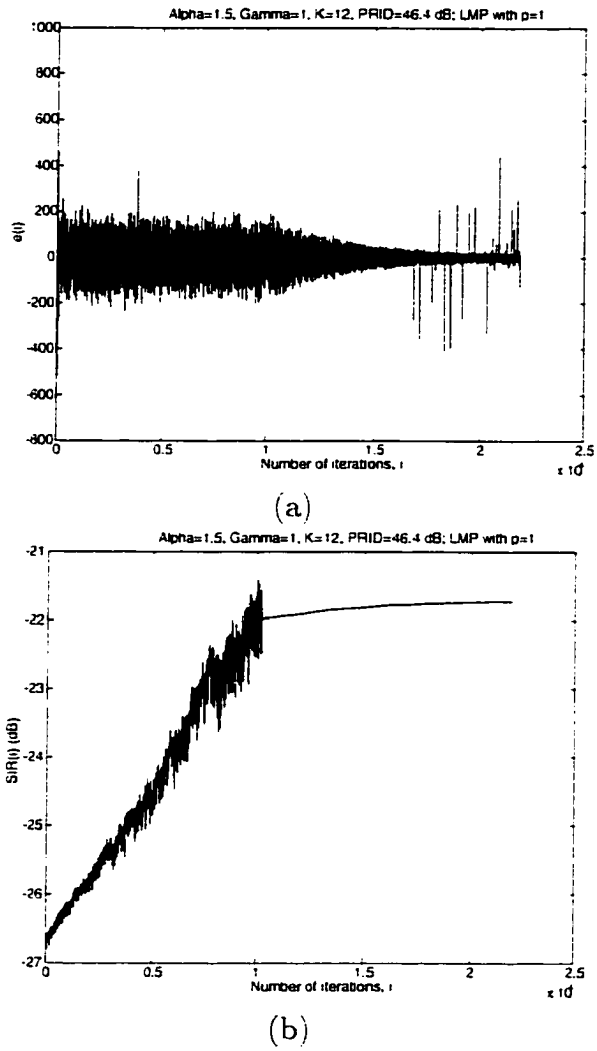

Figure 3.19 Transient behavior of LMP algorithm with $p = 1$ as a function of the number of iterations: $\alpha = 1.5$, $\gamma = 1$, PRID $= 46.4$ dB, $K = 12$, and $K_s = 5$: (a) one realization of error signal $e(i)$ and (b) output SIR in dB.

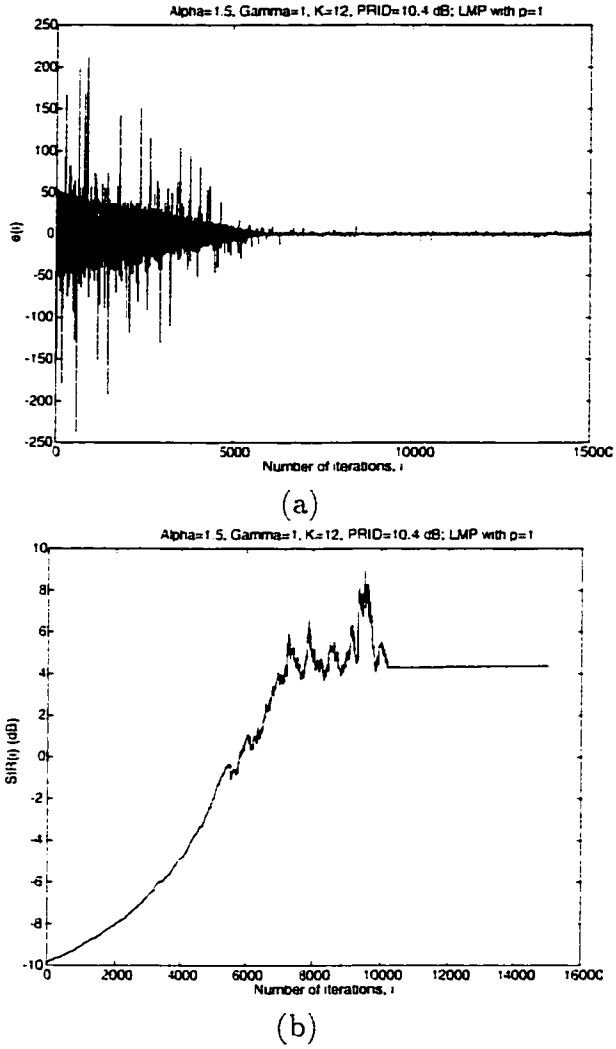

Figure 3.20 Transient behavior of LMP algorithm with $p = 1$ as a function of the number of iterations; $\alpha = 1.5$, $\gamma = 1$, PRID = 10.4 dB, $K = 12$, and $K_s = 5$: (a) one realization of error signal $e(i)$ and (b) output SIR in dB.

CHAPTER 4 LINEAR LEAST L_p-NORM INTERFERENCE SUPPRESSION

4.1 Introduction

The adaptive minimum dispersion (MD) detector [87] has been proposed for interference suppression of DS/CDMA systems in the presence of additive non-Gaussian impulsive noise modeled as a symmetric α-stable ($S\alpha S$) process [60]. The adaptive MD detector uses the least mean p-norm (LMP) algorithm [60] and has good near-far resistance.

The LMP algorithm is a member of the family of stochastic gradient-based algorithms like the LMS algorithm [90]. The LMP algorithm depends on the underlying distributions of all input signals. It is shown in [88] that when input process and desired process are non-Gaussian, the LMP algorithm converges to solutions other than the Wiener solution for various values of p. That is, for each value of p, the LMP algorithm approximates the associated optimal solution derived from ensemble averages. However, for $S\alpha S$ processes, the LMP algorithm has limitation on the values of p (i.e., $1 \leq p < \alpha \leq 2$). After reaching the optimal solution, the LMP algorithm randomly moves around the optimal solution due to the presence of gradient noise like the LMS algorithm. It is known that since the mean squared error (MSE) depends on time i, the estimation error $e(i)$ is nonstationary (see [90] for further details). The LMP algorithm has a slow convergence rate as shown in Chapter 3 and [60].

The above facts and limitation motivate us to consider the method of *least L_p-norm*

for MAI suppression. It is much likely that higher values of p (i.e., $1 \leq p < \infty$) can offer performance improvements over the adaptive MD detector using the LMP algorithm with $1 \leq p < \alpha \leq 2$. The method of *least L_p-norm* solves the linear filtering problem. This method requires no assumptions on the statistics of the input signals unlike the stochastic gradient-based algorithms. Hence the restriction of the values of p can be released in this method. The conventional least squares (LS) (or L_2-norm) method actually belongs to a family of *least L_p-norm* methods. The LS method has been widely used because of its computational simplicity. Rice and White [91] said:

> The principle of LS is normally defended (if at all) on the basis of the assumption that the errors $e(i)$ are normally distributed. It is undoubtedly true that the L_2-norm is efficient in such a situation, probably the most efficient possible. However, we would like to refer the reader to the proposal [92] that all texts on statistics should state: Normality is a myth, there never has been, and never will be, a normal distribution. Lp-norm estimation depends greatly on the distribution of the errors. Furthermore, there is a large variation in the effectiveness of various norms and no single norm is good (or even mediocre) in all situations.

The LS method provides the Wiener solution when the signals are Gaussian-distributed and ergodic. The least L_p-norm method calculates its optimal solution corresponding to a finite set of input signal vectors whenever a new input signal vector $\mathbf{r}(i)$ is available. The optimal solution remains constant during the interval of each data block. This method can be considered for both stationary and nonstationary signals like the LS method. Note that the LMP algorithm was derived under the assumption that the input vector $\mathbf{r}(i)$ applied to the transversal filter is a stationary $S\alpha S$ process.

L_p-norm estimation problem in linear regression has been an active research area of robust data modeling [93], [94], [91]. There have been two successful applications using fast algorithms for L_p-norm deconvolution proposed in [95]: least L_p-norm estima-

tion of autoregressive model coefficients of symmetric α-stable processes [96] and linear predictive modeling for sinusoidal frequency estimation[97].

This chapter considers the problem of interference suppression for DS/CDMA systems in $S\alpha S$ non-Gaussian impulsive noise channels using the L_p-norm estimation. Simulation results show that the detector based on the L_p-norm estimation provides significant performance improvements over the adaptive MD detector in a wide range of near-far situations. The proposed detector indicates superior near-far resistance.

4.2 Problem Formulation

Consider an asynchronous binary phase shift keyed (BPSK) DS/CDMA system in the presence of non-Gaussian impulsive noise modeled as a $S\alpha S$ process as shown in Section 2.1. After the front-end chip-matched filtering the received signal vector $\mathbf{r}(i) \in \Re^N$ at time $t = iT$ is given by

$$\mathbf{r}(i) = b(i)\mathbf{c} + \mathbf{j}(i) + \mathbf{v}(i), \quad -\infty < i < \infty$$

where $b(i)$ is the signal bit of the desired user, $\mathbf{c} \in \Re^N$ is the spreading code vector of the desired user, $\mathbf{j}(i) \in \Re^N$ is the interference vector, and $\mathbf{v}(i) \in \Re^N$ is the additive channel noise vector modeled as a $S\alpha S$ process. Here T is the symbol interval and N is the processing gain (see Section 2.1 for detailed description). The interference suppression can be formulated as a linear least L_p-norm estimation problem: Find an optimal tap weighting vector $\hat{\mathbf{w}}(n) \in \Re^N$ of a transversal filter such that

$$\min_{\mathbf{w}(n)} J_{L_p}(\mathbf{w}(n)), \ 1 \le p < \infty \tag{4.1}$$

where $J_{L_p}(\mathbf{w}(n))$ is a cost function defined as

$$\begin{aligned} J_{L_p}(\mathbf{w}(n)) &\triangleq \sum_{i=1}^{n} |e(i)|^p \\ &= \sum_{i=1}^{n} \left| b(i) - \mathbf{w}(n)^T \mathbf{r}(i) \right|^p . \end{aligned} \tag{4.2}$$

Here $e(i)$ is the estimation error and $\mathbf{w}(i) \in \Re^N$ is the tap weighting vector of the transversal filter. Assume that $n > N$. Then this problem can be viewed as finding a least L_p-norm solution to the overdetermined linear system of equations

$$\mathbf{A}\mathbf{w}(n) = \mathbf{b} \tag{4.3}$$

where

$$\mathbf{A} \triangleq \begin{bmatrix} \mathbf{r}(1)^T \\ \mathbf{r}(2)^T \\ \vdots \\ \mathbf{r}(n)^T \end{bmatrix} \in \Re^{n \times N}, \ \mathbf{b} \triangleq \begin{bmatrix} b(1) \\ b(2) \\ \vdots \\ b(n) \end{bmatrix} \in \Re^n, \text{ and } \mathbf{w}(n) \triangleq \begin{bmatrix} w_0(n) \\ w_1(n) \\ \vdots \\ w_{N-1}(n) \end{bmatrix} \in \Re^N. \tag{4.4}$$

An overdetermined system typically has no exact solution, since $\mathbf{b}$ cannot belong to the range of $\mathbf{A}$, denoted by $R(A)$, a proper subspace of $\Re^n$ [98], [99]. Hence we need to find the optimal vector $\hat{\mathbf{w}}(n)$ such that

$$\min_{\mathbf{w}(n)} J_{L_p}(\mathbf{w}(n)), \ 1 \leq p < \infty \tag{4.5}$$

for some suitable choice of p, where

$$\begin{aligned} J_{L_p}(\mathbf{w}(n)) &= \|\mathbf{e}(n)\|_p^p & (4.6) \\ &= \|\mathbf{b} - \mathbf{A}\mathbf{w}(n)\|_p^p & (4.7) \\ &= \sum_{i=1}^{n} |(\mathbf{b} - \mathbf{A}\mathbf{w}(n))_i|^p & (4.8) \\ &= \sum_{i=1}^{n} \left|(b(i) - \mathbf{w}(n)^T\mathbf{r}(i)\right|^p. & (4.9) \end{aligned}$$

Here $\mathbf{e}(n)$ is a residual vector and $\|\cdot\|_p^p$ represents the pth power of the L_p-norm. Different L_p-norm solutions exist for different values of p [99]. Note that when $p = 2$ the least L_p-norm solution reduces to a conventional least squares (LS) solution and when $p = 1$ it reduces to a L_1-norm or least absolute deviations (LAD) solution. Since the object function $J_{L_p}(\mathbf{w}(n))$ is convex for $1 \leq p < \infty$, the least L_p-norm solution is unique except for $p = 1$ [97].

4.3 Least L_p-Norm Solution

To obtain the least L_p-norm solution to (4.3), we use the approach given in [97]. A reader is referred to [97] for further information. First, we differentiate (4.8) with respect to the tap weights and set the partial derivatives to zero:

$$\frac{\partial J_{L_p}(\mathbf{w}(n))}{\partial w_j(n)} = 0, \quad j = 0, 1, \cdots, N-1 \tag{4.10}$$

or

$$\sum_{i=1}^{n} p\,|(\mathbf{e}(n))_i|^{p-1}\, sgn((\mathbf{e}(n))_i)\,(\mathbf{A})_{ij} = 0, \quad j = 0, 1, \cdots, N-1. \tag{4.11}$$

where $(\cdot)_i$ and $(\cdot)_{ij}$ denote the ith element of the associated vector and the ith row-qth column element of the associated matrix, respectively. Since $sgn((\mathbf{e}(n))_i) = \frac{(\mathbf{e}(n))_i}{|(\mathbf{e}(n))_i|}$, (4.11) becomes

$$\sum_{i=1}^{n} p\,|(\mathbf{e}(n))_i|^{p-2}\,(\mathbf{e}(n))_i\,(\mathbf{A})_{ij} = 0, \quad j = 0, 1, \cdots, N-1. \tag{4.12}$$

Let

$$\mathbf{W}(n) \triangleq diag\left(p\,|(\mathbf{e}(n))_1|^{p-2}, p\,|(\mathbf{e}(n))_2|^{p-2}, \cdots, p\,|(\mathbf{e}(n))_n|^{p-2}\right). \tag{4.13}$$

Then (4.12) can be written as

$$\left(\mathbf{A}^T\mathbf{W}(n)\mathbf{e}(n)\right)_j = 0, \quad j = 0, 1, \cdots, N-1. \tag{4.14}$$

Substituting $\mathbf{e}(n) = \mathbf{b} - \mathbf{A}\mathbf{w}(n)$ into (4.14) yields

$$\mathbf{A}^T\mathbf{W}(n)\left(\mathbf{A}\mathbf{w}(n) - \mathbf{b}\right) = 0 \tag{4.15}$$

or

$$\mathbf{A}^T\mathbf{W}(n)\mathbf{A}\mathbf{w}(n) = \mathbf{A}^T\mathbf{W}(n)\mathbf{b} \tag{4.16}$$

which is known as the *weighted normal equations*. Since the diagonal weighting matrix $\mathbf{W}(n)$ is a function of the residual vector $\mathbf{e}(n)$, the weighted normal equations are nonlinear and usually must be solved via iterative methods such as the *iteratively reweighted least squares* (IRLS) [100], [95], [97] or the *residual steepest descent* (RSD) [95], [101] algorithm. When $p = 2$, the matrix $\mathbf{W}(n)$ becomes a scaled version of an identity matrix and (4.16) thus reduces to the normal equations of the conventional LS. The IRLS algorithm is summarized in Table 4.1. Here an absolute value of the normalized L_p-norm differential of the residual vectors is used as a stopping condition of convergence [96].

$$e_{sc}(n;k+1) = \frac{\left| \|\mathbf{e}(n;k+1)\|_p - \|\mathbf{e}(n;k)\|_p \right|}{\|\mathbf{e}(n;k)\|_p}, \quad k = 0, 1, \cdots. \tag{4.17}$$

Unfortunately, the recursive least L_p-norm algorithm is hard to find because $\mathbf{W}(n)$ is a function of the residual vector $\mathbf{e}(n)$ (see (4.13)). Hence, adaptive algorithms cannot be easily developed for least L_p-norm estimation. The IRLS algorithm converges for $2 \leq p < 3$, while it diverges for $3 \leq p < \infty$ [102], [100], [103], [104]. For $1 \leq p < 2$, the IRLS algorithm also converge under weak conditions [96], [97], [100]. Hence, we restrict our attention to the least L_p-norm solutions with $1 \leq p < 3$. The least L_p-norm ($1 \leq p < 2$) estimates are consistent like the LS and LAD estimates [105], [96].

The IRLS algorithm has more computational complexity than the LMP algorithm. The IRLS algorithm requires the inversion of $\mathbf{A}^T\mathbf{W}(n;k)\mathbf{A} \in \Re^{N \times N}$ of order N^3 complexity [106] as shown in step 4 of Table 4.1. The IRLS algorithm takes $O(K_{it} \cdot N^3)$ per symbol, while the LMP algorithm takes $O(2N)$ per symbol. Here $O(N)$ represents the computational complexity of order N and K_{it} denotes the number of iterations of the IRLS algorithm. However, the IRLS algorithm gives better performance, but at the cost of its computational complexity.

Table 4.1 IRLS Algorithm

Step	Description
1	Initialize tap weighting vector $\mathbf{w}(n;0) = \left(\mathbf{A}^T\mathbf{A}\right)^{-1}\mathbf{A}^T\mathbf{b}$
2	Calculate residual vector $(\mathbf{e}(n;k))_i = (\mathbf{b} - \mathbf{A}\mathbf{w}(n;k))_i,\ i = 1, 2, \cdots, n$
3	Calculate diagonal weighting matrix $(\mathbf{W}(n;k))_{ii} = \begin{cases} \lvert(\mathbf{e}(n;k))_i\rvert^{p-2} & \text{if } \lvert(\mathbf{e}(n;k))_i\rvert \geq \epsilon \\ \epsilon^{p-2} & \text{if } \lvert(\mathbf{e}(n;k))_i\rvert < \epsilon \end{cases},\ i = 1, 2, \cdots, n,$ where ϵ is a positive small value to avoid the ith residual $(\mathbf{e}(n;k))_i$ with value close to zero
4	Update tap weighting vector $\mathbf{w}(n;k+1) = \left(\mathbf{A}^T\mathbf{W}(n;k)\mathbf{A}\right)^{-1}\mathbf{A}^T\mathbf{W}(n;k)\mathbf{b}$
5	Go to step 2 or stop when convergence is achieved, i.e., $e_{sc}(n;k+1)$ is less than ε_{sc}

4.4 Simulation Results

We compare the BER performance of the interference suppression using the least L_p-norm criterion with that of the adaptive MD, MF, MMSE, and HLMF detectors via Monte Carlo simulation in the same simulation environment as in Section 2.2. We consider an asynchronous BPSK DS/CDMA system with $K = 5$ users and $K_s = 2$ users. In step 1 of the IRLS algorithm, the tap weighting vector is initialized as the spreading code vector $\mathbf{c}$ of the desired user instead of the LS solution vector. In each of the simulations the value of p in the least L_p-norm criterion is set to 1, unless stated otherwise.

Figures 4.1 - 4.4 show the BER performance as a function of the PRID for the four condition sets such as $\{\alpha = 1.1 \text{ and } \gamma = 0.2\}$, $\{\alpha = 1.1 \text{ and } \gamma = 1\}$, $\{\alpha = 1.5 \text{ and } \gamma = 0.2\}$, and $\{\alpha = 1.5 \text{ and } \gamma = 1\}$, respectively. Here α is the characteristic exponent and γ is the dispersion of the $S\alpha S$ noise process. We use the following acronyms in Figure 4.1 through Figure 4.4: LP stands for the least L_p-norm detector using the IRLS algorithm, MD for the adaptive minimum dispersion detector using the LMP

algorithm, MF for the conventional matched filter detector, MMSE for the minimum mean squared error detector, and HLMF for the hard-limiting matched filter detector. The performance of the least L_p-norm detector is nearly insensitive to all PRID levels. This shows that the proposed detector gives much better near-far resistance than the adaptive MD detector in a wide range of near-far environments ranging from mild to severe situations. In particular, its BER performance does not degrade even in severe near-far situations unlike the adaptive MD detector. Hence the proposed detector is more effective against severe near-far environments than the adaptive MD detector. In addition, the proposed detector provides significant BER performance improvements over the adaptive MD detector for all PRID levels. The least L_p-norm detector still performs well for all PRID levels even though none of the detectors perform decently with highly impulsive noise with $\gamma = 1$. The steady state performance heavily depends on the number of rows n of matrix $\mathbf{A}$, i.e. data block size to be estimated. It is experimentally observed that $n = 32$ gives best BER performance for the current simulation environment

Figure 4.5 through Figure 4.8 show the BER performance as a function of p for $\gamma = 0.2$ (with o-mark) and $\gamma = 1.0$ (with $*$-mark), and $\alpha = 1.5$, $K = 5$: PRID = 6.02, 18.02, 30.02, and 42.02 dB, respectively. Given $1 \leq p < 3$, the simulation results show that the L_p-norm with $p = 2.9$ is best for PRID = 6.02, 18.02, 42.02 dB, while the L_p-norm with $p = 2.7$ for PRID = 30.02 dB.

Figure 4.9 and Figure 4.10 show the BER performance of the L_p-norm detector as a function of the PRID for different values of p for the two condition sets such as $\{\alpha = 1.5, \gamma = 0.2, K = 5, \text{and } K_s = 2\}$ and $\{\alpha = 1.5, \gamma = 1.0, K = 5, \text{and } K_s = 2\}$, respectively. The detector's BER performance depends on the value of p in the L_p-norm. The BER performance significantly improves as p approaches 3.

Figure 4.11 shows the transient state behavior of the proposed detector using the IRLS algorithm as a function of number of iterations for $\alpha = 1.5$, $\gamma = 0.2$, PRID = 48.02 dB, and $p = 2.7$. In step 5 of Table 4.1, ε_{sc} is set to 10^{-3}. The IRLS algorithm

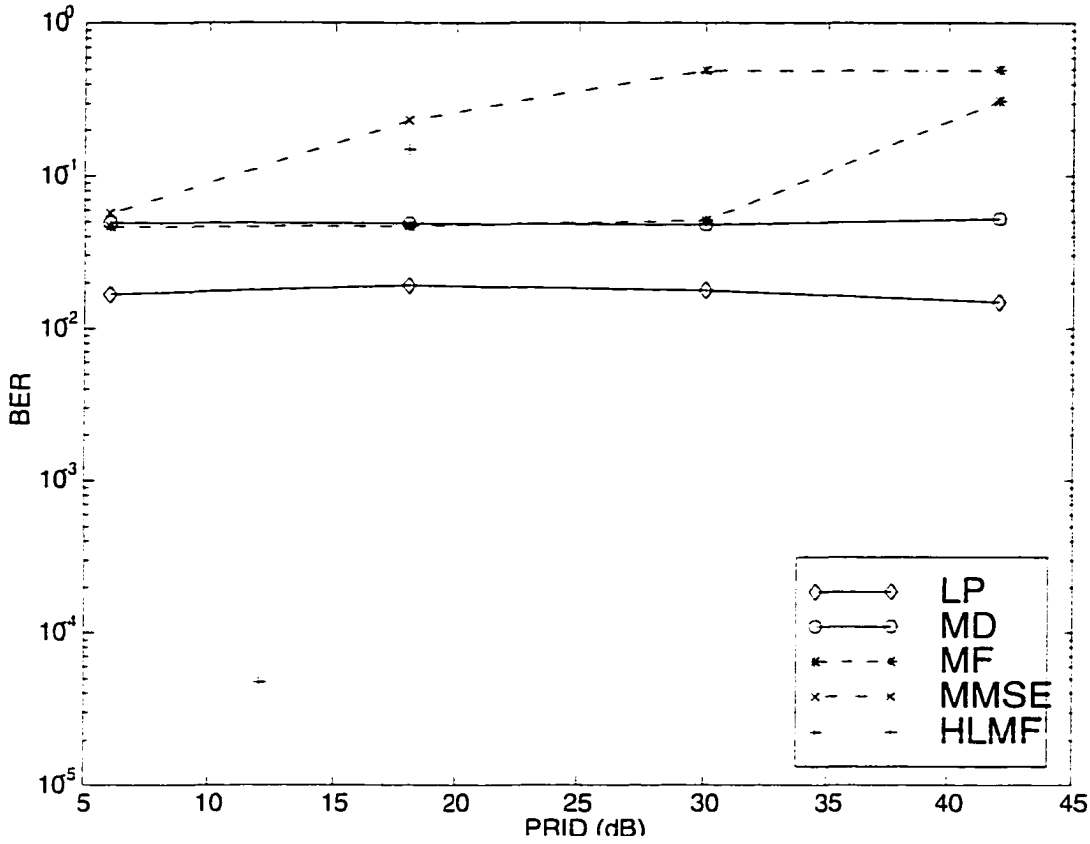

Figure 4.1 BER as a function of the PRID for an asynchronous DS/CDMA system: $\alpha = 1.1$, $\gamma = 0.2$, $K = 5$, $K_s = 2$, and least L_p-norm with $p = 1$.

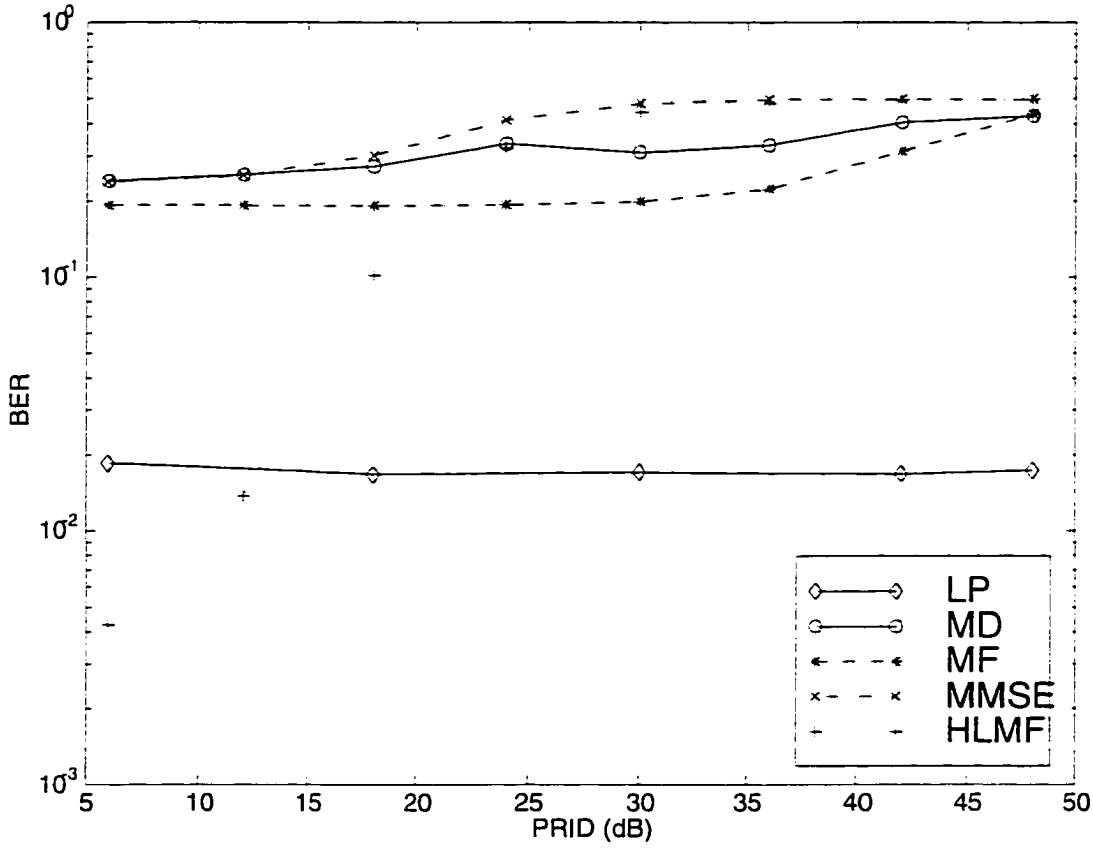

Figure 4.2 BER as a function of the PRID for an asynchronous DS/CDMA system: $\alpha = 1.1$, $\gamma = 1$, $K = 5$, $K_s = 2$, and least L_p-norm with $p = 1$.

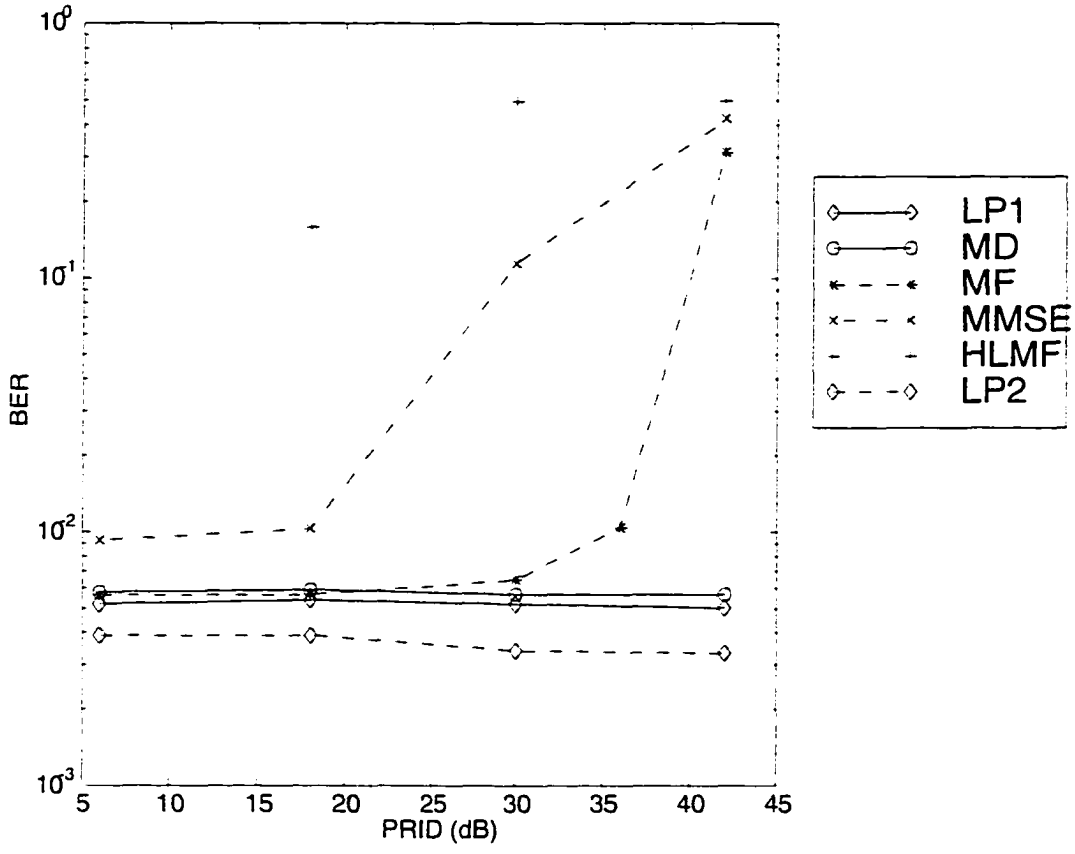

Figure 4.3 BER as a function of the PRID for an asynchronous DS/CDMA system: $\alpha = 1.5$, $\gamma = 0.2$, $K = 5$, $K_s = 2$, and least L_p-norm with $p = 1.49$ (LP1) and $p = 1.6$ (LP2).

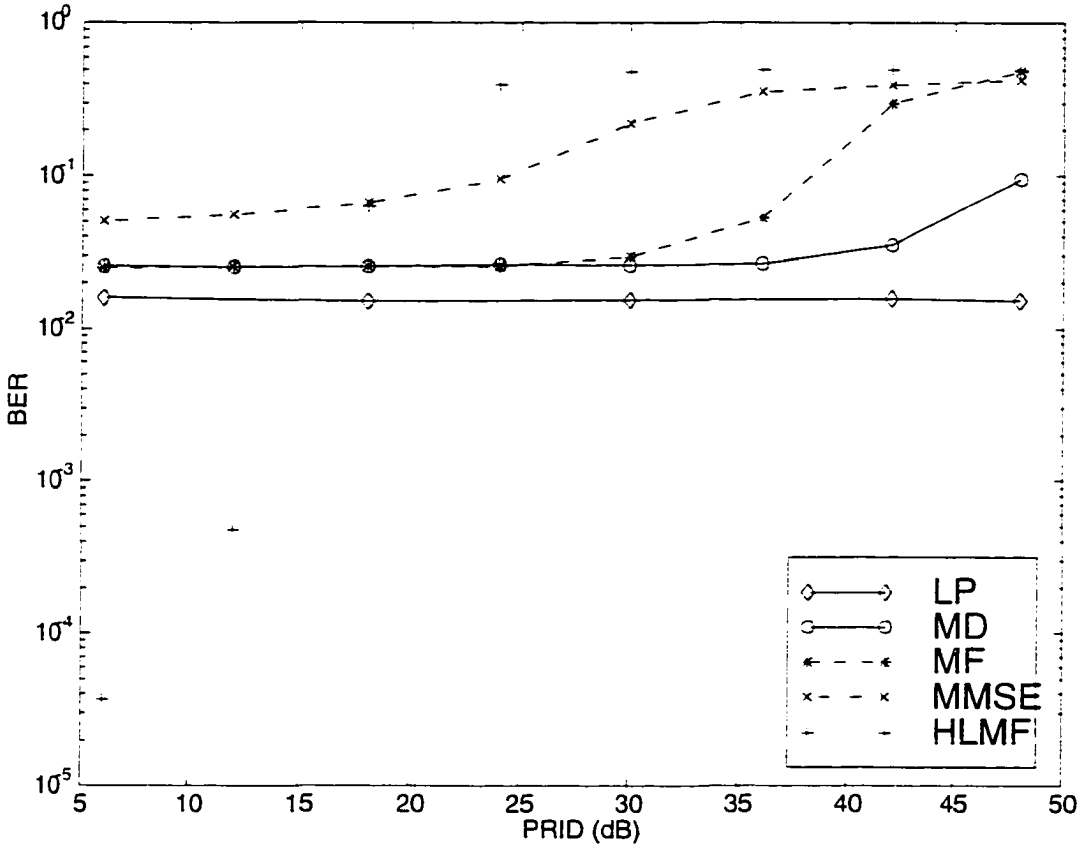

Figure 4.4 BER as a function of the PRID for an asynchronous DS/CDMA system: $\alpha = 1.5$, $\gamma = 1$, $K = 5$, $K_s = 2$, and least L_p-norm with $p = 1$.

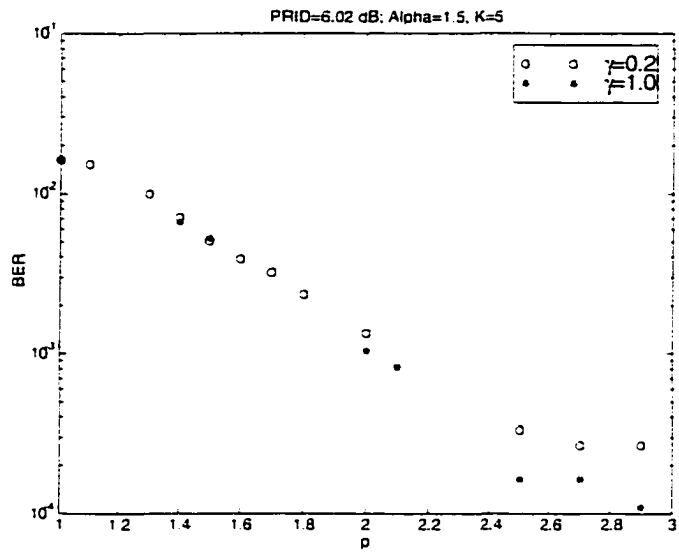

Figure 4.5 BER of the L_p-norm detector as a function of p for different values of γ: $\alpha = 1.5$, $K = 5$, $K_s = 2$, and PRID = 6.02 dB.

takes on the order of a few tens of number of iterations to converge to a steady state for each new symbol. The number of iterations actually depends on the stopping condition value ε_{sc}. If ε_{sc} is larger, fewer iterations are required. In this case, convergence can be obtained within a few iterations. The IRLS algorithm operates on data blocks of symbols, while the LMP algorithm works on a symbol-by-symbol basis. Therefore it is not possible to compare the convergence rates of the IRLS with those of the LMP algorithms quantitatively.

The limitation of the proposed detector is that the IRLS algorithm may have numerical problems. In step 4 of the IRLS algorithm $\mathbf{A}^T\mathbf{W}(n;k)\mathbf{A}$ may be close to singular since, as described in [32], the input correlation matrix $\mathbf{A}^T\mathbf{A}$ is nearly singular when the number of all active users K is less than the number of chips N and the Gaussian noise variance is small compared to signal power. However, it is less likely that this numerical problem will occur in the presence of additive non-Gaussian impulsive noise modeled as a $S\alpha S$ process since it has an infinite variance.

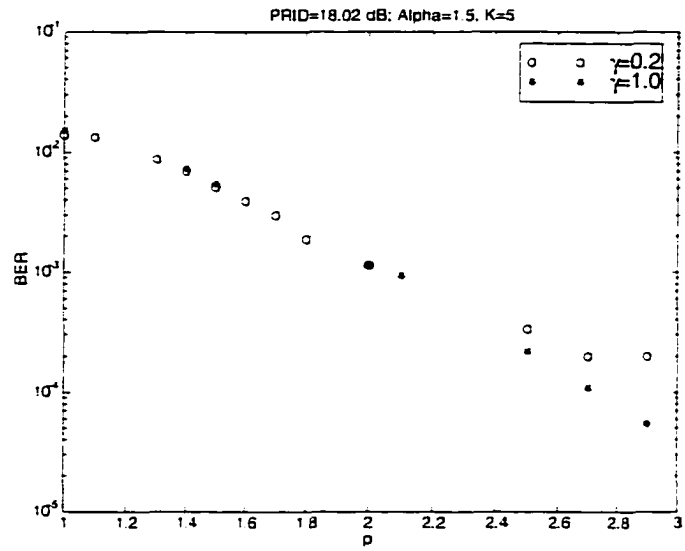

Figure 4.6 BER of the L_p-norm detector as a function of p for different values of γ; $\alpha = 1.5$, $K = 5$, $K_s = 2$, and PRID = 18.02 dB.

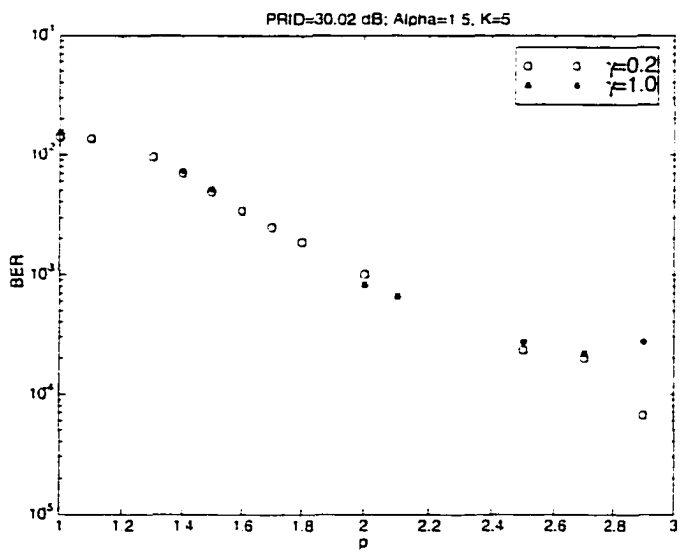

Figure 4.7 BER of the L_p-norm detector as a function of p for different values of γ; $\alpha = 1.5$, $K = 5$, $K_s = 2$, and PRID = 30.02 dB.

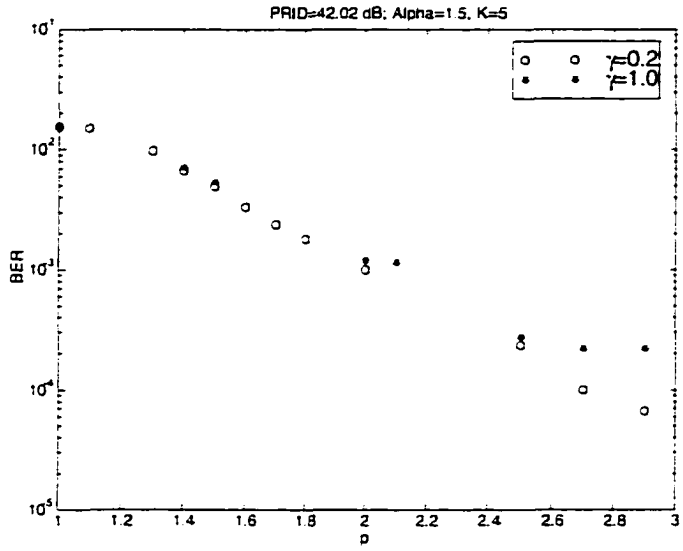

Figure 4.8 BER of the L_p-norm detector as a function of p for different values of γ: $\alpha = 1.5$, $K = 5$, $K_s = 2$, and PRID = 42.02 dB.

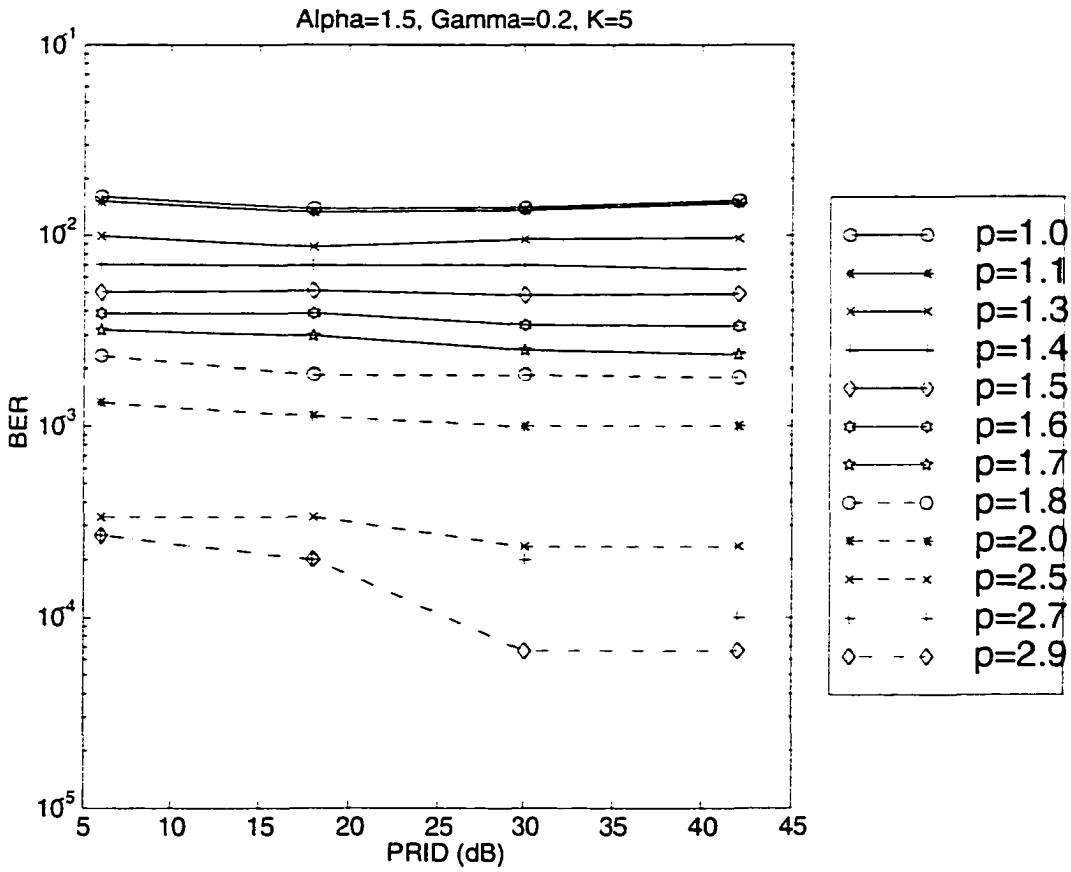

Figure 4.9 BER of the L_p-norm detector as a function of the PRID for different values of p: $\alpha = 1.5$, $\gamma = 0.2$, $K = 5$, and $K_s = 2$.

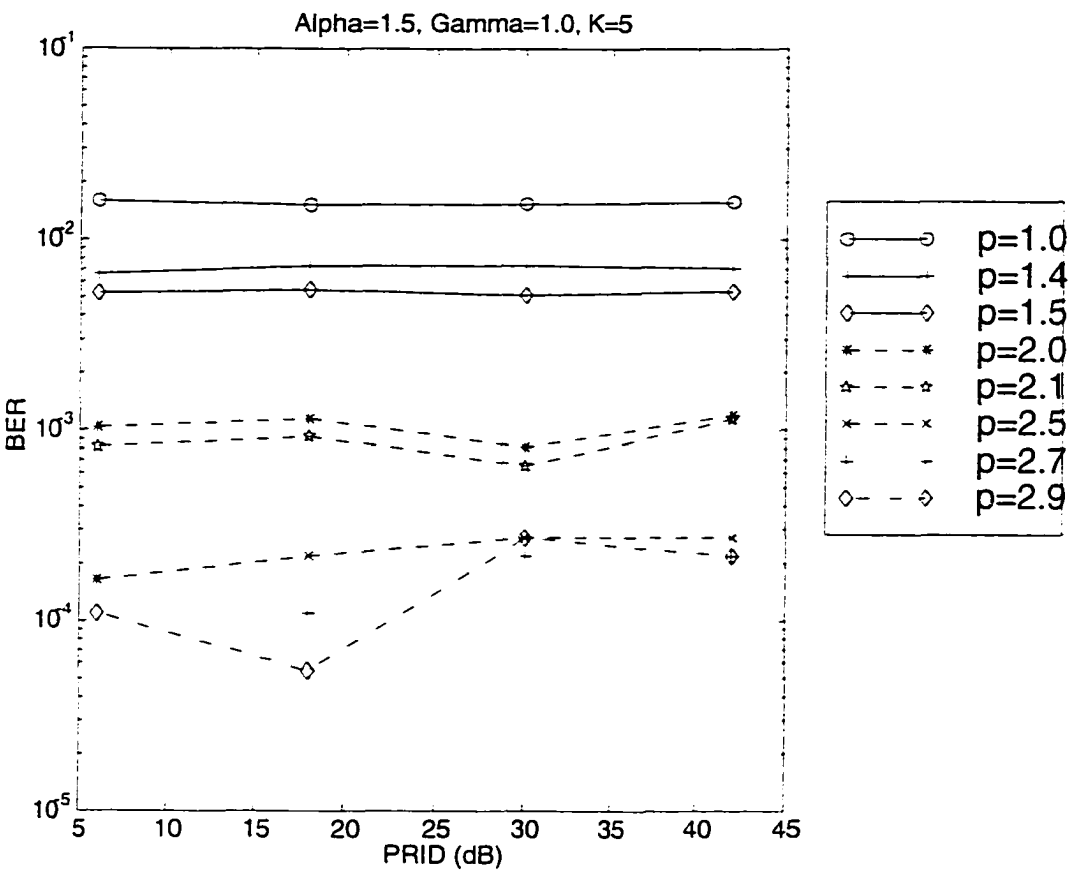

Figure 4.10 BER of the L_p-norm detector as a function of the PRID for different values of p: $\alpha = 1.5$, $\gamma = 1.0$, $K = 5$, and $K_s = 2$.

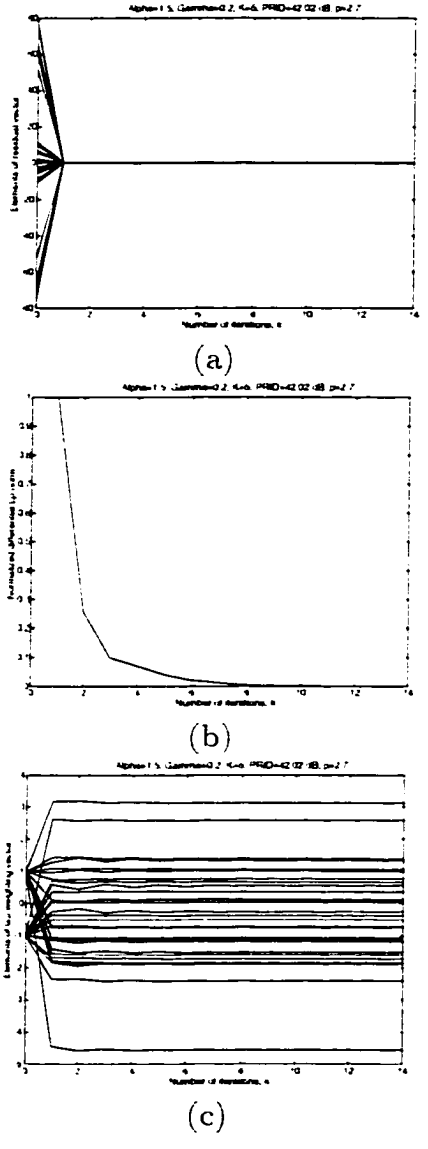

(a)

(b)

(c)

Figure 4.11 Transient behavior of the IRLS algorithm as a function of number of iterations: (a) residual vector $\mathbf{e}(n;k) \in \Re^n$, $n = 32$, (b) $e_{sc}(n;k)$, (c) least L_p-norm solutions for all elements of the tap weighting vector $\mathbf{w}(n;k)$: $\alpha = 1.5$, $\gamma = 0.2$, $K = 5$, $K_s = 2$, PRID = 42.02 dB, and $p = 2.7$.

CHAPTER 5 FUZZY HYBRID INTERFERENCE SUPPRESSION

5.1 Introduction

In this work, we propose a fuzzy hybrid detector for interference suppression in DS/CDMA systems when additive channel noise modeled as a symmetric α-stable ($S\alpha S$) process is present. In multiple-access impulsive noise channels, nonlinear detectors such as the hard-limiting matched filter (HLMF) are more effective than the matched filter (MF) detector against impulsive noise-limited situation. The linear MF detector is more effective against multiple-access interference (MAI)-limited situation than the HLMF detector [58]. However, the linear MF detector has a near-far problem. To combat the near-far problem in multiple-access impulsive noise channels, the adaptive minimum dispersion (MD) detector has been proposed for DS/CDMA systems in the presence of additive channel noise modeled as a $S\alpha S$ process. The adaptive MD detector has good near-far resistance [87]. The performance of the adaptive MD detector is comparable to that of the conventional MF detector and inferior to that of the HLMF detector in impulsive noise-limited environments where additive impulsive noise dominates over MAI. Since the HLMF detector is locally optimum for a Laplacian noise density [75], it performs well in impulsive noise-limited environments [49], [66], [87] (see Chapter 3). A hybrid detector that combines the linear MF and the HLMF was introduced in the form of adaptive detection of signals in single-user impulsive noise environments. This hybrid detector was adaptively implemented such that an incremental signal-to-noise

ratio (SNR) is maximized. This detector performs well in a wide range of the unknown underlying noise environments [107].

These facts motivate us to consider a hybrid detection scheme which combines the best features of the adaptive MD detector for MAI-limited environment and the HLMF detector for impulsive noise-limited environment. The hybrid approach employs a linear combination of the outputs (or test statistics) of the adaptive MD and HLMF detectors. The problem is how to control the mixing parameter effectively. The mixing parameter depends on the underlying channel environments. Simulation results show that the fuzzy hybrid detector makes the best use of the advantages of the adaptive MD and HLMF detectors in a wide range of the underlying channel environments that range from impulsive noise-limited to MAI-limited environments.

5.2 Problem Formulation

Consider an asynchronous binary phase shift keyed (BPSK) DS/CDMA system in the presence of non-Gaussian impulsive noise modeled as a $S\alpha S$ process as shown in Section 2.1. The proposed detector scheme is shown in Figure 5.1. The resulting test statistic is given by

$$Z(i) = \beta \cdot \mathbf{w}(i)^T \mathbf{r}(i) + (1-\beta) \cdot \mathbf{c}^T \mathbf{g}(\mathbf{r}(i)), \quad -\infty < i < \infty \tag{5.1}$$

where $\beta \in [0,1]$ is a mixing parameter, $\mathbf{r}(i) \in \Re^N$ is the received signal vector at ith symbol interval, $\mathbf{w}(i) \in \Re^N$ is the tap weighting vector of adaptive MD detector, $\mathbf{c} \in \Re^N$ is the desired user's spreading code, and $\mathbf{g}(\mathbf{r}(i) \in \Re^N$ is a nonlinear vector function. The first term indicates the scaled test statistic of the adaptive MD detector and the second term indicates that of the HLMF detector. The adaptive MD detector is operated independently using the error signal $e(i) = b(i) - \mathbf{w}(i)^T \mathbf{r}(i)$ where $b(i)$ is a desired signal bit. For the HLMF $\mathbf{g}(\mathbf{r}(i))$ is chosen as $\mathbf{g}(\mathbf{r}(i)) = [sign(r_0(i)), sign(r_1(i)), \cdots, sign(r_{N-1}(i))]^T$. For $\beta = 0$ the test statistic of the hybrid detector reduces to that of the HLMF, while

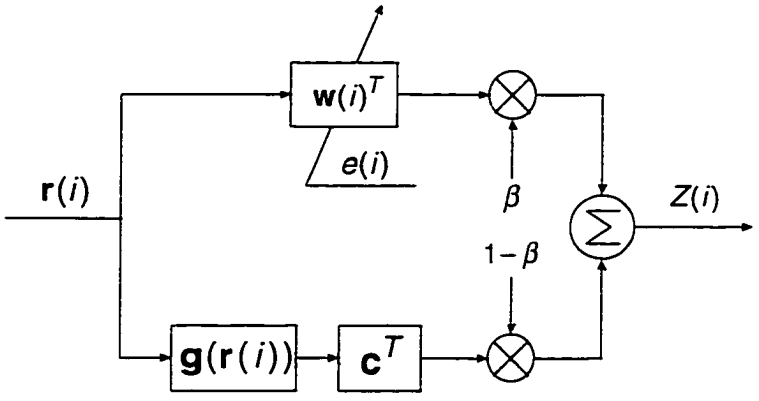

Figure 5.1 Hybrid detector model.

for $\beta = 1$ it reduces to that of the linear adaptive MD detector. A fuzzy system controls the mixing parameter β depending on the underlying channel environments.

5.3 Fuzzy System

The fuzzy system is a single input, single output system. The input variable is the power ratio of the interfering users to the desired user (PRID) given in (2.22). The output variable is the mixing parameter β. The PRID is given for each of the simulations.

Previous simulation results, which are shown in Chapter 3 and [87], show that there is a crossover point beyond which the linear adaptive MD detector is superior to the HLMF detector in terms of BER as the PRID increases. Figure 5.2 is a sketch of the BER performance of the linear adaptive MD and HLMF detectors as a function of the PRID based on the previous simulation results.

This crossover point gets higher as the dispersion of the additive noise increases, i.e., the additive noise becomes more impulsive. In most cases the higher crossover point occurs beyond the desirable range of BER performance as shown in [49]. In our case $\gamma = 1$ is large enough to provide a severe impulsive environment for most α's of the additive impulsive noise. From our specific simulation results, it is observed that the crossover points are roughly located between PRID = 13 dB and PRID = 17 dB (see

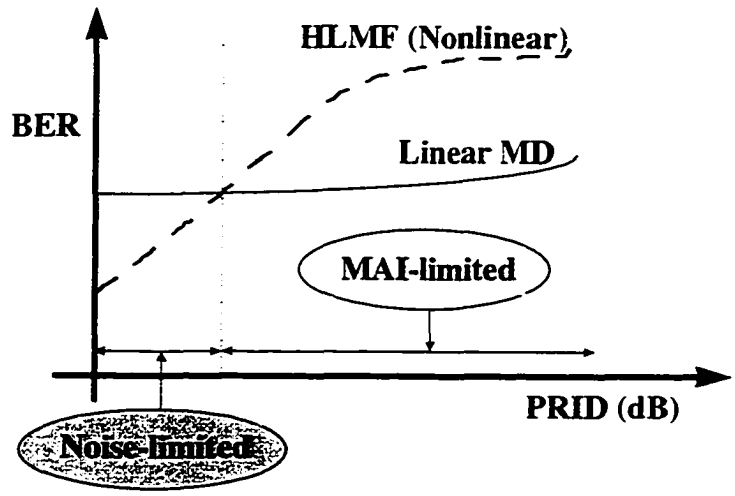

Figure 5.2 Sketch of the BER performance as a function of the PRID for an asynchronous DS/CDMA system.

Figures 3.2 - 3.10). Therefore, we choose PRID = 15 dB as the nominal crossover point for our problem. The channel environments can be divided into two situations: impulsive noise-limited (if the PRID is less than the nominal crossover point) and MAI-limited (if the PRID is larger than the nominal crossover point).

The PRID is a convenient quantity for performance comparison in simulations. However, in practice the carrier-to-interference ratio (CIR) is used. The CIR [108] is given by

$$\mathrm{CIR} = \frac{E_b}{I_o} \cdot \frac{B_c}{R_b} \tag{5.2}$$

where E_b is the energy per bit, I_o is the interference power per Hz, R_b is the bit per second, and B_c is the radio channel bandwidth in Hz. The PRID is closely related to the $\frac{E_b}{I_o}$. Since the $\frac{E_b}{I_o}$ is determined by the measured signal power [9], the PRID can be estimated.

From the observations about the nominal crossover point and the characteristics of the adaptive MD and HLMF detectors, we will determine fuzzy sets corresponding to the input and output variables as shown in Figure 5.3 and Figure 5.4. For the input PRID variable we define two fuzzy sets. The sets are for low (L) and high (H) levels of

the PRID. The membership function $m_{tz}(x)$ of each of the fuzzy sets is a trapezoidal function [109], [110] given by

$$\begin{aligned} m_{tz}(x) &= trapezoid(x; a, b, c, d) \\ &= \max\left(\min\left(\frac{x-a}{b-a}, 1, \frac{d-x}{d-c}\right), 0\right). \end{aligned} \tag{5.3}$$

Table 5.1 shows the parameters for trapezoidal membership functions used in the input fuzzy sets. Each membership function is symmetric about the nominal crossover point at PRID = 15 dB. Figure 5.3 shows the membership functions of the input fuzzy sets.

Table 5.1 Parameters for Trapezoidal Membership Functions

	Parameters	a	b	c	d
Fuzzy sets	L	-18	-12	12	18
(PRID)	H	12	18	80	86

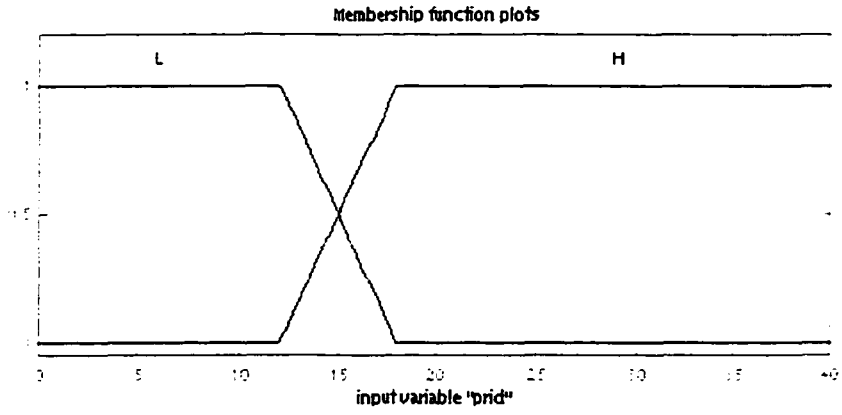

Figure 5.3 Membership functions of the input fuzzy sets.

For the output variable β we define two fuzzy sets such as low(L) and high(H) depending the output value β ranging between 0 and 1. The membership function $m_G(x)$ of each of the fuzzy sets is Gaussian function [110] given by

$$m_G(x) = \exp\left[-\frac{1}{2}\frac{(x-c)^2}{\sigma^2}\right] \tag{5.4}$$

where c is a position parameter and σ is a shape parameter. c's are set to 0 and 1. σ is set to 0.03356. The Gaussian functions are heavily distributed around the vicinity of $\beta = 0$ and $\beta = 1$ according to the characteristics of the adaptive MD and HLMF detectors depending on β as shown in (5.1). Figure 5.4 shows the membership functions of the two output fuzzy sets.

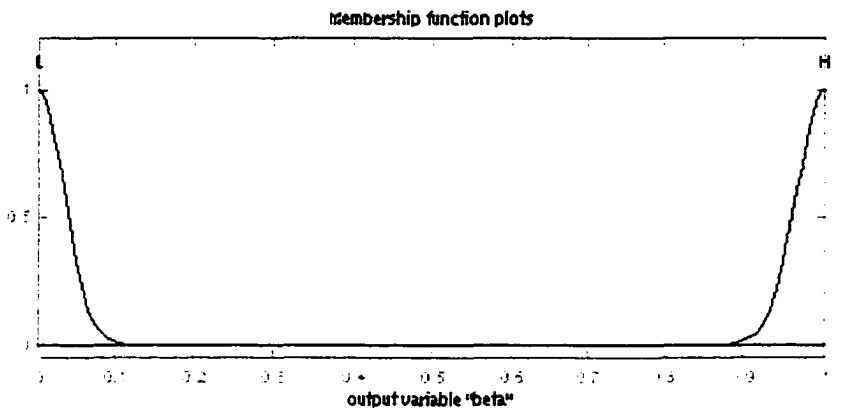

Figure 5.4 Membership functions of the output fuzzy sets.

Fuzzy rules can be written as antecedent-consequent pairs of IF-THEN statements [109], [111]. The two linguistic fuzzy rules are:

IF PRID is L , THEN β is L

and

IF PRID is H , THEN β is H.

Figure 5.5 shows the architecture of the additive [111] (or Mamdani [109]) fuzzy system. Figure 5.6 shows the fuzzy correlation-minimum inference system using minimum and sum for fuzzy implication and aggregation, respectively. Input fuzzy sets map the crisp input value (for example, PRID = 16 dB) of the PRID into antecedent membership or fit values. Each of the antecedent fit values scale the membership function of the consequent fuzzy set with pairwise minimum. The fuzzy system sums the clipped

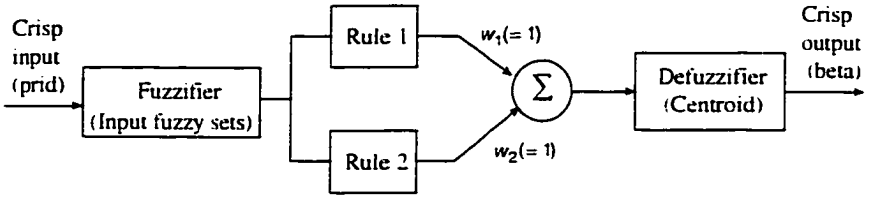

Figure 5.5 Additive fuzzy system.

waveforms of the membership functions corresponding to the consequent fuzzy sets and computes the fuzzy centroid of the output membership functions. This defuzzification produces the crisp system output (for example, $\beta = 0.614$).

Figure 5.7 shows a fuzzy input-output relationship generated by the fuzzy system. This relationship shows how the mixing parameter β varies as a function of the input variable, PRID. The mixing parameter β is close to zero or very small when the PRID is less than 12.021 dB. This indicates that the resulting test statistic comes from the HLMF detector. When the PRID is larger than 18.021 dB, β goes towards one. In this case the adaptive MD detector is selected. When the PRID level is in the range from 12.021 dB to 18.021 dB, β takes on intermediate values between 0 and 1. The fuzzy system is insensitive to the PRID levels when the PRID is either larger than 18.021 dB or less than 12.021 dB, because β remains nearly unchanged. In the transition range from 12.021 dB to 18.021 dB, the fuzzy hybrid detector could suffer from a performance degradation to some extent, but it can be robust to the PRID mismatch. The fuzzy system was designed using the MATLAB fuzzy logic toolbox [110].

5.4 Simulation Results

The fuzzy hybrid detector is tested via Monte Carlo simulation in the same simulation environment as in Section 2.2. We compare the BER performance of the fuzzy hybrid detector with that of other detectors: adaptive MD, MF, and HLMF. We consider an asynchronous BPSK DS/CDMA system with $K = 5$ users and $K_s = 2$ users.

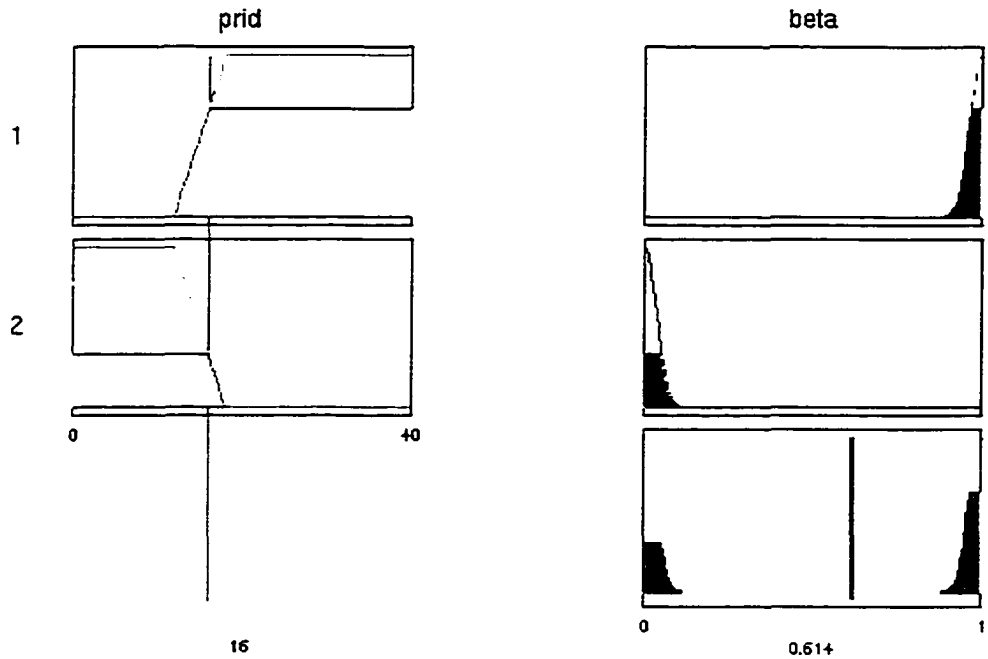

Figure 5.6 The fuzzy correlation-minimum inference system using minimum and sum for fuzzy implication and aggregation, respectively: In this case PRID = 16 dB which gives the membership degree of $m_H(16) = 0.667$, $m_L(16) = 0.333$: The centroid output of the system is $\beta = 0.614$.

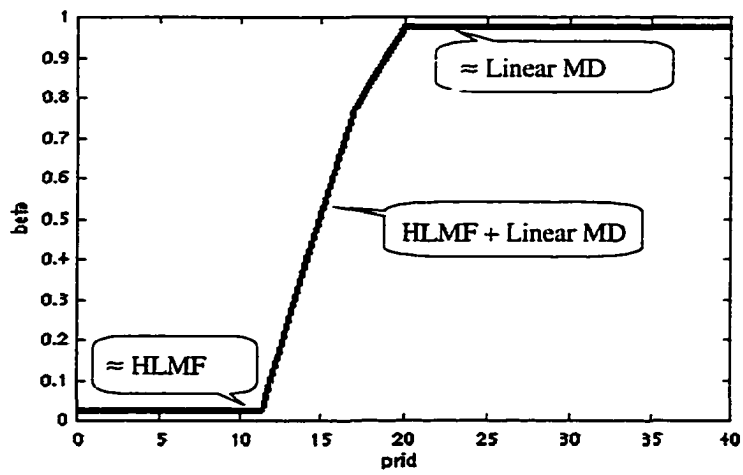

Figure 5.7 Mixing parameter β as a function of the input variable, PRID.

Figure 5.8 through Figure 5.10 show the BER performance as a function of the PRID for the three condition sets such as $\{\alpha = 1.1$ and $\gamma = 0.2\}$, $\{\alpha = 1.5$ and $\gamma = 1\}$, and $\{\alpha = 1.9$ and $\gamma = 1\}$, respectively. Here α is the characteristic exponent and γ is the dispersion of the $S\alpha S$ noise process. For each PRID level the performance of the fuzzy hybrid detector is nearly comparable to whichever detector performs better. Note that the HLMF detector performs better than the adaptive MD detector using the least mean p-norm (LMP) algorithm [60] when the PRID is less than about 18 dB and vice versa elsewhere. The main advantage of the fuzzy hybrid detector is that this detector provides significant performance improvements over the adaptive MD detector for impulsive noise-limited environments (i.e., if the PRID is less than the nominal crossover point of PRID = 15 dB).

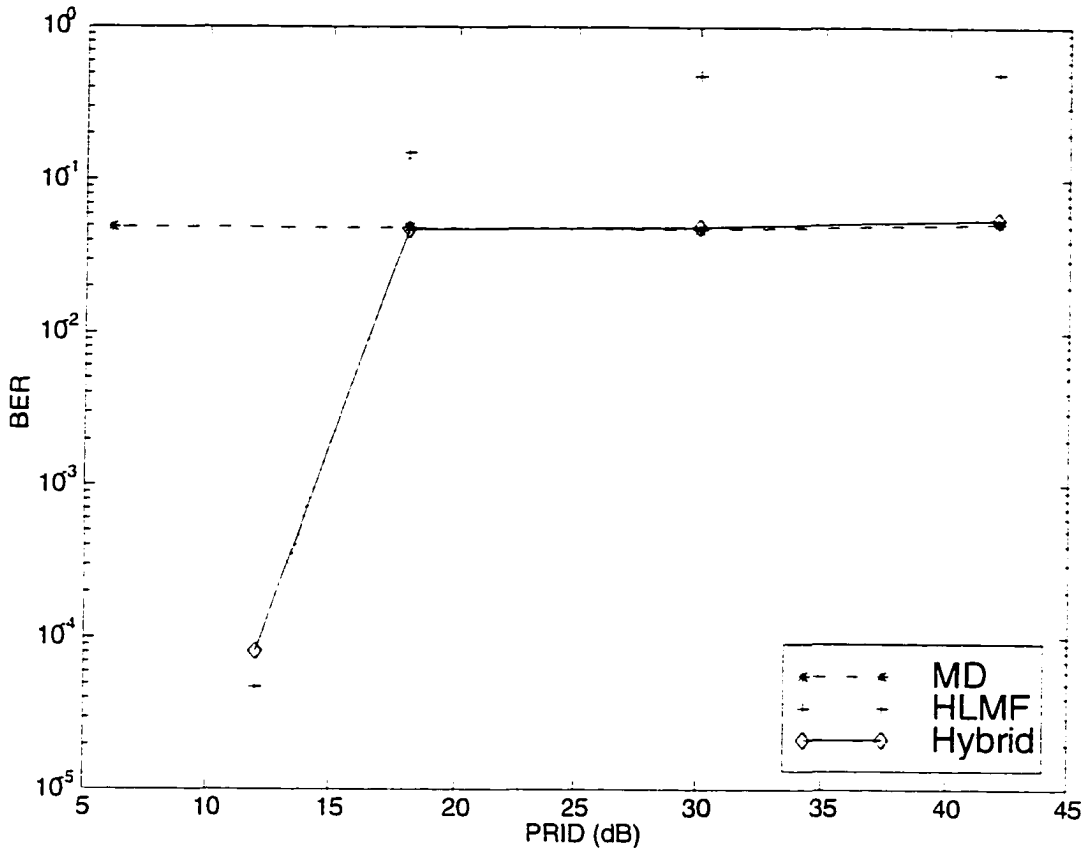

Figure 5.8 BER as a function of the PRID for an asynchronous DS/CDMA system: $\alpha = 1.1$, $\gamma = 0.2$, $K = 5$, $K_s = 2$, and LMP with $p = 1$.

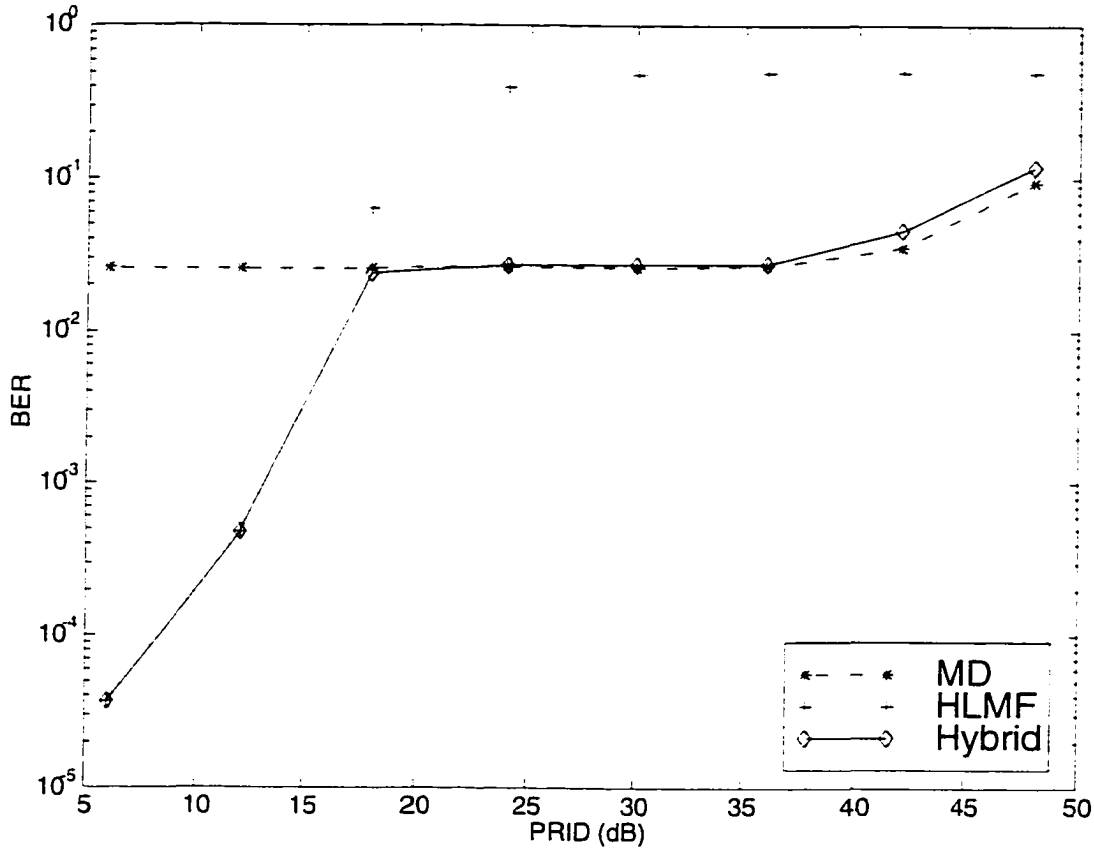

Figure 5.9 BER as a function of the PRID for an asynchronous DS/CDMA system: $\alpha = 1.5$, $\gamma = 1$, $K = 5$, $K_s = 2$, and LMP with $p = 1$.

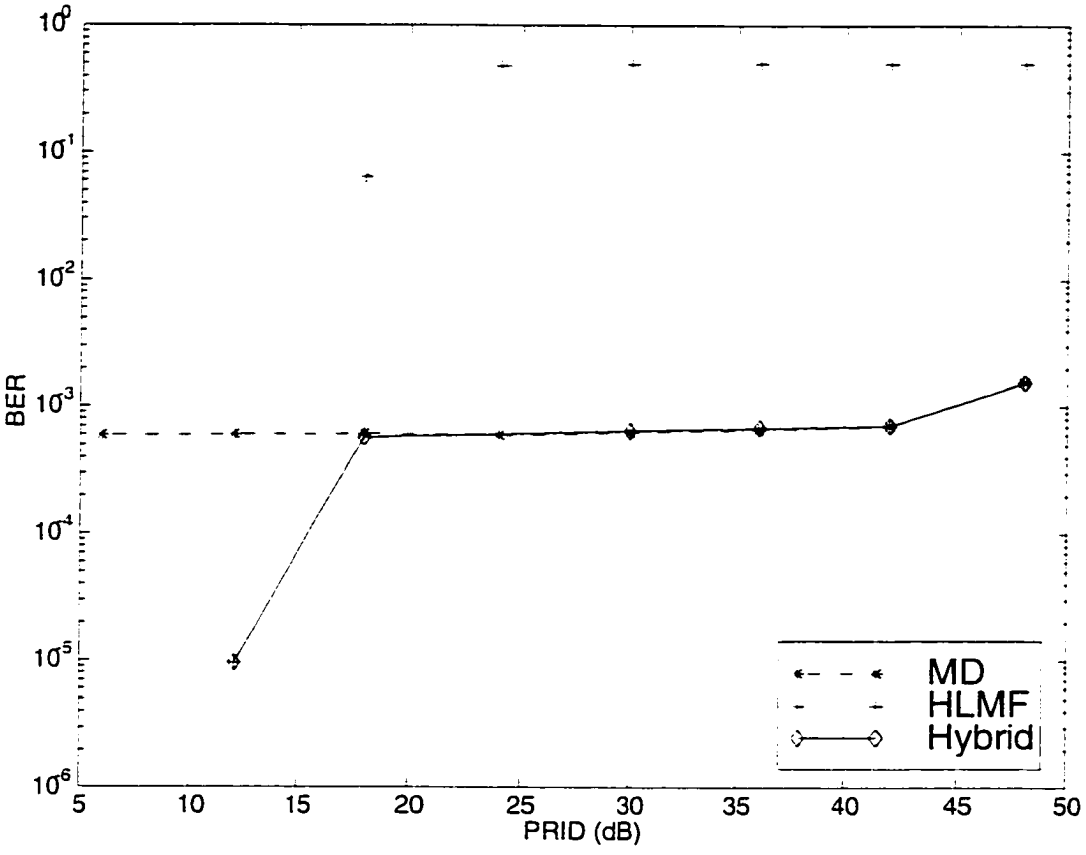

Figure 5.10 BER as a function of the PRID for an asynchronous DS/CDMA system: $a = 1.9$, $\gamma = 1$, $K = 5$, $K_s = 2$, and LMP with $p = 1.3$.

CHAPTER 6 CONCLUSIONS

6.1 Summary

We have considered the problems of multiple-access interference suppression for asynchronous DS/CDMA systems in additive non-Gaussian impulsive noise channels. The additive non-Gaussian impulsive noise was modeled as $S\alpha S$ process with $1 < \alpha < 2$. We primarily focused on the linear detectors based on transversal filters. We compared the BER performance of the proposed detectors with that of different detectors such as the linear MF, HLMF, and MMSE detectors.

In Chapter 3, we presented an interference suppression scheme based on the MD criterion. The LMP algorithm was used to approximate the MD solution for the tap weights. We derived some closed-form expressions for the MD detector in the context of a $S\alpha S$ process under the independence assumptions made in Chapter 3. The closed-form results are analogous to those of MMSE detectors. The performance of the adaptive MD detector was compared with that of previously proposed detectors by extensive Monte Carlo simulation. The simulation results showed that the performance of the adaptive MD detector is much better than that of the other detectors in MAI-limited environments, while it is comparable to that of the conventional MF detector elsewhere. The proposed detector is good near-far resistance in the presence of additive non-Gaussian impulsive noise modeled as a $S\alpha S$ process. In this case the MMSE criterion is not effective. The MD criterion can be used as a possible alternative of the MMSE criterion in $S\alpha S$ non-Gaussian impulsive noise channels. The MD criterion can be viewed as a

generalization of the MMSE criterion to a $S\alpha S$ noise process. Since the LMP algorithm is valid for $p < \alpha \leq 2$, the LMP algorithm with $p = 1$ can be robust to unknown characteristic exponent $\alpha \in (1, 2]$. This observation is consistent with the fact that the minimum L_1-norm error criterion has been successfully used in impulsive noise environments. The limitation of the proposed detector is that the LMP algorithm used in the adaptive implementation of the MD criterion has a slow convergence rate. The LMP algorithm generally takes on the order of several thousand bits to converge to a steady state. Since the covariation is nonlinear, the theoretical analysis for $S\alpha S$ processes is limited.

In Chapter 4, we presented an interference suppression scheme using least L_p-norm estimation. The interference suppression was formulated as a linear L_p-norm estimation problem. This method requires no assumptions on the statistics of the input signals unlike stochastic gradient-based algorithms such as the LMS and LMP algorithms. The L_p-norm solution for the tap weighting vector of the transversal filter was obtained using the IRLS algorithm. The IRLS algorithm converges for $1 \leq p < 3$, while it diverges for $3 \leq p < \infty$. We thus considered the cases for $1 \leq p < 3$. The simulation results showed that the interference suppression scheme using the least L_p-norm estimation offers significant performance improvements over the adaptive MD detector using the LMP algorithm. The detector's BER performance depends on the value of p in the L_p-norm. The BER performance significantly improves as p approaches 3. The least L_p-norm detector has better near-far resistance than the adaptive MD detector at the cost of higher computational complexity. The computational complexity of the IRLS algorithm is $O(K_{it} \cdot N^3)$ per symbol, while the LMP algorithm takes $O(2N)$ per symbol. Here $O(N)$ represents the computational complexity of order N and K_{it} denotes the number of iterations of the IRLS algorithm.

Finally, interference suppression technique using the fuzzy hybrid approach was presented in Chapter 5. This hybrid detector takes advantage of the performance of the

HLMF detector in impulsive noise-limited environments and the performance of the adaptive MD detector in a MAI-limited environments. The hybrid detector linearly combines the test statistics of the adaptive MD and HLMF detectors using the mixing parameter β. This mixing parameter was controlled by a fuzzy system according to the underlying channel environment. The simulation results showed that the performance of the fuzzy hybrid detector is a combination of the better performance characteristics of the adaptive MD and HLMF detectors depending on the underlying channel environments.

6.2 Recommendations for Future Work

Some possible directions for future work are:

- Fast adaptive algorithms can be considered to speed up the convergence rate of the adaptive MD detector. Further study is needed to examine the transient behavior such as the stability conditions in the context of a $S\alpha S$ process. Since the $S\alpha S$ process does not have a finite second-order moment, conventional methods based on the first-order and second-order moments cannot be used.

- The effect of higher values of p ($p \geq 3$) in the least L_p-norm estimation on the steady state performance should be investigated. The IRLS algorithm converges for $1 \leq p < 3$. To get an insight of higher values of p, other algorithms can be introduced. Further study should be focused on adaptive implementations. Methods for reducing computational complexity can be considered.

APPENDIX A COMPLETE DERIVATIONS FOR SECTION 3.3

Derivation of MD Formula and Relevant Solutions

Under the assumptions made in Chapter 3, we can solve (3.1). Starting with (3.1), it follows that

$$\left[r_n(i).b(i) - \tilde{Z}(i)\right]_\alpha = \left[r_n(i).b(i) - \tilde{\mathbf{w}}^T\mathbf{r}(i)\right]_\alpha = 0$$

or

$$\left[b(i)c_n + j_n(i) + v_n(i).b(i) - \sum_{p=0}^{N-1} \tilde{w}_p\left(b(i)c_p + j_p(i) + v_p(i)\right)\right]_\alpha = 0$$

or

$$\left[b(i)c_n + j_n(i) + v_n(i).\left(1 - \sum_{p=0}^{N-1} \tilde{w}_p c_p\right) b(i) - \sum_{p=0}^{N-1} \tilde{w}_p j_p(i) - \sum_{p=0}^{N-1} \tilde{w}_p v_p(i)\right]_\alpha = 0$$

or

$$\overbrace{\left[b(i)c_n.\left(1 - \sum_{p=0}^{N-1} \tilde{w}_p c_p\right) b(i) - \sum_{p=0}^{N-1} \tilde{w}_p j_p(i) - \sum_{p=0}^{N-1} \tilde{w}_p v_p(i)\right]_\alpha}^{A} +$$

$$\overbrace{\left[j_n(i).\left(1 - \sum_{p=0}^{N-1} \tilde{w}_p c_p\right) b(i) - \sum_{p=0}^{N-1} \tilde{w}_p j_p(i) - \sum_{p=0}^{N-1} \tilde{w}_p v_p(i)\right]_\alpha}^{B} +$$

$$\overbrace{\left[v_n(i).\left(1 - \sum_{p=0}^{N-1} \tilde{w}_p c_p\right) b(i) - \sum_{p=0}^{N-1} \tilde{w}_p j_p(i) - \sum_{p=0}^{N-1} \tilde{w}_p v_p(i)\right]_\alpha}^{C}$$

$$= 0 \qquad \text{(A.1)}$$

for all $n \in [0..N-1]$ and $1 < \alpha \leq 2$. Applying the properties of the covariation given in Chapter 2 to the left-hand side of (A.1) yields

$$\begin{aligned} A &= \left[b(i)c_n, \left(1 - \sum_{p=0}^{N-1} \tilde{w}_p c_p\right) b(i) - \sum_{p=0}^{N-1} \tilde{w}_p j_p(i) - \sum_{p=0}^{N-1} \tilde{w}_p v_p(i) \right]_\alpha \\ &= c_n \left\{ (1 - \sum_{p=0}^{N-1} \tilde{w}_p c_p)^{<\alpha-1>} [b(i).b(i)]_\alpha \right\} \\ &= \gamma_b (1 - \tilde{\mathbf{w}}^T \mathbf{c})^{<\alpha-1>} c_n. \end{aligned}$$

$$\begin{aligned} B &= \left[j_n(i), \left(1 - \sum_{p=0}^{N-1} \tilde{w}_p c_p\right) b(i) - \sum_{p=0}^{N-1} \tilde{w}_p j_p(i) - \sum_{p=0}^{N-1} \tilde{w}_p v_p(i) \right]_\alpha \\ &= -\sum_{p=0}^{N-1} \tilde{w}_p^{<\alpha-1>} [\Gamma_j]_{nth} \\ &= -\tilde{w}_n^{<\alpha-1>} \gamma_{j_n}. \end{aligned}$$

and

$$\begin{aligned} C &= \left[v_n(i), \left(1 - \sum_{p=0}^{N-1} \tilde{w}_p c_p\right) b(i) - \sum_{p=0}^{N-1} \tilde{w}_p j_p(i) - \sum_{p=0}^{N-1} \tilde{w}_p v_p(i) \right]_\alpha \\ &= -\sum_{p=0}^{N-1} \tilde{w}_p^{<\alpha-1>} [\Gamma_v]_{nth} \\ &= -\tilde{w}_n^{<\alpha-1>} \gamma_{v_n}. \end{aligned}$$

Substituting A, B, and C into (A.1) yields:

$$\gamma_b \left(1 - \tilde{\mathbf{w}}^T \mathbf{c}\right)^{<\alpha-1>} c_n - \tilde{w}_n^{<\alpha-1>} \gamma_{j_n} - \tilde{w}_n^{<\alpha-1>} \gamma_{v_n} = 0$$

or

$$(\gamma_{j_n} + \gamma_{v_n}) \tilde{w}_n^{<\alpha-1>} = \gamma_b \left(1 - \tilde{\mathbf{w}}^T \mathbf{c}\right)^{<\alpha-1>} c_n \tag{A.2}$$

for all $n \in [0..N-1]$ and $1 < \alpha \leq 2$. In the matrix-form, (A.2) can be written as

$$\Gamma \tilde{\mathbf{w}}_\alpha = \gamma_b \left(1 - \tilde{\mathbf{w}}^T \mathbf{c}\right)^{<\alpha-1>} \mathbf{c} \tag{A.3}$$

which yields (3.3). Let $\alpha = 2$. Then, since $\bar{\mathbf{w}}_\alpha|_{\alpha=2} = \bar{\mathbf{w}}$, (3.3) reduces to

$$\bar{\mathbf{w}} = \gamma_b \left(1 - \bar{\mathbf{w}}^T \mathbf{c}\right) \Gamma^{-1} \mathbf{c}. \tag{A.4}$$

Taking the transpose of both sides of (A.4) and multiplying by $\mathbf{c}$ gives

$$\bar{\mathbf{w}}^T \mathbf{c} = \gamma_b (1 - \bar{\mathbf{w}}^T \mathbf{c}) \mathbf{c}^T (\Gamma^{-1})^T \mathbf{c}.$$

Solving for $\bar{\mathbf{w}}^T \mathbf{c}$ and substituting it into (A.4), we have

$$\bar{\mathbf{w}} = \frac{\gamma_b}{1 + \gamma_b \mathbf{c}^T (\Gamma^T)^{-1} \mathbf{c}} \Gamma^{-1} \mathbf{c} \tag{A.5}$$

where $\bar{\mathbf{w}}$ is the minimum dispersion solution for $\mathbf{w}$. Note that when $\alpha = 2$, $\gamma_b = \frac{1}{2}\sigma_b^2$ and $\Gamma = \frac{1}{2}\mathbf{R} = \frac{1}{2}\mathbf{R}^T$, where $\sigma_b^2 = E\left[\left[|b(i)|^2\right]\right.$ and $\mathbf{R} \triangleq \mathbf{R}_j + \mathbf{R}_v = E[\mathbf{j} \cdot \mathbf{j}^T] + E\left[\mathbf{v} \cdot \mathbf{v}^T\right]$. Hence (A.5) becomes (3.4).

Next, pre-multiplying both sides of (A.3) by $\bar{\mathbf{w}}^T$ gives

$$\bar{\mathbf{w}}^T \Gamma \bar{\mathbf{w}}_\alpha = \gamma_b (1 - \bar{\mathbf{w}}^T \mathbf{c})^{<\alpha-1>} \bar{\mathbf{w}}^T \mathbf{c}. \tag{A.6}$$

From (3.5) and (A.6) it follows that

$$\begin{aligned} J^\alpha_{\alpha,\min} &= J^\alpha_\alpha|_{\mathbf{w}(i)=\bar{\mathbf{w}}, \mathbf{w}_\alpha(i)=\bar{\mathbf{w}}_\alpha} \\ &= \gamma_b (1 - \bar{\mathbf{w}}^T \mathbf{c})(1 - \bar{\mathbf{w}}^T \mathbf{c})^{<\alpha-1>} + \gamma_b (1 - \bar{\mathbf{w}}^T \mathbf{c})^{<\alpha-1>} \bar{\mathbf{w}}^T \mathbf{c} \end{aligned} \tag{A.7}$$

which reduces to (3.6). Let $J_{\min} = E\left[|\tilde{e}(i)|^2\right]$, where $J_{\min}$ is the minimum mean-squared error. Then, when $\alpha = 2$, (A.7) also reduces to

$$J^\alpha_{\alpha,\min} = \frac{1}{2}\sigma^2_{\tilde{e}} = \frac{1}{2} E\left[|\tilde{e}(i)|^2\right] = \frac{1}{2} J_{\min} = \frac{1}{2}\sigma_b^2 (1 - \bar{\mathbf{w}}^T \mathbf{c}) \tag{A.8}$$

Hence we obtain (3.7).

Derivation of Output SIR

By using the properties of the covariation and independence assumptions made in Chapter 3, it follows:

$$\begin{aligned} & \textit{Numerator of (3.8)} \\ = \; & \left[\mathbf{w}(i)^T b(i)\mathbf{c}.\, \mathbf{w}(i)^T b(i)\mathbf{c}\right]_\alpha \\ = \; & \mathbf{w}(i)^T\mathbf{c}(\mathbf{w}(i)^T\mathbf{c})^{<\alpha-1>}\left[b(i).b(i)\right]_\alpha \\ = \; & \mathbf{w}(i)^T\mathbf{c}\left|\mathbf{w}(i)^T\mathbf{c}\right|^{\alpha-1} sign(\mathbf{w}(i)^T\mathbf{c})\gamma_b \\ = \; & \left|\mathbf{w}(i)^T\mathbf{c}\right|^\alpha \gamma_b \end{aligned} \tag{A.9}$$

and

$$\begin{aligned} & \textit{Denominator of (3.8)} \\ = \; & \left[\mathbf{w}(i)^T(\mathbf{j}(i)+\mathbf{v}(i)).\, \mathbf{w}(i)^T(\mathbf{j}(i)+\mathbf{v}(i))\right]_\alpha \\ = \; & \left[\sum_{p=0}^{N-1} w_p(i)(j_p(i)+v_p(i)).\sum_{q=0}^{N-1} w_q(i)(j_q(i)+v_q(i))\right]_\alpha \\ = \; & \sum_{p=0}^{N-1} w_p(i)\left[j_p(i)+v_p(i).\sum_{q=0}^{N-1} w_q(i)(j_q(i)+v_q(i))\right]_\alpha \\ = \; & \sum_{p=0}^{N-1} w_p(i)\left\{\left[j_p(i).\sum_{q=0}^{N-1} w_q(i)(j_q(i)+v_q(i))\right]_\alpha + \left[v_p(i).\sum_{q=0}^{N-1} w_q(i)\,(j_q(i)+v_q(i))\right]_\alpha\right\} \\ = \; & \sum_{p=0}^{N-1} w_p(i)\left\{\sum_{q=0}^{N-1} w_q(i)\left[j_p(i).j_q(i)+v_q(i)\right]_\alpha + \sum_{q=0}^{N-1} w_q(i)\left[v_p(i).j_q(i)+v_q(i)\right]_\alpha\right\} \\ = \; & \sum_{p=0}^{N-1} w_p(i)\left\{\sum_{q=0}^{N-1} w_q(i)\left[j_p(i).j_q(i)\right]_\alpha + \sum_{q=0}^{N-1} w_q(i)\left[v_p(i).v_q(i)\right]_\alpha\right\} \\ = \; & \sum_{p=0}^{N-1} w_p(i)\left\{\sum_{q=0}^{N-1} w_q(i)[\Gamma_j]_{p.q} + \sum_{q=0}^{N-1} w_q(i)\,[\Gamma_v]_{p.q}\right\} \\ = \; & \mathbf{w}^T(i)(\Gamma_j+\Gamma_v)\mathbf{w}_\alpha(i) = \mathbf{w}^T(i)\Gamma\mathbf{w}_\alpha(i). \end{aligned} \tag{A.10}$$

Substituting (A.9) and (A.10) into the definition expression of the output SIR yields (3.9). From (A.6) and (3.6) it follows that

$$
\begin{aligned}
SIR|_{\mathbf{w}(i)=\bar{\mathbf{w}},\mathbf{w}_\alpha(i)=\bar{\mathbf{w}}_\alpha} &= \frac{\gamma_b \left|\bar{\mathbf{w}}^T\mathbf{c}\right|^\alpha}{\bar{\mathbf{w}}^T\Gamma\bar{\mathbf{w}}_\alpha} \\
&= \frac{\gamma_b \left|\bar{\mathbf{w}}^T\mathbf{c}\right|^\alpha}{\gamma_b(1-\bar{\mathbf{w}}^T\mathbf{c})^{<\alpha-1>}\bar{\mathbf{w}}^T\mathbf{c}} \\
&= \frac{\gamma_b \left|\bar{\mathbf{w}}^T\mathbf{c}\right|^\alpha}{J^\alpha_{\alpha.\min}\bar{\mathbf{w}}^T\mathbf{c}} \\
&= \frac{\gamma_b \left|\bar{\mathbf{w}}^T\mathbf{c}\right|^\alpha}{J^\alpha_{\alpha.\min}\left|\bar{\mathbf{w}}^T\mathbf{c}\right| sign(\bar{\mathbf{w}}^T\mathbf{c})} \\
&= \frac{\gamma_b \left|\bar{\mathbf{w}}^T\mathbf{c}\right|^{\alpha-1} sign(\bar{\mathbf{w}}^T\mathbf{c})}{J^\alpha_{\alpha.\min}}. \qquad \text{(A.11)}
\end{aligned}
$$

which leads to (3.10).

When $\alpha = 2$, by using (A.8) and (3.7), (3.10) becomes

$$
\begin{aligned}
SIR_{\max} &= \frac{\gamma_b}{J^\alpha_{\alpha.\min}}\bar{\mathbf{w}}^T\mathbf{c} \\
&= \frac{\frac{1}{2}\sigma_b^2}{\frac{1}{2}J_{\min}}\left(1-\frac{1}{\sigma_b^2}J_{\min}\right)
\end{aligned}
$$

which reduces to (3.11).

Derivation of Probability of Error

By the assumptions made in Chapter 3, the test statistic $Z(i)$ is a $S\alpha S$ random variable. The conditional location parameters are given by

$$
\begin{aligned}
\tilde{\mu}_0 &= E\left[Z(i) \mid b(i) = +1, \mathbf{b}_J(i)\right] \\
&= \mathbf{w}(i)^T\mathbf{c} + \mathbf{w}(i)^T\mathbf{j}_J(i) \qquad \text{(A.12)}
\end{aligned}
$$

and

$$
\begin{aligned}
\tilde{\mu}_1 &= E\left[Z(i) \mid b(i) = -1, \mathbf{b}_J(i)\right] \\
&= -\mathbf{w}(i)^T\mathbf{c} + \mathbf{w}(i)^T\mathbf{j}_J(i). \qquad \text{(A.13)}
\end{aligned}
$$

Let $\check{Z}_0(i) = Z(i)|_{b(i)=+1.\mathbf{b}_J(i)} - \check{\mu}_0$ and $\check{Z}_1(i)|_{b(i)=-1.\mathbf{b}_J(i)} = Z(i) - \check{\mu}_1$. Then for $1 < \alpha \leq 2$ the dispersion $\gamma_{\check{Z}(i)}$ is given by

$$\begin{aligned}\gamma_{\check{Z}(i)} &= \left[\check{Z}_0(i).\check{Z}_0(i)\right]_\alpha = \left[\check{Z}_1(i).\check{Z}_1(i)\right]_\alpha \\ &= \left[\mathbf{w}(i)^T\mathbf{v}(i).\mathbf{w}(i)^T\mathbf{v}(i)\right]_\alpha = \mathbf{w}(i)^T\Gamma_v\mathbf{w}_\alpha(i). \end{aligned} \tag{A.14}$$

From (3.5) and (A.14) we obtain

$$\gamma_{\check{Z}(i)} = J_\alpha^\alpha(\mathbf{w}(i)) - \gamma_b(1 - \mathbf{w}(i)^T\mathbf{c})(1 - \mathbf{w}(i)^T\mathbf{c})^{<\alpha-1>} - \mathbf{w}(i)^T\Gamma_J\mathbf{w}_\alpha(i) \tag{A.15}$$

for $1 < \alpha \leq 2$. $\gamma_{\check{Z}(i)}$ corresponding to the MD solution is thus given by

$$\begin{aligned}\gamma_{\check{Z}(i).\min} &= \gamma_{\check{Z}(i)}(\mathbf{w}(i) = \bar{\mathbf{w}}; \mathbf{w}_\alpha(i) = \bar{\mathbf{w}}_\alpha) \\ &= J_{\alpha.\min}^\alpha - \gamma_b(1 - \bar{\mathbf{w}}^T\mathbf{c})(1 - \bar{\mathbf{w}}_\alpha{}^T\mathbf{c})^{<\alpha-1>} - \bar{\mathbf{w}}^T\Gamma_J\bar{\mathbf{w}}_\alpha. \end{aligned} \tag{A.16}$$

Substituting (3.6) into (A.16) yields

$$\begin{aligned}\gamma_{\check{Z}(i).\min} &= J_{\alpha.\min}^\alpha - J_{\alpha.\min}^\alpha(1 - \bar{\mathbf{w}}^T\mathbf{c}) - \bar{\mathbf{w}}^T\Gamma_J\bar{\mathbf{w}}_\alpha \\ &= J_{\alpha.\min}^\alpha \cdot \bar{\mathbf{w}}^T\mathbf{c} - \bar{\mathbf{w}}^T\Gamma_J\bar{\mathbf{w}}_\alpha. \end{aligned} \tag{A.17}$$

Rearranging (3.10) in terms of $J_{\alpha.\min}^\alpha$ and substituting it into (A.17), we get

$$\begin{aligned}\gamma_{\check{Z}(i).\min} &= \frac{\gamma_b}{SIR_{\max}}(\bar{\mathbf{w}}^T\mathbf{c})^{<\alpha-1>} \cdot \bar{\mathbf{w}}^T\mathbf{c} - \bar{\mathbf{w}}^T\Gamma_J\bar{\mathbf{w}}_\alpha \\ &= \frac{\gamma_b}{SIR_{\max}}\left|\bar{\mathbf{w}}^T\mathbf{c}^{(1)}\right|^\alpha - \bar{\mathbf{w}}^T\Gamma_J\bar{\mathbf{w}}_\alpha \end{aligned} \tag{A.18}$$

for $1 < \alpha \leq 2$.

When $\alpha = 2$,

$$f_\alpha(\xi; \gamma_{\check{Z}(i)}, \check{\mu}_0) = \frac{1}{\sqrt{2\pi\sigma^2_{\check{Z}(i)}}}\exp\left[-\frac{(\xi - \check{\mu}_0)^2}{2\sigma^2_{\check{Z}(i)}}\right] \tag{A.19}$$

where $\sigma^2_{\check{Z}(i)} = 2\gamma_{\check{Z}(i)}$. Substituting (A.19) into (3.12) thus yields

$$\begin{aligned} P_e(\mathbf{b}_J(i)) &= \int_{-\infty}^{0} \frac{1}{\sqrt{2\pi\sigma^2_{\check{Z}(i)}}} \exp\left[-\frac{(\xi-\check{\mu}_0)^2}{2\sigma^2_{\check{Z}(i)}}\right] d\xi \\ &= Q\left(\frac{\check{\mu}_0}{\sqrt{\sigma^2_{\check{Z}(i)}}}\right) \\ &= Q\left(\frac{\mathbf{w}(i)^T\mathbf{c} + \mathbf{w}(i)^T\mathbf{j}_J(i)}{\sqrt{2\gamma_{\check{Z}(i)}}}\right) \\ &= Q\left(\frac{\mathbf{w}(i)^T(\mathbf{c}+\mathbf{j}_J(i))}{\sqrt{2\mathbf{w}(i)^T\Gamma_v\mathbf{w}_\alpha(i)}}\right) \end{aligned}$$

where $Q(x) = \frac{1}{\sqrt{2\pi}}\int_x^\infty e^{-t^2/2}dt$. Hence we obtain (3.13).

BIBLIOGRAPHY

[1] S. Moshavi. "Multi-user detection for DS-CDMA communications." *IEEE Commun. Mag.*, vol. 34, no. 10, pp. 124–136, Oct. 1996.

[2] S. Verdu. "Recent progress in multiuser detection." in *Proc. 1988 Int. Conf. Advances in Communications and Control Systems*, Baton Rouge, LA, Oct. 1988, pp. 27–38.

[3] S. Verdu. "Multiuser detection." in *Advances in Statistical Signal Processing*, vol. 2, pp. 369–409, JAI Press Inc., 1993.

[4] H. V. Poor. "Signal detection in multiple-access channels." in *U.S. Army Research Office Proposal*. (Contract DAAG29-81-K-0062 to Coordinated Science Laboratory, University of Illinois), 1980.

[5] J. D. Laster and J. H. Reed. "Interference rejection in digital wireless communications." *IEEE Signal Processing Mag.*, vol. 14, no. 3, pp. 37–62, May 1997.

[6] K. S. Gilhousen, I. M. Jacobs, R. Padovani, L. A. Weaver Jr., and C. E. Wheatley III, "On the capacity of a cellular CDMA system," *IEEE Trans. Vehic. Technol.*, vol. 40, pp. 303–311, May 1991.

[7] Y. Han, H. G. Bahk, and S. Yang, "CDMA mobile system overview: Introduction, background, and system concepts," *ETRI Journal*, vol. 19, no. 3, pp. 83–97, Oct. 1997.

[8] S. Kim, Y. Oh, H.-Y. Kweon, and H. Lee, "Developement of mobile station in the CDMA mobile system," *ETRI Journal*, vol. 19, no. 3, pp. 202–227, Oct. 1997.

[9] D.-W. Lee, K. Yoo, J.-S. Kim, M. J. Kim, and J.-H. Park, "Developement of the base station transceiver subsystem in the CDMA mobile system," *ETRI Journal*, vol. 19, no. 3, pp. 116–140, Oct. 1997.

[10] L. B. Milstein, "Interference rejection techniques in spread spectrum communications," *Proceedings of the IEEE*, vol. 76, no. 6, pp. 657–671, Jun. 1988.

[11] L. M. Garth and H. V. Poor, "Narrowband interference suppression in impulsive channels," *IEEE Trans. Aerospace and Electronic Systems*, vol. 28, no. 1, pp. 15–34, Jan. 1992.

[12] L. A. Rusch and H. V. Poor, "Narrowband interference suppression in CDMA spread spectrum communications," *IEEE Trans. Commun.*, vol. 42, no. 2, part 3, pp. 1969–1979, Apr. 1994.

[13] S. Verdu, "Adaptive multiuser detection," in *Code Division Multiple Access Communications*, S. G. Glisic and P. A. Leppanen, Eds., chapter 3, pp. 97–116, Kluwer, The Netherlands, 1995.

[14] A. Duel-Hallen, J. Holtzman, and Z. Zvonar, "Multiuser detection for CDMA systems," *IEEE Pers. Commun.*, vol. 2, no. 2, pp. 46–58, Apr. 1995.

[15] S. Verdu, "Minimum probability of error for asynchronous Gaussian multiple-access channels," *IEEE Trans. Inform. Theory*, vol. IT-32, no. 1, pp. 85–96, Jan. 1986.

[16] R. Lupas and S. Verdu, "Linear multiuser detectors for synchronous code-division multiple access channels," *IEEE Trans. Inform. Theory*, vol. 35, no. 1, pp. 123–136, Jan. 1989.

[17] R. Lupas and S. Verdu. "Near-far resistance of multiuser detectors in asynchronous channels." *IEEE Trans. Commun.*, vol. 38, no. 4, pp. 496–508, Apr. 1990.

[18] Z. Xie, R. T. Short, and C. K. Rushforth, "A family of suboptimum detectors for coherent multi-user communications." *IEEE J. Select. Areas Commun.*, vol. 8, no. 4, pp. 683–90, May 1990.

[19] A. J. Viterbi, "Very low rate convolutional codes for maximum theoritical performance of spread-spectrum multiple-access channels." *IEEE J. Select. Areas Commun.*, vol. 8, no. 4, pp. 641–49, May 1990.

[20] P. Patel and J. Holtzman, "Analysis of a simple successive interference cancellation." *IEEE J. Select. Areas Commun.*, vol. 12, no. 5, pp. 796–807, Jun. 1994.

[21] K. I. Pedersen, T. E. Kolding, I. Seskar, and J. M. Holtzman, "Practical implementation of succesive interference cancellation." Available HTTP: http://winwww.rutgers.edu/pub/publications/Index.html. WINLAB, Rutgers Univ., Newark, NJ, 1998.

[22] M. K. Varanasi and B. Aazhang, "Multistage detection for asynchronous code-division multiple-access communications." *IEEE Trans. Commun.*, vol. 38, pp. 509–519, Apr. 1990.

[23] R. Kohno, H. Imai, M. Hatori, and S. Pasupathy, "Combination of an adaptive array antenna and a canceller of interference for direct-sequence spread-spectrum multiple-access system." *IEEE J. Select. Areas Commun.*, vol. 8, no. 4, pp. 675–682, May 1990.

[24] A. Duel-Hallen, "Decorrelation decision-feedback multi-user detector for synchronous code-division multiple access channels." *IEEE Trans. Commun.*, vol. 41, no. 2, pp. 285–90, Feb. 1993.

[25] A. Duel-Hallen, "A family of multi-user decision-feedback detectors for asynchronous code-division multiple access channels," *IEEE Trans. Commun.*, vol. 43, no. 2/3/4, pp. 421–34, Feb./Mar./Apr. 1995.

[26] H. V. Poor and S. Verdu, "Single-user detectors for multiuser channels," *IEEE Trans. Commun.*, vol. 36, no. 1, pp. 50–60, Apr. 1988.

[27] B. Aazhang, B.-P. Paris, and G. C. Orsak, "Neural networks for multiuser detection in code-division multiple-access communications," *IEEE Trans. Commun.*, vol. 40, no. 7, pp. 1212–1222, Jul. 1992.

[28] U. Mitra and H. V. Poor, "Neural network techniques for adaptive multiuser demodulation," *IEEE J. Select. Areas Commun.*, vol. 12, no. 9, pp. 1460–1470, Dec. 1994.

[29] M. Abdulrahman, D. Falconer, and A. Sheikh, "Equalization for interference cancellation in spread spectrum multiple-access systems," in *Proc. IEEE 42nd Vehicular Technology Conf.*, May 1992, pp. 71–74.

[30] U. Madhow and M. L. Honig, "Minimum mean squared error interference suppression for direct sequence spread-spectrum code-division multiple-access," in *Proc. 1st Int. Conf. Universal and Personal Communications*, Dallas, TX, Sept. 28-Oct. 1 1992, pp. 10.04/1–5.

[31] U. Madhow and M. L. Honig, "Error probability and near-far resistance of minimum mean squared error interference suppression schemes for CDMA," in *Proc. IEEE Global Telecommunications Conf.*, Dallas, TX, Dec. 6-9 1994, vol. 3, pp. 1339–43.

[32] E. K. B. Lee. "Rapid converging adaptive interference suppression for direct-sequence code-division multiple-access systems." in *Proc. IEEE Global Telecommunications Conf.*, 1993. pp. 1683–1687.

[33] P. B. Rapajic and B. S. Vucetic. "Linear adaptive fractionally spaced single-user receiver for asynchronous CDMA systems." in *Proc. 1993 IEEE International Symposium on Information Theory*, 1993. p. 45.

[34] U. Madhow and M. L. Honig, "MMSE interference suppression for direct-sequence spread-spectrum CDMA." *IEEE Trans. Commun.*, vol. 42, no. 12, pp. 3178–3188. Dec. 1994.

[35] P. Rapajic and B. Vucetic. "Adaptive receiver structures for asynchronous CDMA systems." *IEEE J. Select. Areas Commun.*, vol. 12, no. 4, pp. 685–697. May 1994.

[36] E. G. Strom and S. L. Miller. "Optimum complexity reduction of minimum mean square error DS-CDMA receivers." in *Proc. IEEE Vehicular Technology Conf.*, 1994. pp. 568–72.

[37] N. B. Mandayam and B. Aazhang. "An adaptive multiuser interference rejection algorithm for direct-sequence code division multiple access." in *Proc. 1994 IEEE International Symposium on Information Theory*, Trondheim, Norway, Jun. 1994.

[38] S. L. Miller. "An adaptive direct-sequence code-division multiple-access receiver for multiuser interference rejection." *IEEE Trans. Commun.*, vol. 43, no. 2/3/4. pp. 1746–1755. Feb./Mar./Apr. 1995.

[39] U. Mitra and H. V. Poor. "Adaptive receiver algorithms for near-far resistant CDMA." *IEEE Trans. Commun.*, vol. 43, no. 2/3/4. pp. 1713–1724. Feb./Mar./Apr. 1995.

[40] M. Tahernezhad and L. Zhu. "Performance evaluation of LMS-based adaptive suppression schemes in asynchronous CDMA." *Int. J. Electronics*. vol. 79. no. 5. pp. 541–550. 1995.

[41] S. L. Miller. "Training analysis of adaptive interference suppression for direct-sequence code-division multiple-accesssystems." *IEEE Trans. Commun.*. vol. 44. no. 4. pp. 488–495. Apr. 1996.

[42] C. Pateros and G. Saulnier. "Interference suppression and multipath mitigation using an adaptive correlator direct sequence spread spectrum receiver." in *Proc. Int. Conf. Communications*. 1992. pp. 662–666.

[43] R. A. Iltis. "A GLRT-based spread-spectrum receiver for joint channel estimation and interference suppression." *IEEE Trans. Commun.*. vol. 37. no. 3. pp. 277–288. Mar. 1989.

[44] M. L. Honig, U. Madhow. and S. Verdu. "Blind adaptive multiuser detection." *IEEE Trans. Inform. Theory*. vol. 41. no. 4. pp. 944–960. Jul. 1995.

[45] D. Middleton. "Statistical-physical models of urban radio-noise environments - part I: Foundations." *IEEE Trans. Electromagn. Compat.*. vol. 14. pp. 38–56. 1972.

[46] D. Middleton. "Man-made noise in urban environments and transportation systems." *IEEE Trans. Commun.*. vol. COM-21. pp. 1232–1241. Nov. 1973.

[47] E. N. Skomal. *Man-Made Radio Noise*. Van Nostrand Reinhold. Princeton. NJ. 1978.

[48] K. Vastola. "Threshold detection in narrow-band non-Gaussian noise." *IEEE Trans. Commun.*. vol. COM-32. no. 2. pp. 134–139. Feb. 1984.

[49] B. Aazhang, *Performance of DS/SSMA Communications in Impulsive Channels*. Ph.D. thesis, University of Illinoise at Urbana-Champaign, 1986.

[50] G. A. Tsihrintzis and C. L. Nikias, "Performance of optimum and suboptimum receivers in the presence of impulsive noise modeled as an alpha-stable process," *IEEE Trans. Commun.*, vol. 43, no. 2/3/4, pp. 904–914, Feb./Mar./Apr. 1995.

[51] U. Mitra and H. V. Poor, "Detection of spread-spectrum signals in a multi-user environment," in *Proc. IEEE ICASP*, 1995, pp. 1844–1847.

[52] D. Middleton, "Statistical-physical models of man-made radio noise, part I: First-order probability models of the instantaneous amplitude," Number OT-Report 74-36, Office of Telecommunications, Washington, D.C., 20402, 1974.

[53] D. Middleton, "Statistical-physical models of man-made and natural radio noise, part II: First-order probability models of the envelope and phase," Number OT-Report 76-86, Office of Telecommunications, Springfield, VA, Apr. 1976.

[54] D. Middleton, "Statistical-physical models of electromagnetic interference," *IEEE Trans. Electromagn. Compat.*, vol. EMC-19, no. 3, pp. 106–127, Aug. 1977.

[55] A. D. Spaulding and D. Middleton, "Optimum reception in an impulsive interference environment-part I: Coherent detection," *IEEE Trans. Commun.*, vol. COM-25, no. 9, pp. 910–923, Sept. 1977.

[56] A. D. Spaulding and D. Middleton, "Optimum reception in an impulsive interference environment-part II: Incoherent reception," *IEEE Trans. Commun.*, vol. COM-25, no. 9, pp. 924–934, Sept. 1977.

[57] A. D. Spaulding, "Locally optimum and suboptimum detector performance in a non-Gaussian interference environment," *IEEE Trans. Commun.*, vol. COM-33, no. 6, pp. 509–517, Jun. 1985.

[58] B. Aazhang and H. V. Poor, "Performance of DS/SSMA communications in impulsive channels-part I: Linear correlation receivers," *IEEE Trans. Commun.*, vol. com-35, no. 11, pp. 1179–1188, Nov. 1987.

[59] M. Shao and C. L. Nikias, "On symmetric stable models for impulsive noise," Tech. Rep. USC-SIPI-231, University of Southern California, Los Angeles, CA, Feb. 1993.

[60] M. Shao and C. L. Nikias, "Signal processing with fractional lower order moments: Stable processes and their applications," *Proceedings of the IEEE*, vol. 81, no. 7, pp. 986–1010, Jul. 1993.

[61] S. Ambike, J. Ilow, and D. Hatzinakos, "Detection for binary transmission in a mixture of Gaussian noise and impulsive noise modeled as an alpha-stable process," *IEEE Signal Processing Letters*, vol. 1, no. 3, pp. 55–57, Mar. 1994.

[62] J. How, D. Hatzinakos, and A. N. Venetsanopoulos, "Performance of FH SS radio networks with interference modeled as a mixture of Gaussian and alpha-stable noise," in *Proc. IEEE ICASP*, 1995, pp. 1852–1855.

[63] G. Samorodnitsky and M. S. Taqqu, *Stable Non-Gaussian Random Processe: Stochastic Models with Infinite Variance*, Chapman & Hall, New York, NY, 1994.

[64] C. L. Nikias and M. Shao, *Signal Processing with Alpha-Stable Distributions and Applications*, John Wiley & Sons, New York, NY, 1995.

[65] S. Cambanis and G. Miller, "Linear problems in pth order and stable processes," *SIAM J. Appl. Math.*, vol. 41, no. 1, pp. 43–69, Aug. 1981.

[66] B. Aazhang and H. V. Poor, "Performance of DS/SSMA communications in impulsive channels-part II: Hard-limiting correlation receivers," *IEEE Trans. Commun.*, vol. 36, no. 1, pp. 88–97, Jan. 1988.

[67] N. B. Mandayam. "Adaptive linear detection for DS-CDMA communications in impulsive channels." in *Proc. 1995 IEEE 45th Vehicular Technology Conf.*, Chicago, IL, Jul. 25-28 1995, pp. 699–703.

[68] N. B. Mandayam. "Adaptive interference suppression for DS-CDMA with impulsive noise." in *Proc. 1995 IEEE International Symposium on Information Theory*, Whistler, British Columbia, Sept. 17-22 1995, p. 26.

[69] J. F. Weng, S. H. Leung, W. H. Lau, and G. G. Bi. "A new neural network based multiuser detector in impulse noise." in *Proc. Int. Conf. Communications*, Dallas, TX, Jun. 23-27 1996, pp. 541–545.

[70] J. Shen, W.-K. Cheng, and C. L. Nikias. "General $L^{(p,q)}$-metric estimators of arbitrary interference in communication receivers." in *Proc. IEEE Globecom Communication Theory Mini-Conference*, London, UK, 1996, pp. 193–197.

[71] L. A. Rusch and H. V. Poor. "Multiuser detection techniques for narrowband interference suppression in spread spectrum communications." *IEEE Trans. Commun.*, vol. 43, no. 2/3/4, pp. 1725–1737, Apr. 1995.

[72] M. Grigoriu, *Applied Non-Gaussian Processes*, Prentice Hall, Englewood Cliffs, NJ, 1995.

[73] J. M. Chambers, C. L. Mallows, and B. W. Stuck. "A method for simulating stable random variables." *J. of the American Statistical Association*, vol. 71, no. 354, pp. 340–344, Jun. 1976.

[74] K. S. Shanmugan, V. L. Frost, and W. H. Tranter. "Computer-aided analysis and design of communication systems." in *One-Day Tutorial IEEE MILCOM 86*, 1986.

[75] S. A. Kassam. *Signal Detection in Non-Gaussian Noise*. Springer-Verlag. New York. NY. 1988.

[76] V. M. Zolotarev. *One-Dimensional Stable Distributions*. American Mathematical Society. Providence. RI. 1986.

[77] W. Feller. *An Introduction to Probability Theory and its Applications*. Wiley. New York. NY. 1971.

[78] B. V. Gnedenko and A. N. Kolmogorov, *Limited Distributions for Sums of Independent Random Variables*. Addison-Wesley. Reading, MA. 1968. 1954.

[79] G. Miller. "Properties of certain symmetric stable distribution." *J. of Multivariate Anal.*, vol. 8. pp. 346–360. 1978.

[80] B. W. Stuck. "Minimum error dispersion linear filtering of scalar symmetric stable processes." *IEEE Trans. Automatic Control*. vol. AC-23. no. 3. pp. 507–509. Jun. 1978.

[81] I. Singer. *Best Approximation in Normed Linear Space by Elements of Linear Subspaces*. Springer. New York. NY. 1970.

[82] S. S. Rappaport and L. Kurz. "An optimal nonlinear detector for digital data transmission through non-Gaussian channels." *IEEE Trans. Commun. Technology*. vol. COM-14. no. 3. pp. 266–274. Jun. 1966.

[83] E. J. Wegman. S. G. Schwartz. and J. B. Thomas. *Topics in Non-Gaussian Signal Processing*. Academic Press. New York. NY. 1989.

[84] A. R. Milne and J. H. Ganton. "Ambient noise under arctic sea ice." *J. Acoust. Soc. Amer.*, vol. 36. pp. 855–863. May 1964.

[85] D. W. Lytle, "Characteristic problems of underwater communications," in *Proc. IEEE Int. Conf. Communications*, Seattle, WA, Jun. 1973, pp. 38–1–38–3.

[86] H. V. Poor, *An Introduction to Signal Detection and Estimation*, Springer-Verlag, New York, NY, 2nd edition, 1994.

[87] S. Lee and J. Dickerson, "Adaptive minimum dispersion interference suppression for DS/CDMA systems in non-Gaussian impulsive channels," in *Proc. IEEE Military Communications Conf.*, Monterey, CA, Nov. 2-5 1997.

[88] S.-C. Pei and C.-C. Tseng, "Least mean p-power error criterion for adaptive FIR filter," *IEEE J. Select. Areas Commun.*, vol. 12, no. 9, pp. 1540–1547, Dec. 1994.

[89] O. Arikan, A. E. Cetin, and E. Erzin, "Adaptive filtering for non-Gaussian stable processes," *IEEE Signal Processing Letters*, vol. 1, no. 11, pp. 163–165, Nov. 1994.

[90] S. Haykin, *Adaptive Filter Theory*, Prentice-Hall, Englewood Cliffs, NJ, 2nd edition, 1991.

[91] J. R. Rice and J. S. White, "Norms for smoothing and estimation," *SIAM Rev.*, vol. 6, no. 3, pp. 243–256, 1964.

[92] R. C. Geary, "Testing for normality," *Biometrika*, vol. 34, pp. 209–242, 1947.

[93] R. Gonin, *Nonlinear L_p-Norm Estimation*, Marcel Dekker, New York, NY, 1989.

[94] J. Claerbout and F. Muir, "Robust modeling with erratic data," *Geophysics*, vol. 38, no. 5, pp. 826–844, Oct. 1973.

[95] R. Yarlagadda, J. B. Bednar, and T. L. Watt, "Fast algorithms for l_p-norm deconvolution," *IEEE Trans. Acoust. Speech Signal Processing*, vol. ASSP-33, no. 1, pp. 174–182, Feb. 1985.

[96] E. E. Kuruoglu, P. J. W. Rayner, and W. J. Fitzgerald, "Least l_p-norm estimation of autoregressive model coefficients of symmetric α-stable processes," *IEEE Signal Processing Letters*, vol. 4, no. 7, pp. 201–203, Jul. 1997.

[97] J. Schroeder, R. Yarlagadda, and J. Hershey, "L_p-normed minimization with applications to linear predictive modeling for sinusoidal frequency estimation," *Signal Processing*, vol. 24, no. 2, pp. 193–216, Aug. 1991.

[98] B. N. Datta, *Numerical Linear Algebra*, Brooks/Cole Publishing Company, Pacific Grove, CA, 1995.

[99] G. H. Golub and C. F. Van Loan, *Matrix Computations*, Johns Hopkins Univ. Press, Baltimore, MD, 1983.

[100] R. H. Byrd and D. A. Payne, "Convergence of the iteratively reweighted least squares algorithm for robust regression," Tech. Rep. 313, Dept. of Math. Sci., The Johns Hopkins Univ., Baltimore, MD, Jun. 1979.

[101] J. Schroeder and R. Yarlagadda, "Linear predictive spectral estimation via the l_1 norm," *Signal Processing*, vol. 17, pp. 19–29, 1989.

[102] C. S. Burrus, J. A. Barreto, and I. W. Selesnick, "Iteratively reweighted least-squares design of FIR filters," *IEEE Trans. Signal Processing*, vol. 42, no. 11, pp. 2926–2936, Nov. 1994.

[103] G. Merle and H. Spath, "Computational experiences with discrete l_p-approximation," *Comput.*, vol. 12, pp. 315–321, 1974.

[104] R. Fletcher, J. A. Crant, and M. D. Hebden, "The calculation of linear best l_p approximations," *Comput. J.*, vol. 14, pp. 276–279, 1971.

[105] E. E. Kuruoglu, P. J. W. Rayner, and W. J. Fitzgerald. "On the consistency of least l_p-norm estimates of autoregressive model coefficients of symmetric alpha-stable processess." Tech. Rep. CUED/F-INFENG/TR.293, Dept. Eng., Univ. Cambridge, Cambridge, UK, 1997.

[106] D. S. Watkins. *Fundamentals of Matrix Computations*, John Wiley & Sons, New York, NY, 1991.

[107] J. W. Modestino, "Adaptive detection of signals in impulsive noise environments," *IEEE Trans. Commun.*, vol. com-25, no. 9, pp. 1022–1027, Sept. 1977.

[108] W. C. Y. Lee, "Overview of cellular CDMA," *IEEE Trans. Vehic. Tech.*, vol. 40, no. 2, pp. 291–302, May 1991.

[109] J.-S. R. Jang and C.-T. Sun, "Neuro-fuzzy modeling and control," *Proceedings of the IEEE*, vol. 83, no. 3, pp. 378–406, Mar. 1995.

[110] J.-S. R. Jang and N. Gulley, *The Fuzzy Logic Toolbox for Use with MATLAB*, The MathWorks, Natick, MA, 1995.

[111] B. Kosko, *Neural Networks and Fuzzy Systems*, Prentice Hall, Englewood Cliffs, NJ, 1992.

IMAGE EVALUATION TEST TARGET (QA-3)

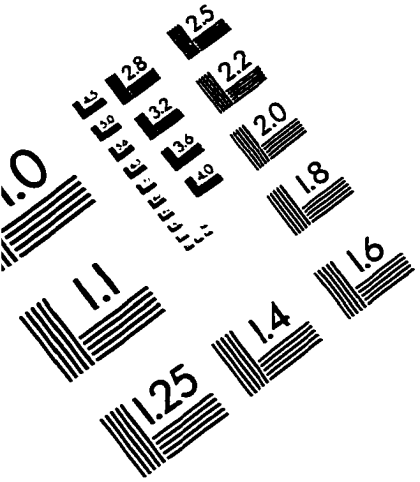

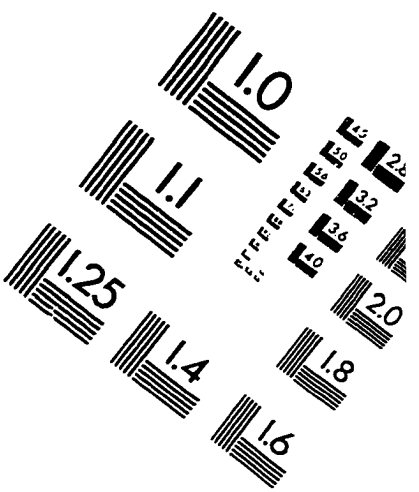

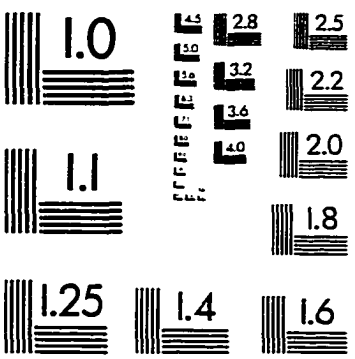

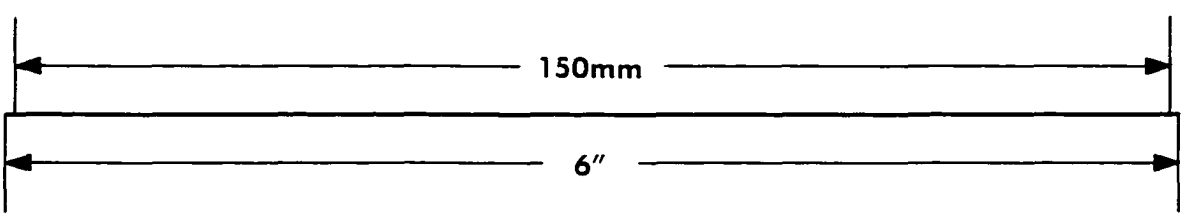

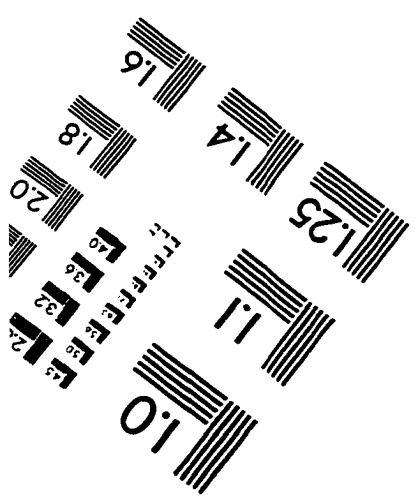

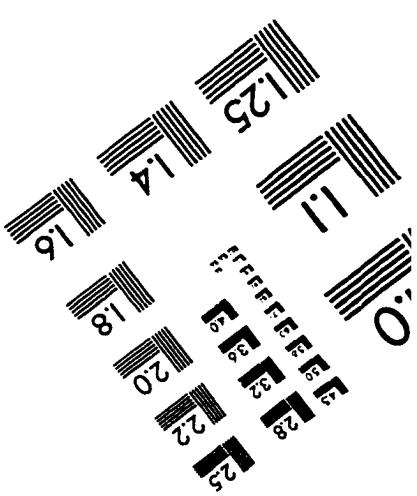

APPLIED IMAGE, Inc
1653 East Main Street
Rochester, NY 14609 USA
Phone: 716/482-0300
Fax: 716/288-5989